Applications note
Ultra-High Mass-Resolution MALDI-TOFMS System

Solutions for Innovation

JMS-S3000 SpiralTOF

Biomolecules Applications Notebook

Edition July 2016

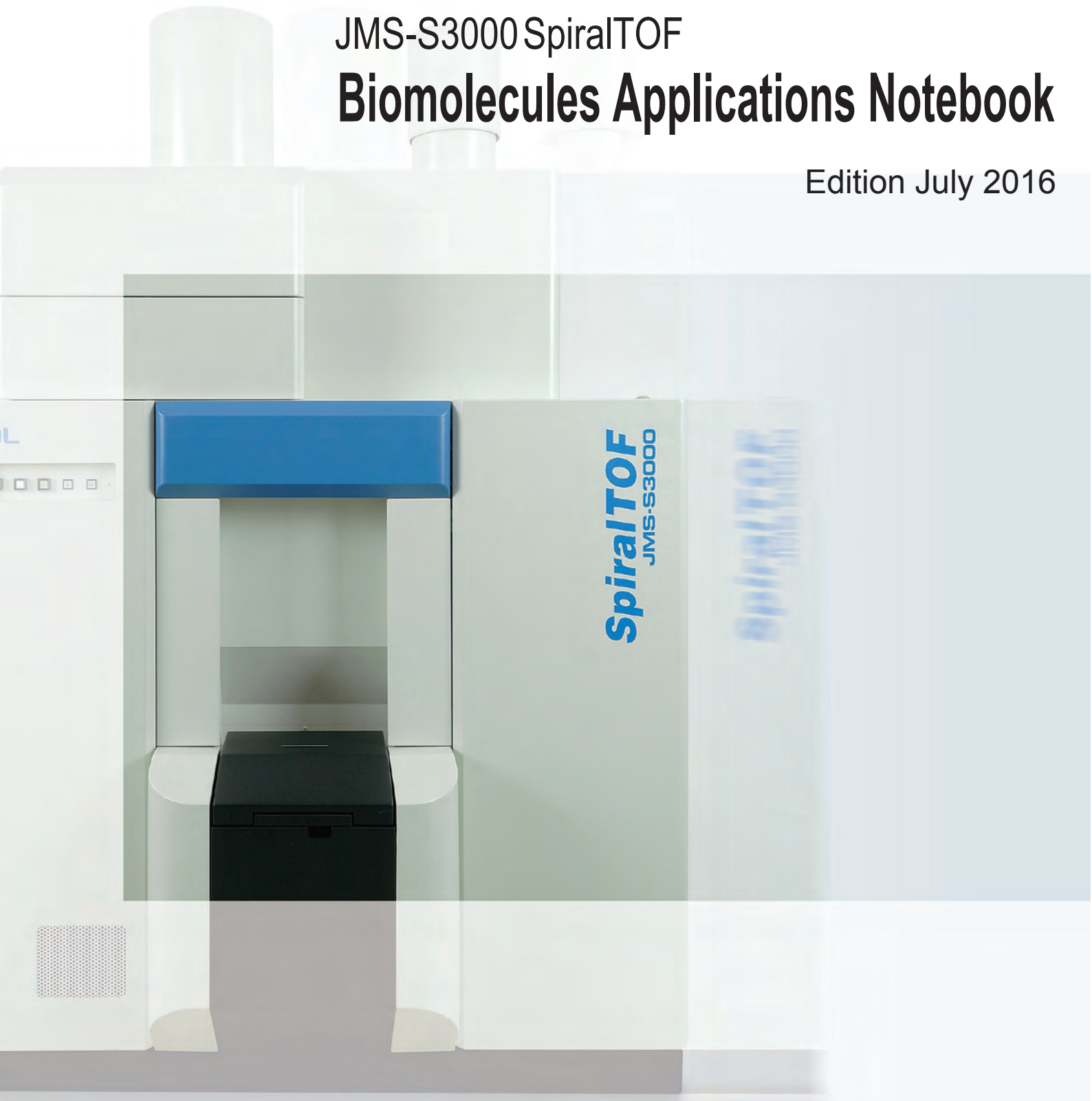

JEOL Ltd.

JMS-S3000 SpiralTOF

Biomolecules Applications Notebook

Edition July 2016

Table of Contents

Development of JMS-S3000: MALDI-TOF/TOF Utilizing a Spiral Ion Trajectory

Takaya Satoh

MS Business Unit, JEOL Ltd.

We have developed the JMS-S3000, matrix assisted laser/desorption ionization time-of-flight mass spectrometer (MALDI-TOFMS). An innovative ion optical system, which achieved a spiral ion trajectory, surpassed basic specification of the reflectron ion optical system presently used in most commercially available TOFMSs. Furthermore, we have developed the TOF-TOF option for the JMS-S3000. In the case of attaching the TOF-TOF option, a spiral ion optical system is adopted for the first TOFMS, whereas a reflectron ion optical system with offset parabolic reflectron is adopted for the second one. Utilizing the spiral trajectory ion optical system, the JMS-S3000 provides unprecedentedly high mass resolution and high precursor ion selectivity. In this paper, we demonstrate not only the high mass resolution of more than 60,000 (FWHM) at *m/z* 2093 but also achievement of high mass resolution over a wide mass range. In addition, we present the high selectivity that enables selection of monoisotopic ions of precursor ions. By selecting only monoisotopic ions of precursor ions, one signal peak corresponding to each fragmentation channel is observed on a product ion spectrum. Consequently, the analysis of the product ion spectrum is made clearer.

Introduction

The time-of-flight mass spectrometer (TOFMS) is one of mass spectrometry techniques, which include the quadrupole mass spectrometer, the magnetic sector mass spectrometer, the ion trap mass spectrometer and the Fourier transform ion cyclotron resonance mass spectrometer. In the case of TOFMS, ions of various *m/z* values, which are generated in the ion source, are accelerated to the detection plane by a pulse voltage applied from a starting time of data acqisition. Since the time-of-flight of ions at the detection plane are proportional to the square root of their *m/z* values, the ions generated in the ion source can be separated. One of the TOFMS feature is fast measurement, which is due to the unnecesity of scan for any physical parameters such as electric or magnetic fields. Recently, not only a single type mass spectrometer, but also a tandem type mass spectrometer connected with the quadrupole mass spectrometer (Q/TOF) or tandemly connected two TOFMSs (TOF/TOF) are available.

The mass resolution of TOFMS is expressed by $T/2\Delta T$, where ΔT is the time-of-flight distribution of the ion group with the same *m/z* value(ion packet) at the detection plane (that is, spatial distribution of the ion packet in the flight direction at the detection plane) and, T is centroid of the time-of-flight distribution. Since TOFMS was invented in 1964 [1], its mass resolution has been improved by increasing T and decreasing ΔT. In 1955, a unique acceleration technique was developed, which focuses the initial space and energy distributions at the detector surface in the flight direction. Applying this technique, the mass resolution was increased by decreasing ΔT [2]. Furthermore, in the early 1970s, a new technique was developed. In this technique, the focus position defined by the above-mentioned acceleration technique is chosen as the start point, and an ion optical system that is composed of ion mirror [3] or elerctrostatic sectors [4] is placed at the post stage. This innovation made it possible to increase the time-of-flight T without increasing ΔT, and led to a dramatic improvement of the mass resolution. Recently, most of commercially available TOFMS instruments use ion mirrors, and their flight paths are 1 to 3 m. For further improvement in the mass resolution of TOFMS, another types of ion optical systems have been proposed. They are the multi-reflecting type [5] and the multi-turn type [6-7] ion optical system where ions fly multiple times on the certain trajectory. These two ion optical systems theoretically achieve an infinitely long flight path in a compact space, and impoved the mass resolution. However, they have the limitation of the mass range because ions with large speed (ions with small *m/z*) lap the ions with small speed (ions with large *m/z*) when the ions flying on the same trajectory multiple times.

We have developed an original ion optical system that utilizes a spiral ion trajectory. This ion optical system can overcome the "lap" problem present in multi-reflecting and multi-turn type ion optical systems. In addition, it is possible to achieve mass resolution and mass accuracy higher than those of widely used reflectron ion optical systems. In this paper, we describe the design of the spiral trajectory

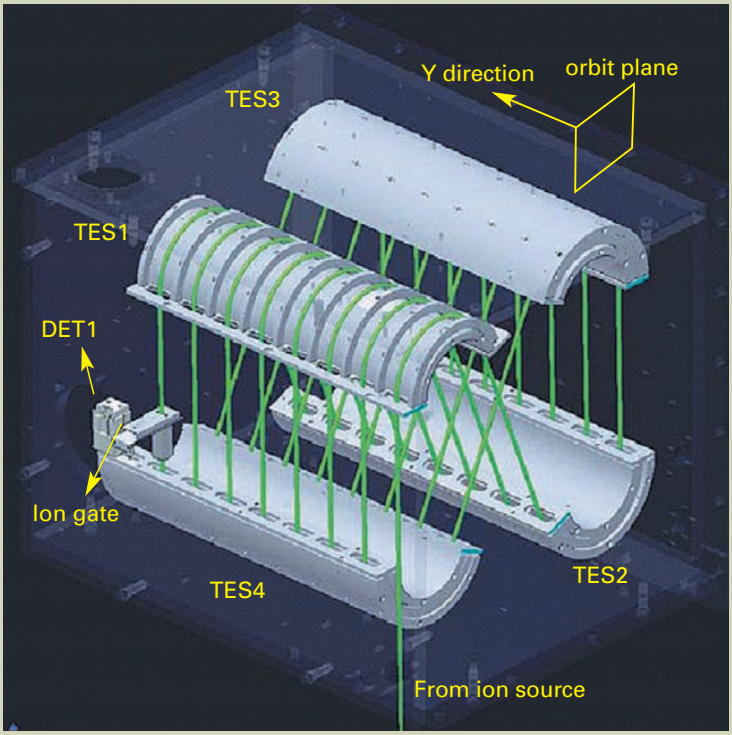

Fig. 1 Spiral ion trajectory ion optical system.

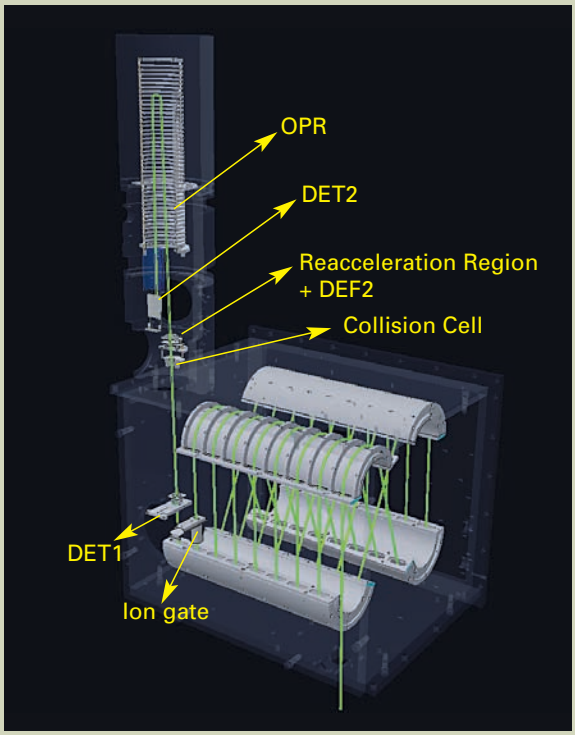

Fig. 2 MALDI-TOF/TOF utilizing the spiral ion trajectory ion optical system.

type ion optical system, and basic performance of a MALDI-TOF/TOF system applying it. The system consistsed of the spiral trajectory type ion optical system and reflectron type ion optical system using offset parabolic reflectron for the first and second TOFMSs, respectively. The instrument achieves higher mass resolution, mass accuracy and precursor ion selectivity due to utilizing a spiral ion optical system for the first TOFMS, thus enabling more precise analysis.

Design of the spiral trajectory ion optical system

Multi-turn type ion optical system technique was applied for development of the spiral trajectory ion optical system. Especially, a combination of the "perfect focusing" and "multi-turn" [12] techniques developed at Osaka University, which achieved highest mass resolution in the world, was considered the most suitable for development of the spiral trajectory ion optical system. For conversion of a multi-turn type ion optical system for a spiral trajectory ion optical system, it is necessary to move ion trajectory perpendicular to the orbit plane. In order to achieve this, we have designed the system so that ion injection is slightly tilted to the orbit plane. The advantage of the design is that there is no need for the mechanism to transfer the ions to the next layer. There are concerns about degradation of mass resolution due to the trajectory deviation from a multi-turn type ion optical system. However, the effect should be negligible by keeping the injection angle to several degrees.

Practically, we have designed the spiral trajectory ion optical system based on MULTUM II [7] construction, which consists of four toriodal electrostatic sectors (cylindrical electrodes with two Matsuda plates). The schematic of the ion optical system is shown in **Fig. 1**. To achieve a spiral trajectory, we have constructed a layered toriodal electric field (TES) by placing (number of cycles +1) Matsuda plates into the cylindrical electrostatic sectors. The Matsuda plates are arranged within certain equal distances L_y in the space L_x between the external and internal electrodes. The three types of voltages applied on TESs 1 to 4 is that of the internal electrode, external electrodes and Matsuda plates. Corresponding voltages are supplied to every Matsuda plates, internal and external electrodes of TESs 1 to 4.

Also, four TESs were placed so that they correspond to MULTUM II when looked from the orbit plane. Y direction was set perpendicular to the periodic orbit plane. In development of the MALDI-TOF/TOF, we have made Y direction to horizontal. The TES1 in the Fig. 1 shows the external electrode is removed so that it can be seen the Matsuda plates are equally spaced. Ions fly through the center of the space, formed by L_x and L_y. Ion passes the same layer of TESs 1 to 4, and after passing the TES 4, it enters to the next layer of TES 1. The process is repeated for several cycles; the ion thus draws a spiral trajectory and reaches the detector (DET1) (Green line in the Figure 1 represents the ion trajectory). The injection angle θ into the layered toriodal electric field can be expressed as follows,

$$\tan\theta = (L_y + L_m) / L_c \quad \cdots\cdots\cdots (1)$$

where, L_m is the thickness of a Matsuda plate and L_c is the one cycle length.

As mentioned above, owing to the usage of four TESs of the same structure in it's construction, the ion optical system can achieve a complicated trajectory within a simple structure.

Production of MALDI-TOF/TOF utilizing spiral trajectory ion optical system

We have developed MALDI-TOF/TOF utilizing the spiral trajectory ion optical system. It consisted of the first TOFMS using the spiral trajectory ion optical system and the second TOFMS using the reflectron ion optical system. The mass spectrum measurement in the first TOFMS is referred as spiral mode, and the product ion spectrum measurement in the second TOFMS as TOF/TOF mode.

An schematic of the system is shown in **Fig. 2** (ion source and the detector DET1 of the first TOFMS are omitted). Spiral trajectory is set to eight cycles of 2.093 m per each. A distance between central trajectories of the adjacent layers is 58 mm, an injection angle is 1.6 degree according to equation (1). Y direction is set as horizontal, so the injection angle is achieved by tilting the extraction direction of the ion source 1.6 degrees from a horizontal plase.

In the spiral mode, ions fly a spiral trajectory and are detected with the spiral mode detector (though not specified in Fig. 2, it is located similarly to DET1 in Fig. 1). Ion gate is placed in the 7th cycle. It allows eliminating high-intensity matrix ions , which are outside of the data acquisition *m/z* range.

In TOF/TOF mode, selection width of the ion gate is made narrower and monoisotopic ions of precursor ions are selected out of all isotpic ions of them. It is possible to mechanically move the spiral mode detector out of the trajectory so that precursor ions can be introduced into the collision cell. Ions, that entered a collision cell, collide with rare gas inside of the cell with a kinetic energy of approximately

20 keV, and generate fragment ions. Precursor ions and fragment ions are mass-separated in a reflectron ion optical system that combines an offset parabolic reflectron (OPR) [13] and a reacceleration mechanism. OPR is a reflectron connecting a linear and parabolic electric fields. It allows simultaneous observation of ions, from low *m/z* fragment ions up to precursor ions. In addition, in order to increase transmission of ions, fine adjustment of the ion trajectory is enabled by installing two deflectors (DEF1 and DEF2) on both sides of the collision cell.

Evaluation of MALDI-TOF/TOF with spiral trajectory ion optical system utilized

Figure 3 shows mass spectrum of six types of peptide mixtures (in order of *m/z* increase: Bradykinin fragment 1-7, Angiotensin II, Angiotensin I, P14R, ACTH fragment 1-17, ACTH fragment 18-39). The mass spectrum of Angiotensin II and ACTH fragment 1-17 are also displayed as an enlarged image. Mass resolution is 58000 (FWHM) and 73000 (FWHM) respectively. The mass error of ACTH fragment 1-17 is 0.16 ppm, when internal calibration is performed among five peptides except ACTH fragment 1-17. It became clear from the above mentioned facts that distance of flight for spiral trajectory ion optical system is 17 m, which is 5 times longer than that of the conventional reflectron type ion optical systems. This allows enhancement of mass resolution and mass accuracy.

Figure 4 shows the relation between *m/z* value and mass resolution when mass resolution is adjusted with ACTH fragment 1-17. Figure 4 shows that it is possible to achieve high mass resolution simultaneously in a wide *m/z* range. This overcomes the problem of MALDI-TOFMS utilizing conventional reflectron type ion optical system that could achieve high mass resolution only in a narrow *m/z* range.

Figure 5.a shows a product ion spectrum diagram of Poly (oxypropylene), acquired in TOF/TOF mode. Selected precursor ions are monoisotopic ions from $[M+Na]^+$ series with *m/z* 1027. A numbers of fragmentation channels from sodium ions as fragment ion to precursor ion ion are observed. The enlarged spectrum around *m/z* 780 is shown in Fig. 5.b. The system is able to select only monoisotopic ions of precursor ions, therefore each fragment channels can be observed as one peak without any isotopic peaks. Two peaks in Fig. 5.b indicate different fragmentation channels. It indicates that 2u different fragmentation channels can be clearly separated. Figure 5.c displays an image of the same *m/z* range as in Fig. 5.b when measured with conventional MALDI-TOF/TOF. Pecursor ion selectivity of traditional TOF/TOF is insufficient so that the fragment ions from all isotopic ions of precursor ions are analyzed in the second TOFMS. Thus every fragmentation channels of product ion spectrum include isotopic peaks. As a result, when *m/z* values of monoisitopc ions of two fragment channels are close, such as 2 u, their isotopic peaks are overlapped and are impossible to be clearly identified. The high precursor ion selectivity originated from the spiral trajectory ion optical system used in this system makes the structual analysis of chemical compounds much easier.

Conclusion

This paper reports on the development of the spiral trajectory ion optical system. Also, the paper describes the development of MALDI-TOF/TOF, which combines a spiral trajectory ion optical system and reflectron type ion optical system utilizing offset parabolic ion mirrors. Innovative ion optical system introduced to the JMS-S3000 has overcome preexisting problems related to conventional MALDI-TOF and MALDI-TOF/TOF. Thus, the JMS-S3000 is expected to play a significant role in various areas.

References

[1] W. E. Stephens. *Phys. Rev.*, **69**, 691 (1946)
[2] W.C.Wiley and I. H. McLaren, *Rev. Sci. Instrum.*, **26**, 1150 (1955).
[3] B. A .Mamyrin, V. I. Karataev, D. V. Shmikk and V. A. Zagulin, *So. Phys. JETP*, 3745(1973).
[4] W. P. Poschenrieder, *Int. J. Mass Spectrom. Ion. Phys.*, **6**, 357 (1972).

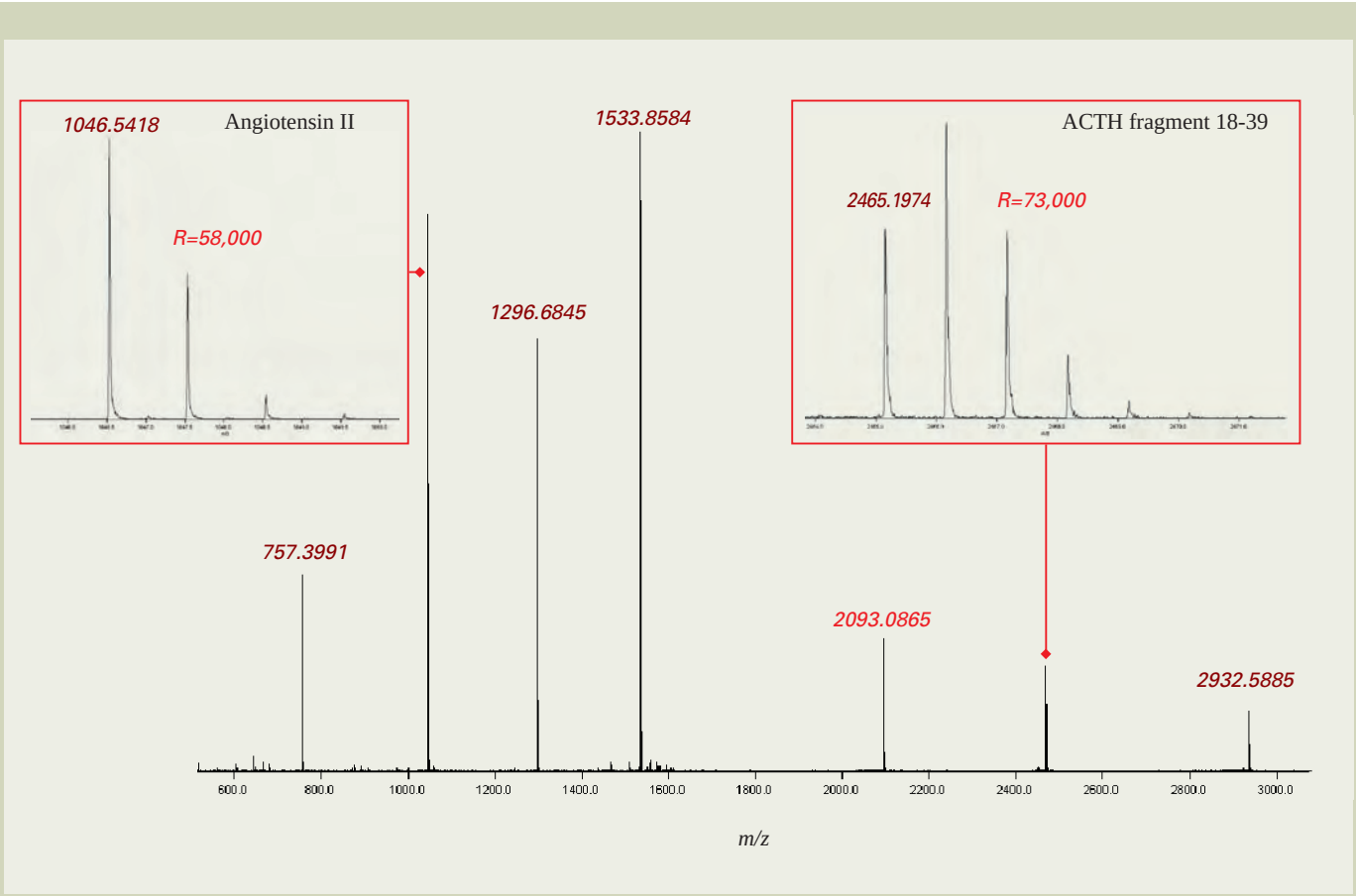

Fig. 3 Mass spectrum of peptide mixtures.

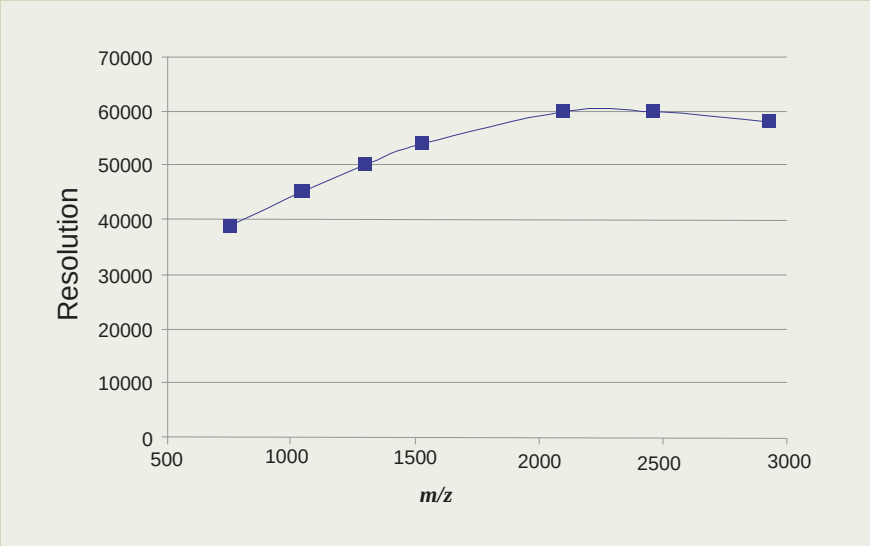

Fig. 4 Relation between *m/z* value and mass resolution.

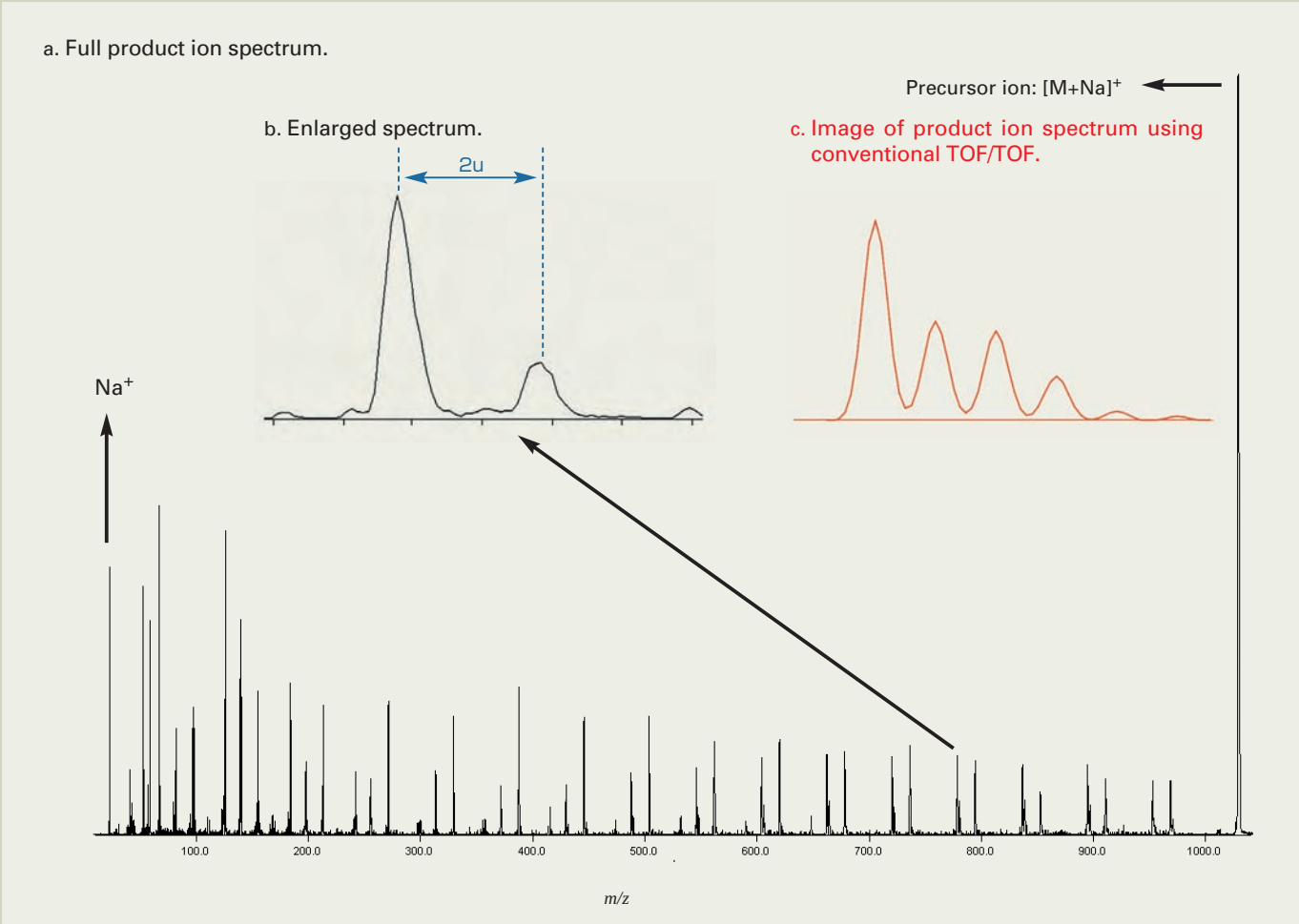

Fig. 5 Product ion spectrum of Poly(oxypropylene).

[5] H. Wollnik and A. Casares, *Int. J. Mass Spectromety*, **227**, 217 (2003).
[6] M. Toyoda, M. Ishihara, S. Yamaguchi, H. Ito, T. Matsuo, R. Reinhard and H. Rosenbauer, *J. Mass Spectrom.*, **35**, 163 (2000).
[7] D. Okumura, M. Toyoda, M. Ishihara and I. Katakuse, *J. Mass Spectom. Soc. Jpn.*, **51**, 349 (2003).
[8] M. Yavor, A. Verentchikov, J. Hasin, B. Kozlov, M. Gavrik and A. Trufanov, Physics Procedia 1 391 (2008)
[9] T. Satoh, H. Tsuno, M. Iwanaga, Y. Kammei, *J. Am. Soc. Mass Spectrom.*, **16**, 1969 (2005).
[10] T. Satoh, H. Tsuno, M. Iwanaga, and Y. Kammei, *J. Mass Spectrom. Soc. Jpn.*, **54**, 11 (2006).
[11] T. Satoh, T. Sato, and J. Tamura, *J. Am. Soc. Mass Spectrom.* **18**, 1318 (2007).
[12] M. Ishihara, M. Toyoda and T. Matsuo, *Int. J. Mass Spectrom.*, **197**, 179 (2000).
[13] E. N. Nikolaev, A. Somogyi, D. L. Smith, C. Gu, V. H. Wysocki, C. D. Martin and G. L. Samuelson, *Int. J. Mass Spectrom.*, **212**, 535 (2001)

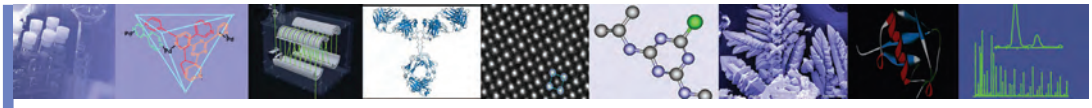

SpiralTOF™

The Relationship between Crystal Condition and Mass Resolving Power, Mass Accuracy

Introduction

The JMS-S3000 SpiralTOF™ has a unique 17 m flight path that offers the highest resolution MALDI-TOF MS system currently available. With an extended flight distance, the SpiralTOF reduces topographic effect of matrix crystal to a minimum and achieves highly reproducible mass resolving power and high mass accuracy with external mass calibration.

In this work, we demonstrate the measurement of a polymer standard with 4 types of matrices that are typically used for MALDI polymer measurement by using the JEOL SpiralTOF system. Additionally, we looked at the crystal condition using the JEOL JSM-7600F thermal field emission scanning electron microscope (FE-SEM).

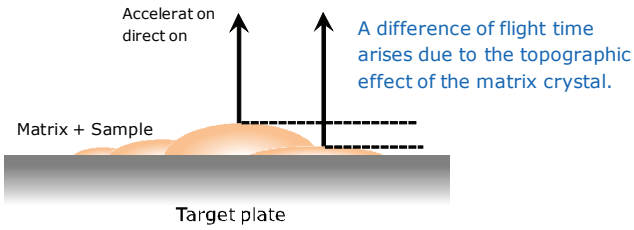

Figure 1. Reduced topographic effect of matrix crystal.

Experimental

Sample information and preparation conditions are shown in Table 1. PEG1500 was dissolved in water at a concentration of 10 mg/mL. Each matrix was dissolved in THF at a concentration of 10 mg/mL. NaI used as the cationization agent was dissolved in THF at a concentration of 1 mg/mL. Next, the PEG1500, NaI and matrix solutions were mixed together 1:1:2 (1:1:4 for DIT) by volume. Afterwards, 0.75 µL of this mixture was placed on the hairline finish stainless steel plate (MTP format, 384 spots for samples and 96 spot for calibrant). Finally, the dried sample was measured using the JMS-S3000 SpiralTOF MS system. We also obtained SEM images for each crystal condition with the JSM-7600F.

Polymer standard	Conc.	Solvent
Polyethylene glycol (PEG) 1500	10 mg/mL	Water
Cationization agent		
NaI	1 mg/mL	Water
Matrix		
α-Cyano-4-hydroxycinnamic acid (CHCA)	10 mg/mL	Tetrahydrofuran (THF)
2,5-Dihydroxybenzoic acid (DHB)	10 mg/mL	THF
Dithranol (DIT)*	10 mg/mL	THF
trans-3-Indoleacrylic acid (IAA)	10 mg/mL	THF
Sample		
PEG1500/NaI/Matrix = 1/1/2 (v/v) * PEG1500/NaI/DIT = 1/1/4 (v/v)		
0.75 µL of this sample solution mixture was placed on the MALDI target plate		
JSM-7600F conditions		
Sample preparation	Uncoated	
Acceleration voltage	1 kV	
Magnification	x500 and x2,000	

Table 1. Sample information and preparation conditions.

Figure 3. JMS-3000 SpiralTOF.

Figure 4. JSM-7600F Thermal FE-SEM.

Results & discussion:

The MALDI mass spectra of PEG1500 are shown in Figure 4 for each matrix. We set the delay time to achieve the maximum mass resolving power at *m/z* 1537.9. Therefore, the resolving power was approximately 70,000 for the $[HO(C_2H_4O)_{34}H + Na]^+$ peaks, well in excess of that needed to separate isotope peaks. Additionally, we observed excellent mass distributions.

We determined the average mass resolving power (n=10) and external mass accuracy (n=8) for *m/z* 1097.6, *m/z* 1537.9 and *m/z* 1978.2 for each matrix. The results are shown in Figure 5 and 6, respectively. We achieved high mass resolving power for the three selected ions with each matrix. In addition, we obtained excellent mass error (less than 10 ppm) with external calibration for each matrix.

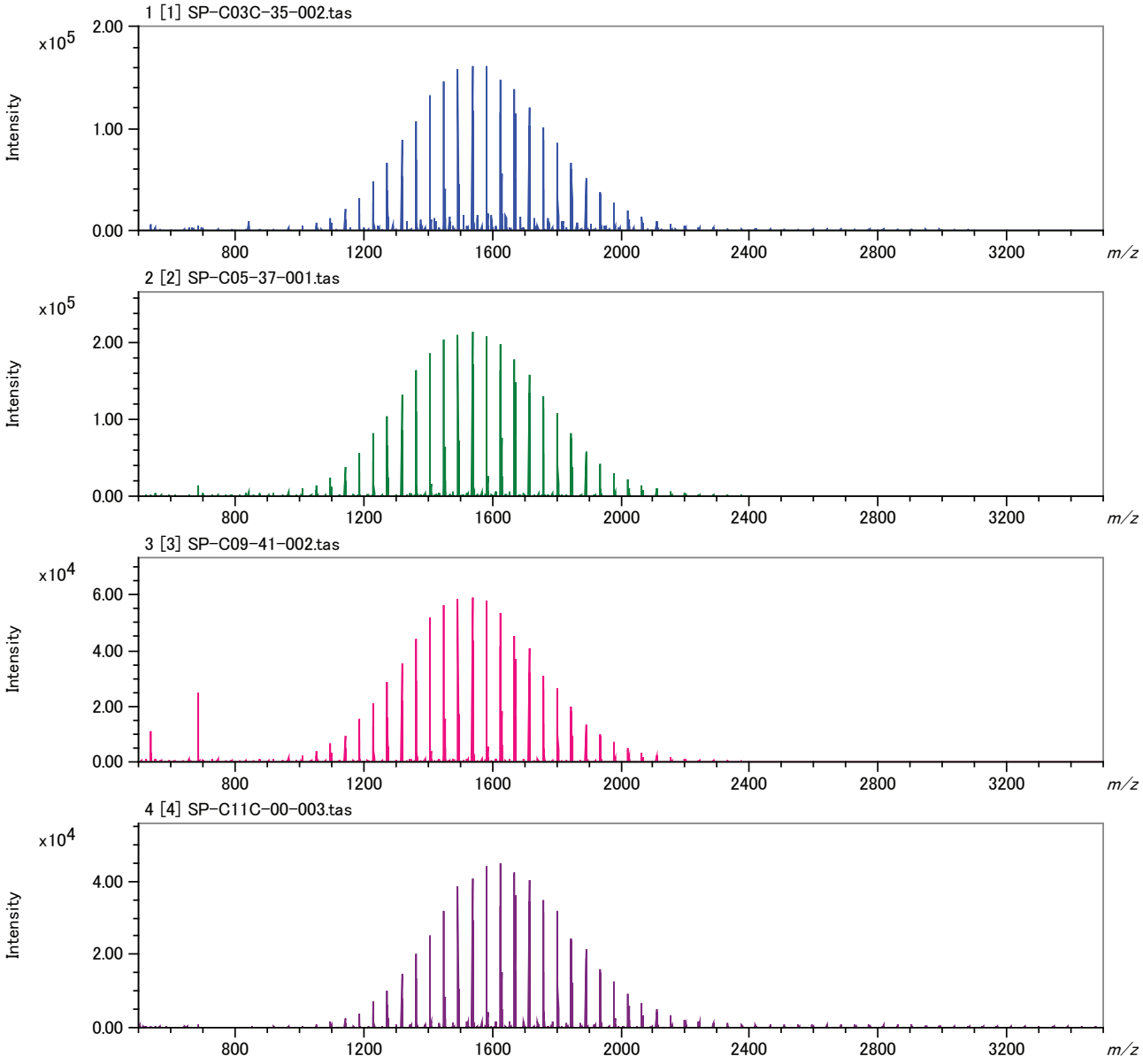

Figure 4. MALDI mass spectra of PEG1500.

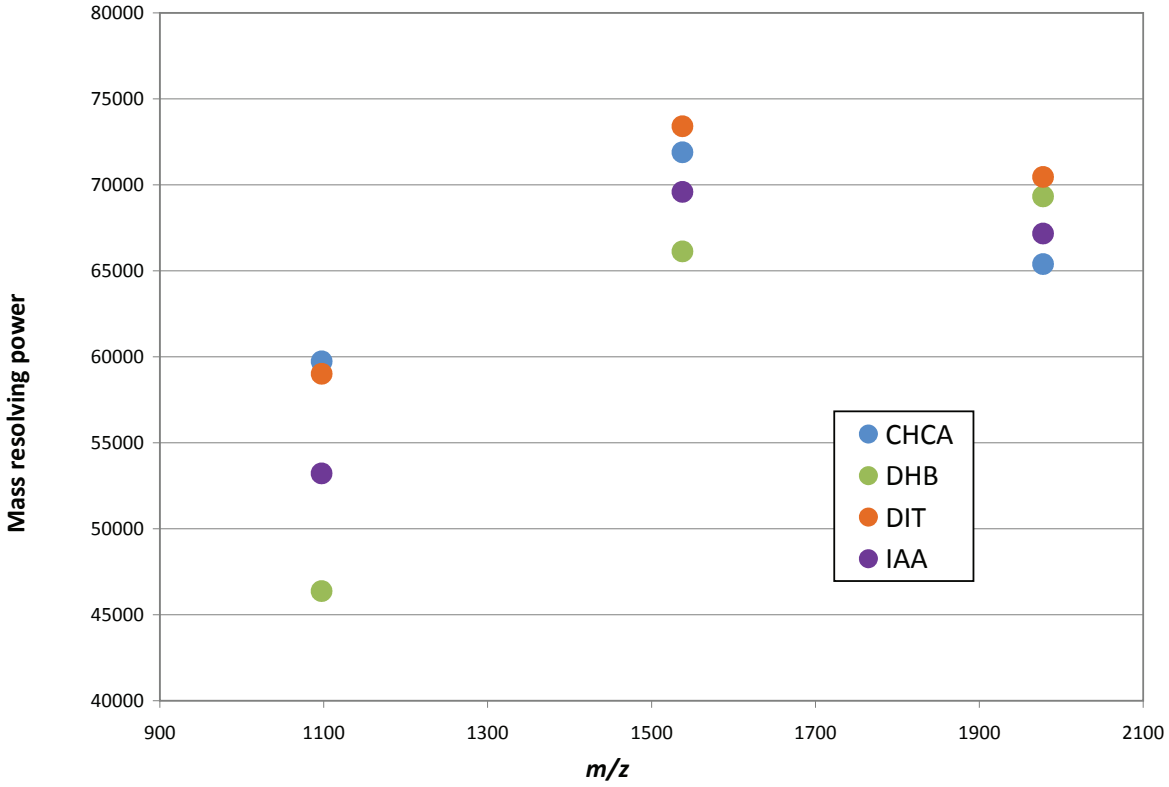

Figure 5. Averaged mass resolving power (n=10) for *m/z* 1097.6, *m/z* 1537.9 and *m/z* 1978.2.

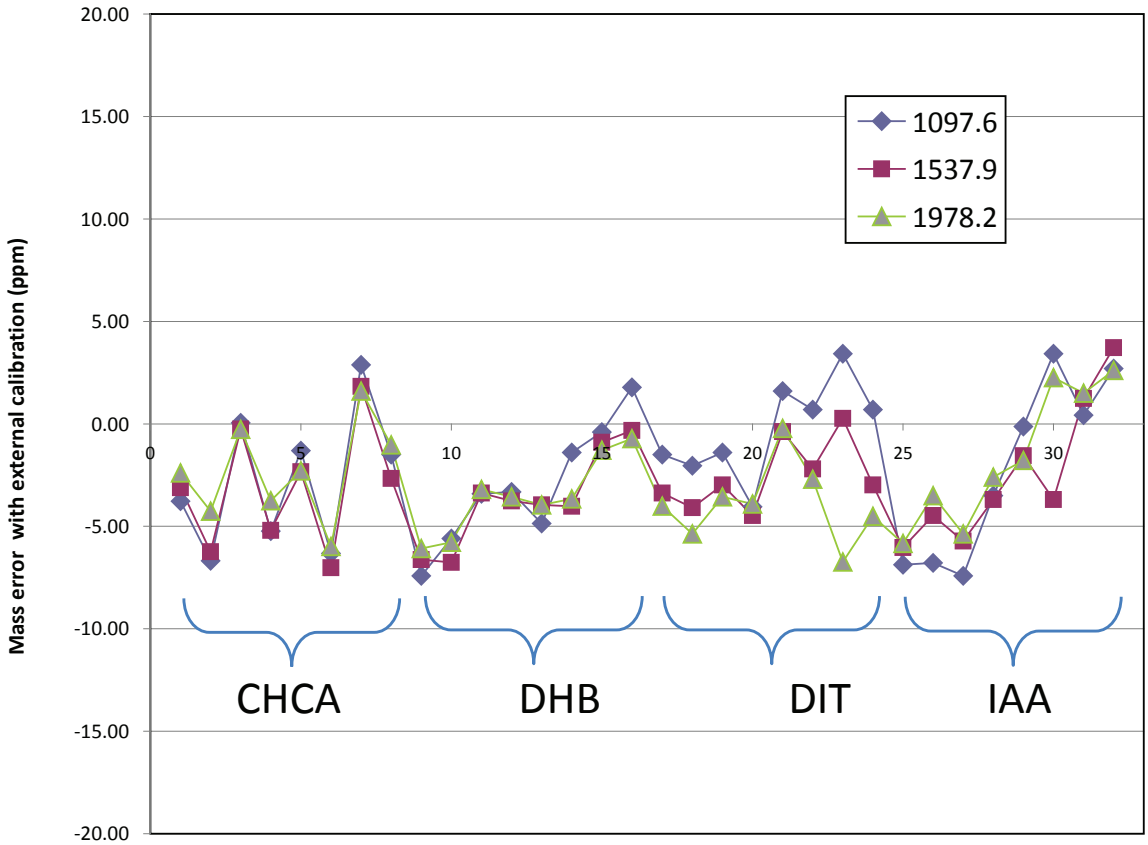

Figure 6. Mass error with external calibration (n=8) for *m/z* 1097.6, *m/z* 1537.9 and *m/z* 1978.2.

We examined the crystal condition with the JEOL JSM-7600F thermal field emission scanning electron microscope. The SEM images are shown Figures 7-10. The crystal shape, size and dispersion were quite different in each matrix crystal. However, SpiralTOF performance was not affected by the topographic effects because these spatial differences were a negligible fraction of the 17 m flight path.

Conclusions

SpiralTOF achieved highly reproducible mass resolving power and high mass accuracy with external mass calibration for all samples. These values were not significantly influenced by the different crystal morphologies for the different matrices. This is attributed to the SpiralTOF's very long (17 meter) flight path.

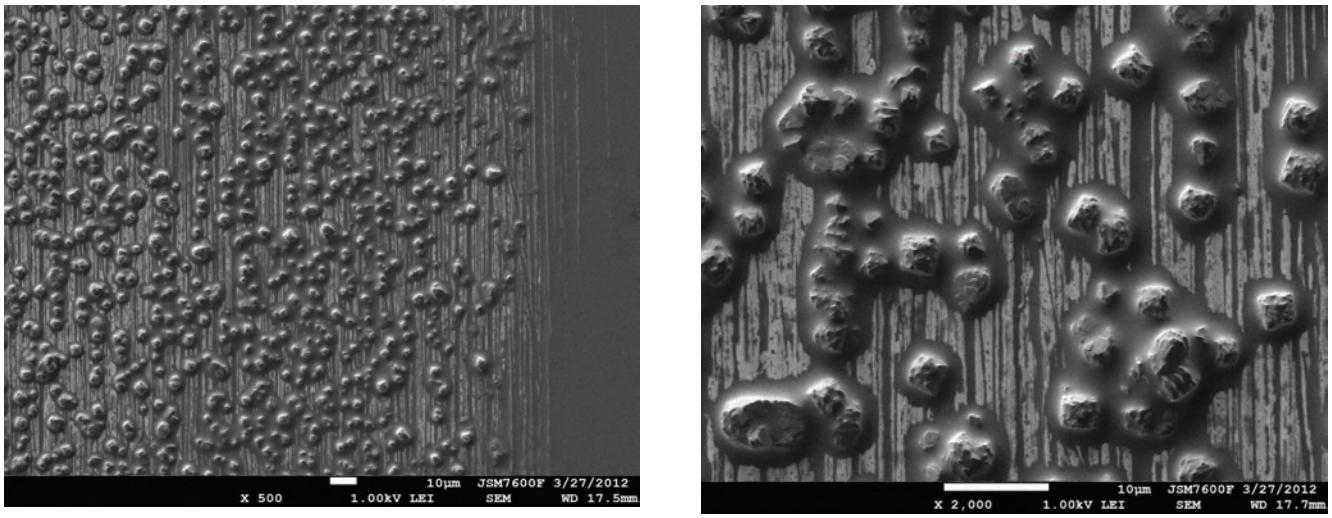

Figure 7. SEM images of CHCA crystal with PEG1500: left: x500, right: x2,000.

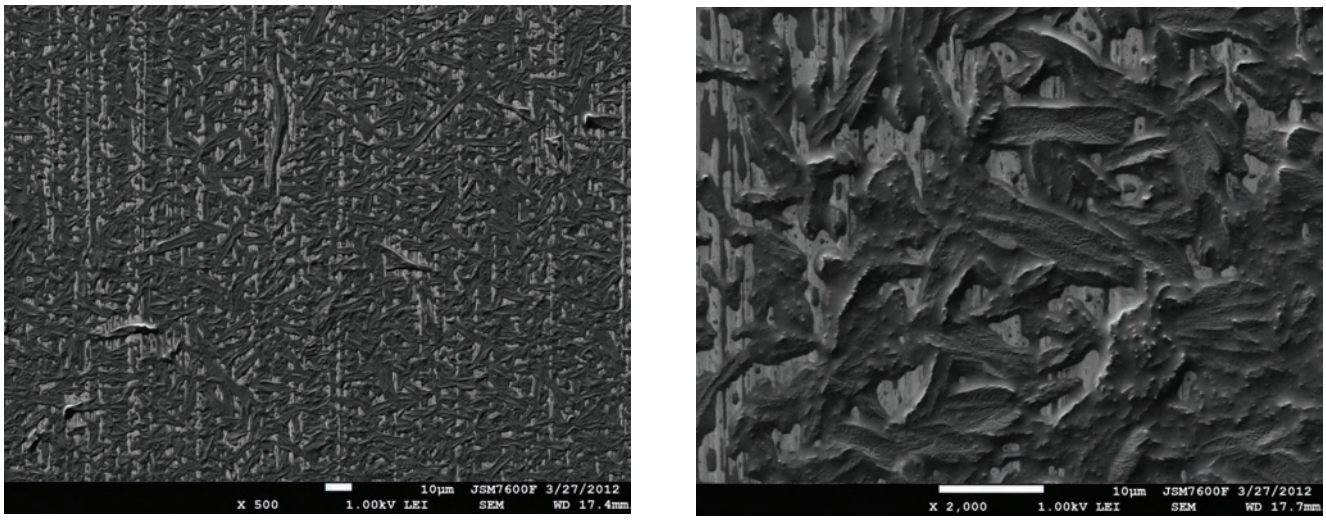

Figure 8. SEM images of DHB crystal with PEG1500: left: x500, right: x2,000.

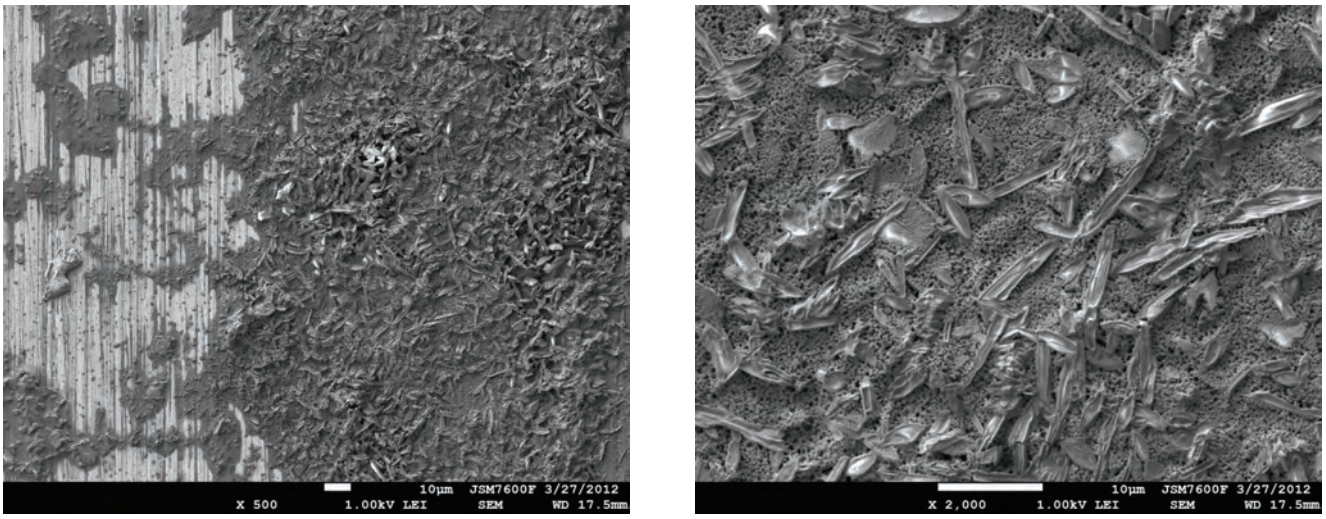

Figure 9. SEM images of DIT crystal with PEG1500: left: x500, right: x2,000.

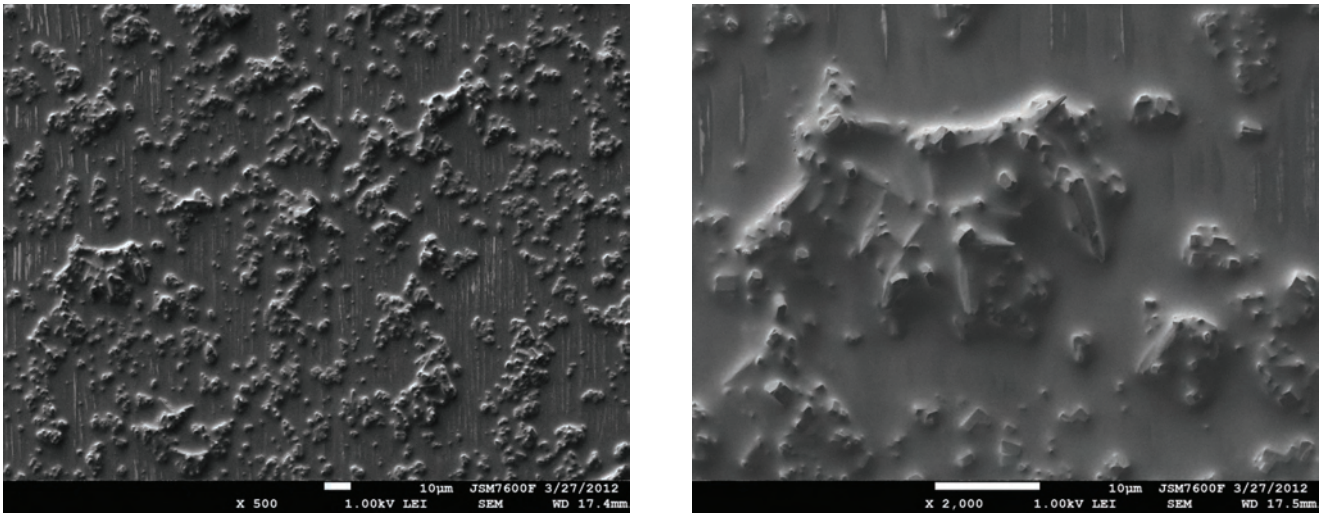

Figure 10. SEM images of IAA crystal with PEG1500: left: x500, right: x2,000.

This page intentionally left blank for layout purpose.

J. Am. Soc. Mass Spectrom. (2013) 24:684 689
DOI: 10.1007/s13361 012 0513 9

FOCUS: DEVELOPMENT AND APPLICATION OF TOF AND TOF/TOF MS: RESEARCH ARTICLE

Structural Analysis of Triacylglycerols by Using a MALDI-TOF/TOF System with Monoisotopic Precursor Selection

Ayumi Kubo,[1] Takaya Satoh,[1] Yoshiyuki Itoh,[1] Masahiro Hashimoto,[1] Jun Tamura,[1] Robert B. Cody[2]

[1]JEOL Ltd., Tokyo, Japan
[2]JEOL USA, Inc., Peabody, MA 01960, USA

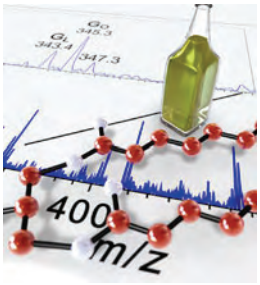

Abstract. A new MALDI-TOF/TOF system with monoisotopic precursor selection was applied to the analysis of triacylglycerols in an olive oil sample. Monoisotopic precursor selection made it possible to obtain product-ion mass spectra without interference from species that differed by a single double bond. Complete structure determination of all triacylglycerols, including structural isomers, was made possible by interpreting the charge-remote fragmentation resulting from high-energy collision-induced dissociation (CID) of the sodiated triacylglycerols.

Key words: MALDI, TOF/TOF, Charge-remote fragmentation, High-energy CID, Triacylglycerols, MS/MS, Lipids, Collision-induced dissociation

Received: 29 March 2012/Revised: 22 June 2012/Accepted: 22 June 2012/Published online: 18 December 2012

Introduction

Triacylglycerols (TAGs or triglycerides) are comprised of three fatty acids esterified with glycerol. Because TAGs are the major components in animal fats and vegetable oils, the analysis of TAGs is biologically important and crucial for quality control of food products.

Recent mass spectrometric approaches to the analysis of TAGs have made use of atmospheric pressure chemical ionization (APCI) [1–5] or electrospray ionization (ESI) [6–10] and tandem mass spectrometry (MS/MS).

Using ESI and a triple quadrupole mass spectrometer, Hsu and Turk [6] reported that collisional activation of lithium adducts of TAGs can provide structural information about the acyl groups. Low-energy collision-induced dissociation (CID) of cationized TAGs does not provide information about the position of the double bonds. However, the CID fragments of unusual dilithiated species was shown to be dependent on double bond location. Byrdwell and Neff [7] reported a method based on dual parallel ESI and APCI combined with tandem mass spectrometry for the analysis of TAGs and their oxidation products. McAnoy et al. [8] used ESI with a linear ion trap to characterize TAG components within a complex mixture of neutral lipids from cell extracts.

Correspondence to: Robert Cody; *e-mail:* cody@jeol.com

High-energy CID is an especially attractive approach for TAG analysis because charge-remote fragmentation [11–22] provides a great deal of information about lipid structure. The complete structural characterization of TAGs was reported in 1998 by Cheng et al. using fast atom bombardment (FAB) and tandem magnetic sector mass spectrometry with high-energy CID fragmentation of the $[M + Na]^+$ species [21]. All TAG structural features could be determined except stereochemistry.

However, large tandem magnetic sector mass spectrometers have fallen out of favor in recent years and high-energy CID appeared destined to become a "lost art" until the introduction of tandem time-of-flight (TOF/TOF) mass spectrometers by Cotter and Cornish in 1993 [22]. Recently, Pittenauer and Allmaier showed that TOF/TOF mass spectrometers have the potential to provide the same complete structural information as a tandem magnetic sector mass spectrometer [23]. The principal limitation of this method was found to be the poor MS-I selectivity (a 4 to 6 u window) of the TOF/TOF system, making it impractical to select precursor ions for TAGs with compositions that differ by two hydrogens. The authors concluded that a LC/MALDI-MS/MS approach might be required to make use of charge-remote fragmentations to characterize TAGs in complex mixtures.

We have developed a tandem time-of-flight mass spectrometer featuring high precursor ion selectivity that resolves the problem of poor MS-I selectivity [24]. The mass

spectrometer uses multi-turn and "perfect focusing" ion optics [25] to fit a very long (17-m) flight path into a compact space [26]. In TOF/TOF mode, an ion gate positioned at the 15 m point in the spiral ion flight path is used to isolate and guide the precursor ion into a gas-filled collision chamber. The long flight path provides ample time separation prior to precursor ion selection, resulting in unit precursor selectivity. The precursor ions undergo 20 kV collisions with a target gas and are subjected to a 9 kV post-acceleration into an offset parabolic reflectron with wide energy acceptance.

Monoisotopic precursor selection combined with high-energy CID is the key to using TOF/TOF for structural analysis of triacylglycerols in complex mixtures. This paper describes the method for structural analysis with this system and reports the complete structural analysis of TAGs, including isomers, in a commercial olive oil sample.

Experimental

Materials and Chemicals

A triacylglycerol standard (1-palmitoyl-2-oleoyl-3-linoleoyl-rac-glycerol), matrix (2,5-dihydroxybenzoic acid or DHB), and cationizing agent (sodium trifluoroacetate), were purchased from Sigma-Aldrich (St. Louis, MO). A trioleoylglycerol (triolein) standard was purchased from TCI. Tetrahydrofuran (THF) was purchased from Wako (Osaka, Japan) and olive oil was purchased from local stores. The triacylglycerol standard, including triolein, and the olive oil were dissolved in THF at respective concentrations of 100 pmol/uL and 10 ug/uL. A solution of sodium trifluoroacetate and DHB was dissolved in THF at respective concentrations of 1 ug/uL and 20 ug/uL, and added to the samples at a volume ratio of 1:1:2. The resulting mixture was loaded onto an MTP 96-hole hairline plate (JEOL Ltd., Akishima Japan) at a volume of 1 uL per spot.

MALDI Mass Spectrometry

A JMS-S3000 Spiral TOF (JEOL Ltd., Akishima, Japan) equipped with the TOF/TOF option was used for all measurements. The laser was a Nd-YLF laser operated at a wavelength of 349 nm. The laser intensity and the detector voltage were set to prevent triacylglycerol peaks from saturating. The extraction delay was optimized to 400 ns to provide a resolving power (FWHM) of approximately 50,000 for the TAG peaks in MS-I mode. For product-ion mass spectrum acquisition, helium collision gas was introduced to attenuate the precursor ion abundance to approximately 50 % of the initial value. The laser was operated at a repetition rate of 1000 Hz. Spectra were acquired at a rate of two spectra per s and 500 spectra were accumulated for each product-ion mass spectrum shown here.

Results and Discussion

Figure 1 shows the structure of 1-palmitoyl-2-oleoyl-3-linoleoyl-rac-glycerol. The structure shows (18:1) oleic acid, (16:0) palmitic acid, and (18:2) linoleic acid substituents at position *sn-2* (the site that determines the stereochemistry) and positions *sn-1 and sn-3*, respectively. In this article, we have labeled the fatty acid substituents at positions *sn-1* and *sn-3* as "*sn-1*/*sn-3*." The substituents at *sn-1* and *sn-3* are indistinguishable by mass spectrometry because the steric structure of triacylglycerol cannot be identified by mass spectrometry. Each fragmentation path is assigned as shown in Figure 1, and is labeled alphabetically. Each letter represents the initial letter of the fatty acid, and the accompanying number represents the bonding position in each fatty acid. The labeling for TAGs such as "TAG(54:3)" follows the convention where the numeral on the left in parentheses represents the total number of acyl carbon chains and the numeral on the right represents the total number of unsaturated bonds at fatty acid moieties.

The major species observed for 1-palmitoyl-2-oleoyl-3-linoleoyl-rac-glycerol was the sodiated molecule $[M + Na]^+$. Figure 2 shows the product ion spectrum acquired by selecting the monoisotopic ion of this species. The resulting fragment ions are solely monoisotopic ions as well because a monoisotopic precursor ion was selected. Thus, each fragmentation path is observed as a single peak on the product-ion mass spectrum. Figure 2a shows the entire mass range of the product-ion spectrum. The Na^+ peak detected at m/z 23.0 confirms that the precursor ion is indeed $[M + Na]^+$. Peaks characteristic of fatty acid fragmentation are predicted as A-, B-,

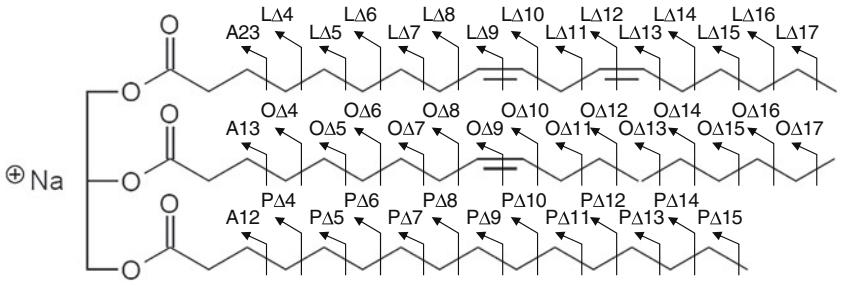

Figure 1. Structure and charge-remote fragmentation of sodiated 1-palmitoyl-2-oleoyl-3-linoleoyl-rac-glycerol

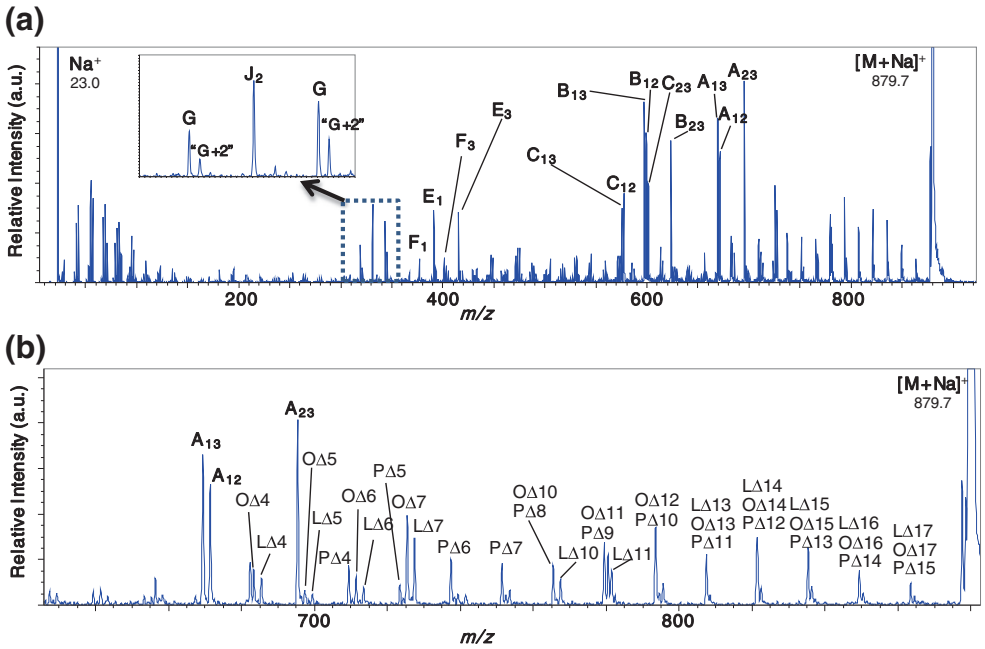

Figure 2. Product-ion mass spectrum for sodiated 1-palmitoyl-2-oleoyl-3-linoleoyl-rac-glycerol, (**a**) entire mass range; (**b**) *m/z* 650–890 magnified

C-, E-, G-, and J-type ions using the nomenclature defined in reference [21]. Figure 2a demonstrates that all of A-, B-, C-, E-, G-, and J-type ions predicted in reference [21] were observed for this example and "G+2" ions (mentioned in reference [21]) were observed. The structure of "G+2" ions and their fragmentation pathway are not clear, but "G+2" ions were also observed in the product ion spectrum of the of triolein standard (shown in Figure 5b) at a relatively lower intensity than that of the G-type ions. Figure 2b also shows that signals resulting from charge-remote fragmentation were detected in the high mass range above *m/z* 650. When the fragment ion at each bonding position is defined as in Figure 1, the peaks can be assigned as shown in Figure 2b. The intensities of fragment ions corresponding to unsaturated bonding positions, such as LΔ9, LΔ12, and OΔ9, are relatively weak or are not observed, resulting in a peak pattern that reflects the structure of 3 fatty acids.

In the analysis of triacylglycerols in the olive oil sample, particular attention was focused on the G- and J-type ions. These ions have the structure where two molecules of fatty acid are eliminated from the precursor ion [21]. These ions help determine the numbers of carbon chains and unsaturated bonds in each fatty acid. In the G-type ion, fatty acids remain at *sn-1*/*sn-3*, while the J-type ion, where a fatty acid remains at *sn-2*, has one less CH_2 at the end. This makes it possible to estimate the bonding positions of three fatty acids because fatty acids having an odd acyl carbon number rarely exist in the natural world.

Figure 3 shows the mass spectrum of the olive oil. Sodiated triacylglycerols $[M + Na]^+$ were observed for this sample that included TAG (52:3) (*m/z* 879.7), TAG (52:2) (*m/z* 881.7), TAG (54:4) (*m/z* 905.8), and TAG (54:3) (*m/z* 907.8). The monoisotopic ions of these four TAGs were selected as the precursor ions, and their product-ion mass spectra were acquired. Figure 4 shows the spectra of ions at *m/z* 905.8 acquired before and after the precursor ion selection. The figure demonstrates that only the ions at *m/z* 905.8 were selected, completely eliminating ions at other mass values.

Figure 5 shows comparison between the product-ion mass spectra of TAG (54:3) $[M + Na]^+$ at *m/z* 907.8 from olive oil and from triolein standard. Given that olive oil is

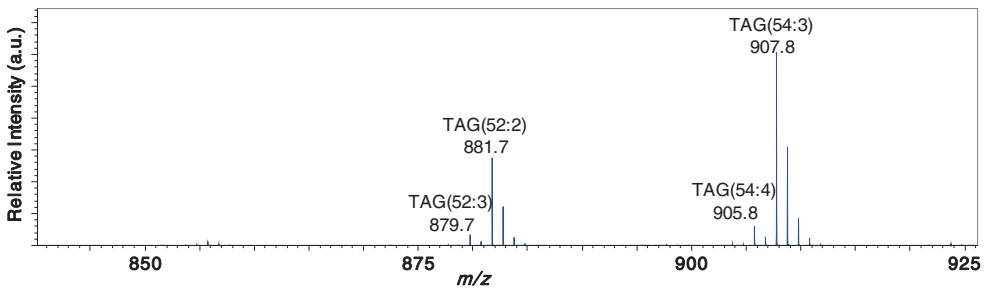

Figure 3. Mass spectrum of olive oil sample showing sodiated TAGs

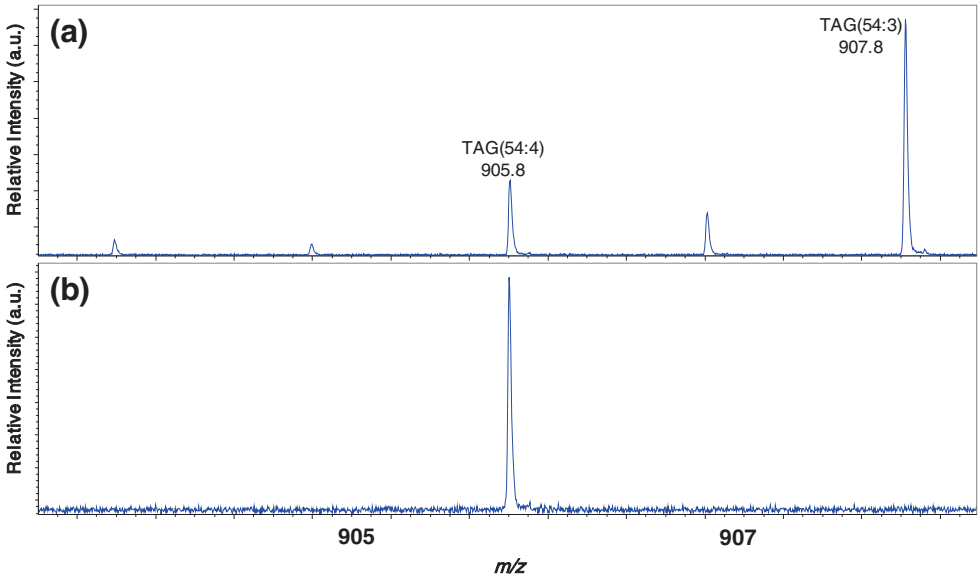

Figure 4. Precursor-ion selection for ions at *m/z* 905.8 (**a**) before selection, (**b**) after selection

rich in oleic acid, the ion at *m/z* 907.8 is expected to contain three oleic acids (18:1). Both of the product-ion mass spectra show a J_2-type ion at *m/z* 331.3, indicating that an oleic acid is bonded at the *sn-2* position, and a G-type ion at *m/z* 345.3, indicating that an oleic acid is bonded at the *sn-1*/*sn-3* positions. The spectra show only one peak that is considered an A-, B-, and C-type ion, suggesting that TAG (54:3) is trioleoylglycerol, which contains three oleic acid molecules. The signals in high mass region resulting from charge-remote fragmentation were identical between the sample and standard, and the spectral patterns were consistent with structure of oleic acid.

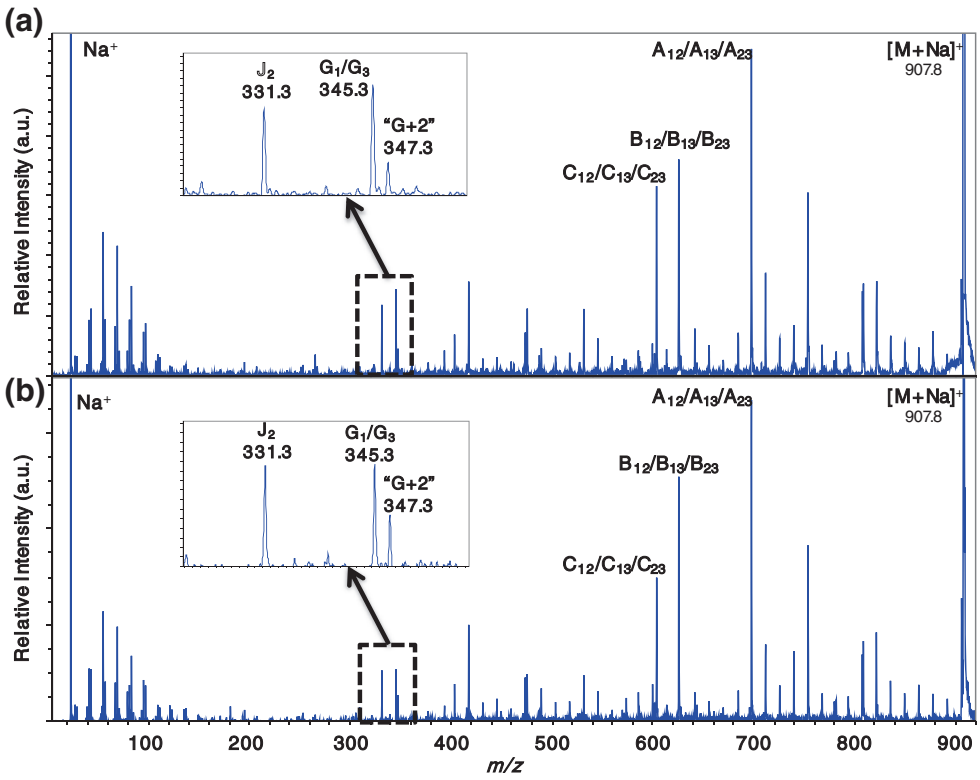

Figure 5. Comparison of product-ion mass spectra for the precursor at *m/z* 907.8 with that of sodiated triolein standard, (**a**) the ions at *m/z* 907.8 from olive oil, (**b**) triolein standard

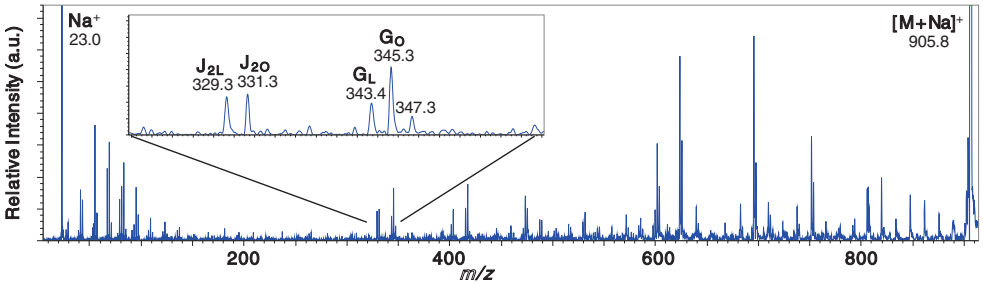

Figure 6. Product-ion mass spectrum for the precursor at *m/z* 905.8

Next, the ion at *m/z* 905.8 was selected as the precursor ion. The *m/z* value of this ion suggests that it is a monoisotopic $[M + Na]^+$ ion of TAG (54:4). Figure 6 shows the product-ion mass spectrum. It is expected that this triacylglycerol is also composed of two (18:1) oleic acids and one (18:2) linoleic acid, given that the major component of olive oil is oleic acid. The product-ion mass spectrum shows fragment ions assigned as G-type ions, at *m/z* 343.4 and *m/z* 345.3. If the ion at *m/z* 343.4 is a G-type ion, the fatty acid molecule at *sn-1/sn-3* is linoleic acid, and if the ion at *m/z* 345.4 is a G-type ion, the fatty acid molecules at *sn-1/sn-3* are oleic acid. The ion at *m/z* 347.3 is assigned as a "G+2" ion because in the product-ion mass spectrum "G+2" ions were observed at lower intensity than G-type ions as discussed above, and the intensity of the ion at *m/z* 347.3 is relatively lower than that of the ion at *m/z* 345.3. This is consistent with the assignment of G+2 ions by Cheng et al. in reference [21]. Since the G-type ion suggests that both oleic acid and linoleic acid are bonded, the remaining fatty acid is (18:1) oleic acid. Next, the product-ion spectrum shows J-type ions: a J-type ion containing oleic acid (J_{2O}) and a J-type ion containing linoleic acid (J_{2L}) at *m/z* 331.3 and *m/z* 329.3, respectively. In the high-mass region, the signals resulting from charge-remote fragmentation were consistent with the structures of oleic acid and linoleic acid. This demonstrates that *m/z* 905.8 is triacylglycerol that contains two molecules of oleic acid and one molecule of linoleic acid and is a mixture of the structural isomers 1,3-dioleoyl-2-linoleoyl-glycerol and 1,2-dioleoyl-3-linoleoyl-glycerol. Table 1 summarizes the structures of triacylglycerols determined for the olive oil samples from the product-ion mass spectra. The ions associated with the peak at *m/z* 879.7 are a mixture of the structural isomers 1-palmitoyl-2-oleoyl-3-linoleoyl-glycerol and 1-palmitoyl-2-linoleoyl-3-oleoyl-glycerol.

Table 1. Summary of TAGs Found in the Olive Oil Sample

m/z	Acyl carbon number and number of double bond	Composition of each fatty acid	
879.7	52:3	(16:0,18:1,18:2)	(16:0,18:2,18:1)
881.7	52:2	(16:0,18:1,18:1)	
905.8	54:4	(18:1,18:1,18:2)	(18:1,18:2,18:1)
907.8	54:3	(18:1,18:1,18:1)	

Conclusion

Monoisotopic precursor selection was demonstrated for TOF/TOF analysis of a standard TAG and TAGs in an olive oil sample. This selectivity made it possible to use charge-remote fragmentation to determine the complete structure (except stereochemistry) for all of the TAGs, including structural isomers, present in the sample. Multiple structural isomers in the precursor ion were identified through the observation of G- and J-type ions. These results demonstrate that the MALDI-TOF-TOF system with high precursor ion selectivity can fully analyze the structure of triacylglycerols without prior chromatographic separation, and that the method is effective for the analysis of complex fat composites in food.

Open Access

References

1. Byrdwell, W.C., Emken, E.A.: Analysis of triglycerides using atmospheric pressure chemical ionization mass spectrometry. *Lipids* **30**, 173 175 (1992)
2. Neff, W.E., Byrdwell, W.C.: Soybean oil triacylglycerol analysis by reversed-phase high-performance liquid chromatography coupled with atmospheric pressure chemical ionization mass spectrometry. *J. Am. Oil Chem. Soc.* **72**, 1185 1191 (1995)
3. Byrdwell, W.C., Emken, E.A., Neff, W.E., Adlof, R.O.: Quantitative analysis of triglycerides using atmospheric pressure chemical ionization mass spectrometry. *Lipids* **31**, 919 935 (1996)
4. Byrdwell, W.C.: Atmospheric pressure chemical ionization mass spectrometry for the analysis of lipids. *Lipids* **36**, 327 346 (2001)
5. Xu, Y., Brenna, J.T.: Atmospheric pressure covalent adduct chemical ionization tandem mass spectrometry for double bond location in monoene- and diene-containing triacylglycerols. *Anal. Chem.* **79**, 2525 2536 (2007)
6. Hsu, F., Turk, J.: Structural characterization of triacylglycerols as lithiated adducts by electrospray ionization mass spectrometry using low-energy collisionally activated dissociation on a triple stage quadrupole instrument. *J. Am. Soc. Mass Spectrom.* **10**, 587 599 (1999)
7. Byrdwell, W.C., Neff, W.E.: Dual parallel electrospray ionization and atmospheric pressure chemical ionization mass spectrometry (MS),MS/MS and MS/MS/MS for the analysis of triacylglycerols and triacylglycerol oxidation products. *Rapid Commun. Mass Spectrom.* **16**, 300 319 (2002)
8. McAnoy, A., Wu, C., Murphy, R.: Direct qualitative analysis of triacylglycerols by electrospray mass spectrometry using a linear ion trap. *J. Am. Soc. Mass Spectrom.* **16**, 1498 1509 (2005)

9. Ham, B.M., Jacob, T.J., Keese, M.M., Cole, R.B.: Identification, quantification and comparison of major non-polar lipids in normal and dry eye tear lipidomes by electrospray tandem mass spectrometry. *J. Mass Spectrom.* **39**, 1321 1336 (2004)
10. Lévêque, N.L., Héron, S., Tchapla, A.: Regioisomer characterization of triacylglycerols by non-aqueous reversed-phase liquid chromatography/electrospray ionization mass spectrometry using silver nitrate as a postcolumn reagent. *J. Mass Spectrom.* **45**, 284 296 (2010)
11. Gross, M.L.: Charge-remote fragmentations: method, mechanism and applications. *Int. J. Mass Spectrom. Ion Process.* **118/119**, 137 165 (1992)
12. Griffiths, W.J., Yang, Y., Lindgren, J.Å.: Charge Remote Fragmentation of Fatty Acid Anions in 400 eV Collisions with Xenon Atoms. *Rapid Commun. Mass Spectrom.* **10**, 21 28 (1996)
13. Deterding, J.D., Gross, M.L.: Tandem mass spectrometry for identifying fatty acid derivatives that undergo charge-remote fragmentations. *Org. Mass Spectrom.* **23**, 169 177 (1988)
14. Deterding, J.D., Gross, M.L.: Fast-atom-bombardment and tandem mass spectrometry for determining structures of fatty acids as their picolinyl ester derivatives. *Anal. Chim. Acta* **200**, 431 455 (1987)
15. Cordero, M.M., Wesdemiotis, C.: Characterization of the Neutral Products Formed upon Charge-Remote Fragmentation of Fatty Acid Ions. *Anal. Chem.* **66**, 861 866 (1994)
16. Murphy, R.C., Fiedler, J., Hevko, J.: Analysis of nonvolatile lipids by mass spectrometry. *Chem. Rev.* **101**(2), 479 526 (2001)
17. Ann, Q., Adams, J.: Structure determination of ceramides and neutral glycosphingolipids by collisional activation of $[M + Li]^+$ ions. *J. Am. Soc. Mass Spectrom.* **3**, 260 263 (1992)
18. Trimpin, S., Clemmer, D.E., Mcewen, C.N.: Charge-remote fragmentation of lithiated fatty acids on a TOF-TOF instrument using matrix-ionization. *J. Am. Soc. Mass Spectrom.* **18**, 1967 1972 (2007)
19. Jensen, N.J., Tomer, K.B., Gross, M.L.: FAB MS/MS for phosphatidylinostitol, -glycerol, -ethanolamine, and other complex phospholipids. *Lipids* **22**, 480 489 (1987)
20. Shimma, S., Kubo, A., Satoh, T., Toyoda, M.: Detailed structural analysis of lipids directly on tissue specimens using a MALDI-SpiralTOF-Reflectron TOF mass spectrometer. *PLoS One* **7**, 5 (2012)
21. Cheng, C., Gross, M.L., Pittenauer, E.: Complete structural elucidation of triacylglycerols by tandem sector mass spectrometry. *Anal. Chem.* **70**, 4417 4426 (1998)
22. Cornish, T.J., Cotter, R.J.: Collision-induced dissociation in a tandem time-of-flight mass spectrometer with two single-stage reflectrons. *Org. Mass Spectrom.* **28**(10), 1129 1134 (1993)
23. Pittenauer, E., Allmaier, G.: The renaissance of high-energy CID for structural elucidation of complex lipids: MALDI-TOF/RTOF-MS of alkali cationized triacylglycerols. *J. Am. Soc. Mass Spectrom.* **20**, 1037 1047 (2009)
24. Satoh, T., Sato, T., Kubo, A., Tamura, J.: Tandem Time-of-Flight Mass Spectrometer with high precursor ion selectivity employing spiral ion trajectory and improved offset parabolic reflectron. *J. Am. Soc. Mass Spectrom.* **22**, 797 803 (2011)
25. Ishihara, M., Toyoda, M., Matsuo, T.: Perfect Spatial and Isochronous Focusing Ion Optics for Multi-turn Time of Flight Mass Spectrometer. *Int. J. Mass Spectrom.* **197**, 179 189 (2000)
26. Satoh, T., Tsuno, H., Iwanaga, M., Kammei, Y.: The design and characteristic features of a new time-of-flight mass spectrometer with a spiral ion trajectory. *J. Am. Soc. Mass Spectrom.* **16**(12), 1969 1975 (2005)

SpiralTOF-TOF

Structural Analysis of Tristearin

Introduction:

The JMS-S3000 SpiralTOF™ is a MALDI-TOF MS that uses an innovative spiral ion optical system to achieve the highest resolution currently available for a MALDI instrument. Additionally, this system can be equipped with a TOF-TOF option that can acquire high-energy collision-induced dissociation (HE-CID) product ion spectra for monoisotopically selected precursor ions. The resulting HE-CID product ion spectra provide detailed structural information about compounds like triglycerides by means of charge-remote fragmentation (CRF).[1]

Tristearin is a triglyceride found in fats that consists of three stearic acid moieties (Fig. 1). In this work, we report the structural analysis of tristearin by using the HE-CID capabilities of the SpiralTOF-TOF.

Results and Discussion:

The sample was dissolved with NaI in methanol to promote Na^+ adduct formation. PEG 1000 was used as an external calibration standard. Initially, the sample was measured in Spiral mode and showed a signal at *m/z* 913.8231 (Fig. 2). This ion was consistent with the expected $[M+Na]^+$ calculated mass of 913.8194. Next, the product ion spectrum of this monoisotopically selected *m/z* was obtained using the TOF-TOF mode (Fig. 3). The resulting mass spectrum showed a fragmentation pattern consistent with the occurrence of CRF. Fig. 4 shows the enlarged *m/z* 600-920 mass range in which the labeled peaks are clearly reflected in the structure shown in Fig. 5. It should be noted that these fragment ions were detected when CRF occurred to one of the three stearin branches present in the molecule.

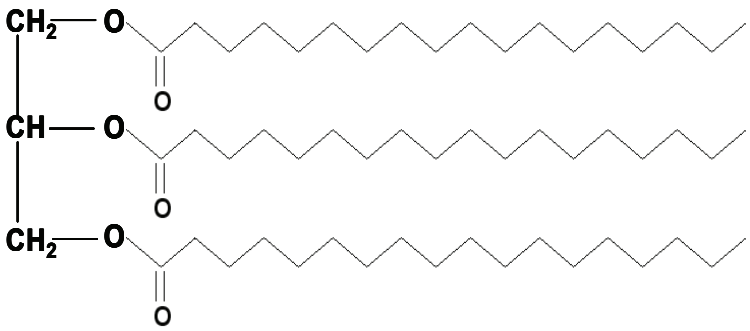

Figure 1. Structure of tristearin.

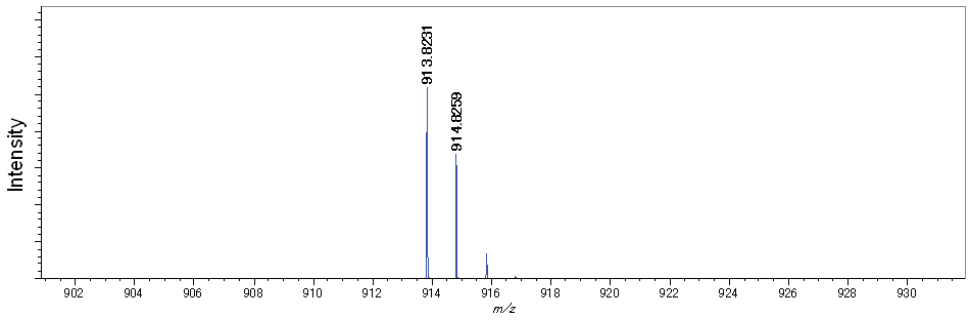

Figure 2. Mass spectrum of tristearin.

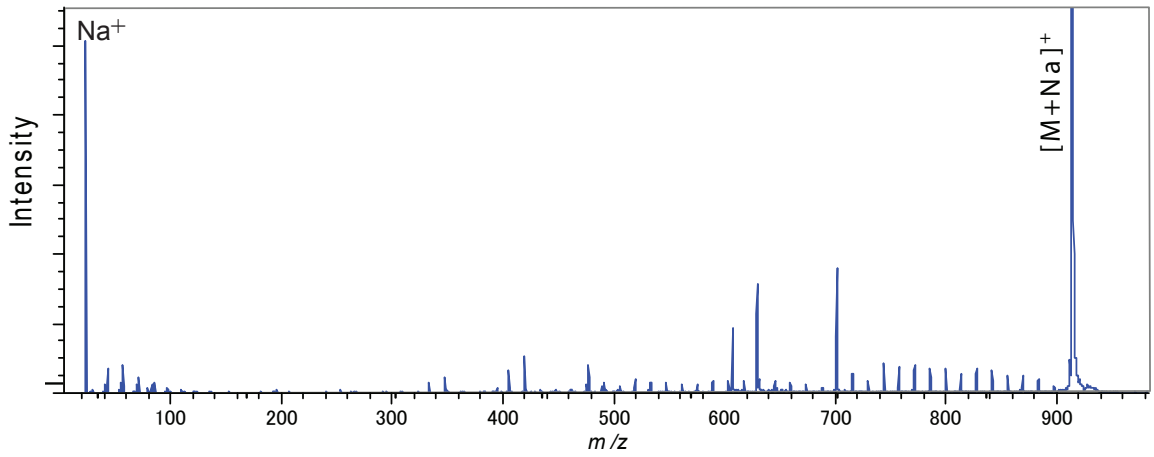

Figure 3. Product ion spectrum for the sodium adduct of tristearin.

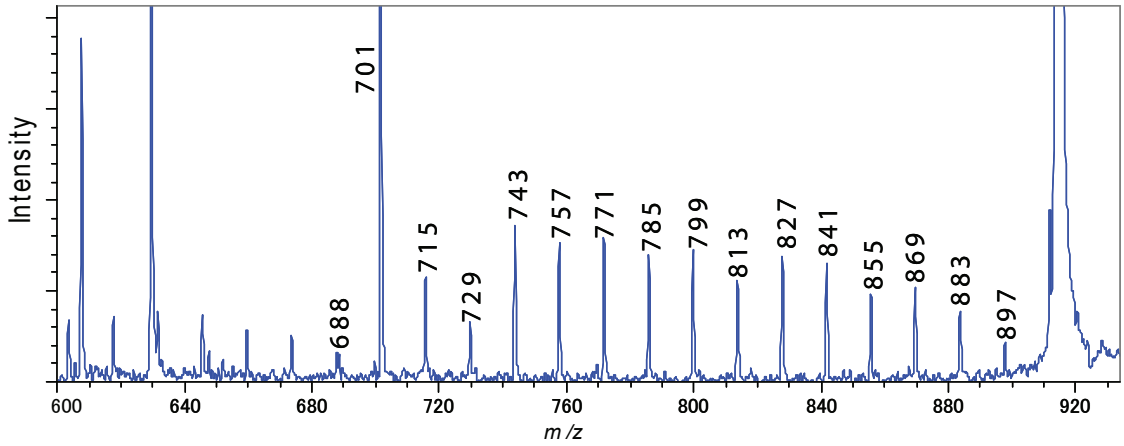

Figure 4. Product ion spectrum for the sodium adduct of tristearin (enlarged between *m/z* 600-920).

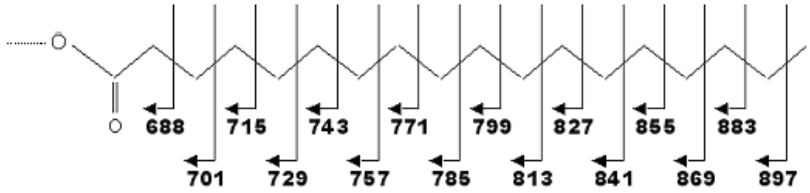

Figure 5. Peak assignments for the product ion spectrum.

Conclusions:

Using the TOF-TOF method, the JMS-S3000 "Spiral-TOF" can acquire HE-CID product ion spectra that show clear CRF mass spectral patterns. Therefore, the structural analyses of compounds like tristearin are easily performed using this technique.

References:

1) Kubo, A., et al., JASMS, 2012. in press.

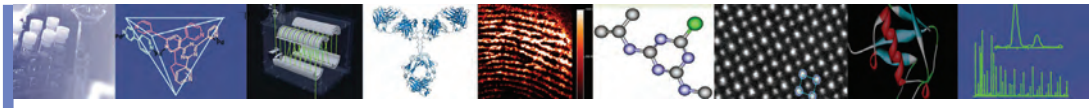

SpiralTOF-TOF

Structural Analysis of Triolein

Introduction:

The JMS-S3000 "SpiralTOF™" is a MALDI-TOF MS that uses an innovative spiral ion optical system to achieve the highest resolution currently available for a MALDI instrument. Additionally, this system can be equipped with a TOF-TOF option that can acquire high-energy collision-induced dissociation (HE-CID) product ion spectra for monoisotopically selected precursor ions. The resulting HE-CID product ion spectra provide detailed structural information about compounds like triglycerides by means of charge-remote fragmentation (CRF).[1] In this work, we report the structural analysis of triolein, a triglyceride that contains 3 oleic acid moieties (Fig. 1), by using HE-CID capabilities of the SpiralTOF-TOF.

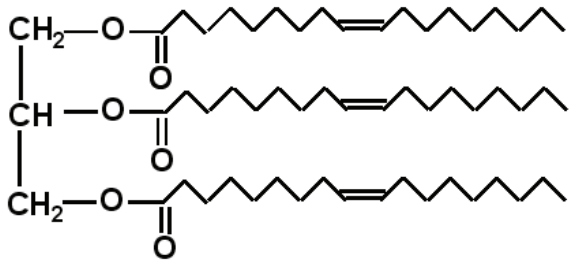

Figure 1. Structure of triolein.

Results and Discussion:

The sample was dissolved with NaI in methanol to promote Na^+ adduct formation. PEG 1000 was used as an external calibration standard. Initially, the sample was measured in Spiral mode and showed a signal at *m/z* 907.7782 (Fig. 2). This ion was consistent with the expected $[M+Na]^+$ calculated mass of 907.7725. Next, the product ion spectrum for this peak was acquired using the TOF-TOF mode (Fig. 3). The resulting mass spectrum showed a fragmentation pattern consistent with the occurrence of CRF. Fig. 4 shows the enlarged *m/z* 600-920 mass range in which the labeled peaks are reflected in the structure shown in Fig. 5. Each of the major peaks between *m/z* 684-753 and between *m/z* 807-821 (except *m/z* 808) shows a difference of 14Da which is consistent with successive losses of CH_2 along the oleic acid backbone. However, the *m/z* 808, which is 1Da from *m/z* 807, is a peak that specifically appears when unsaturated bonds are present in the structure.[2] Additionally, the low intensity peaks between *m/z* 753-807 also confirm the presence of the unsaturated bonds at this position. As noted previously, all of these product ion peaks are consistent with CRF occurring along an oleic acid branch within triolein.

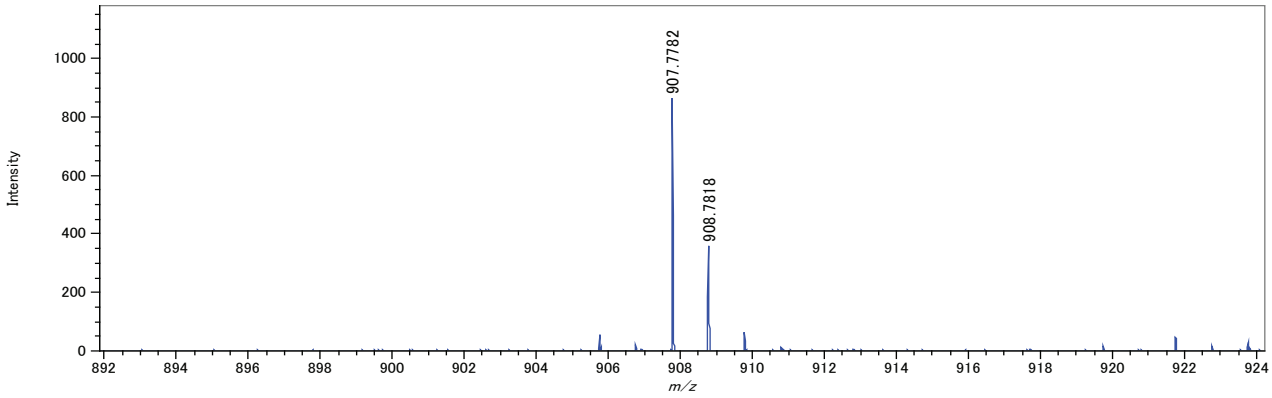

Figure 2. Mass spectrum for the sodium adduct of triolein.

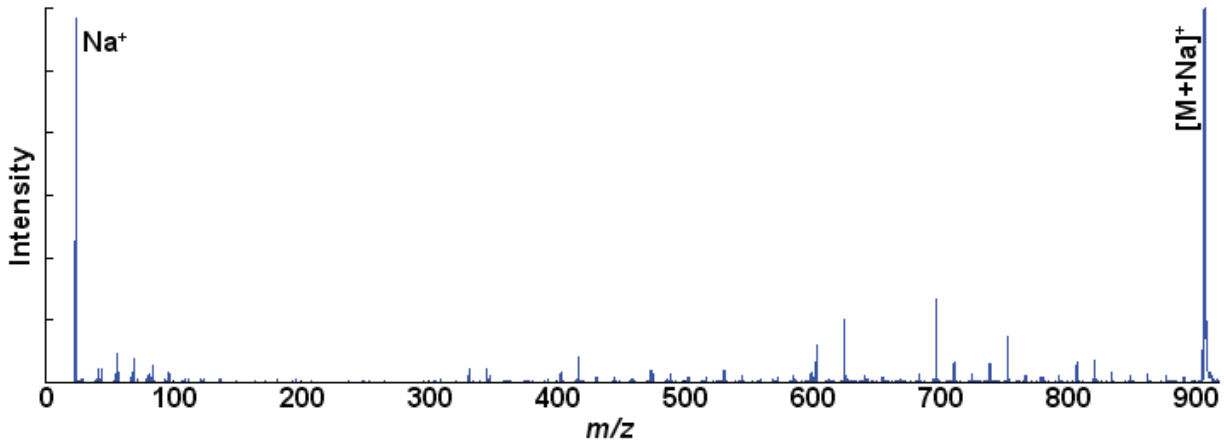

Figure 3. Product ion spectrum for the sodium adduct of triolein.

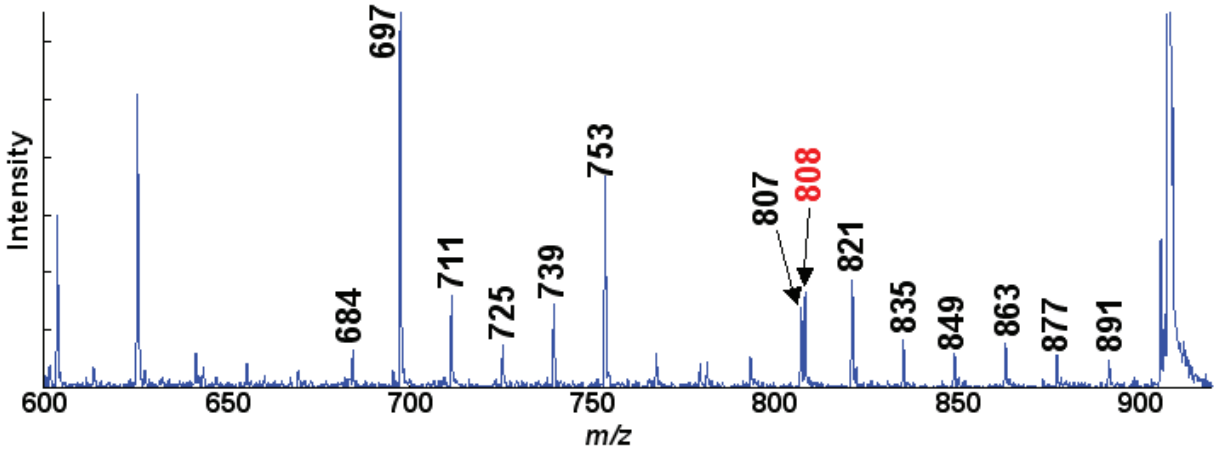

Figure 4. Product ion spectrum for the sodium adduct of triolein (enlarged between *m/z* 600-920).

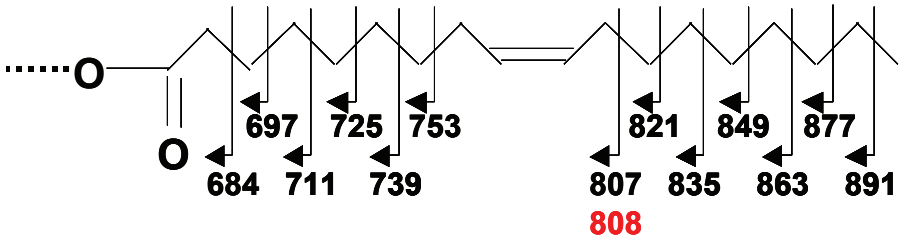

Figure 5. Peak assignments for the product ion spectrum.

Conclusions:

The data for triolein demonstrates that the JMS-S3000 "SpiralTOF" can acquire HE-CID product ion spectra with clear CRF mass spectral patterns. Additionally, this method allows for easy determination of unsaturated bond locations in the carbon chains.

References:

1) Kubo, A., et al., JASMS, 2012. in press.
2) N. Akimoto, *Journal of the Mass Spectrometry Society of Japan* 46 (1998) 228.

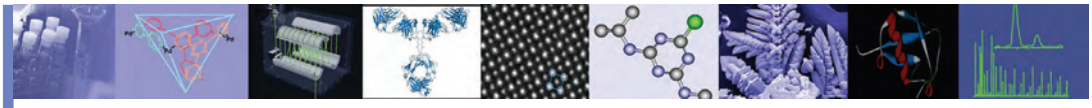

SpiralTOF-TOF

Structural Analysis of Oxidized Triolein

Introduction:
In previous work, we showed that the JEOL SpiralTOF-TOF system's high-energy collision-induced dissociation (HE-CID) is useful for the structural analysis of triglycerides.[1] The resulting HE-CID mass spectra provided detailed information about the fatty acid moieties such as the positions of double bonds, branching, hydroxylation, and oxidation by means of charge-remote fragmentation (CRF).[2]

In this work, we report the structural analysis of oxidized triglycerides by HE-CID using the SpiralTOF-TOF.

Experimental:
Triolein, a triglyceride with 3 oleic acid moieties (Fig.1), was used in this experiment. The triolein sample was kept at 160°C for 60min so that thermal oxidation would occur. The resulting sample was then dissolved in tetrahydrofuran (THF) at a concentration of 10 mg/mL. 2',4',6'-Trihydroxyacetophenone monohydrate (THAP) was used as the matrix and sodium trifluoroacetate (NaTFA) as the cationizing reagent. The THAP and NaTFA were dissolved in THF at a concentration of 10mg/mL and 1mg/mL, respectively. These two solutions and the sample solution were then mixed 1:1:1 by volume. Afterwards, 0.5 µL of this mixture solution was deposited and dried on the MALDI target plate.

Results:
The MALDI mass spectrum of oxidized triolein is shown in Fig. 2. PEG1000 was used as an external calibrant. A series of sodiated peaks were observed for non-oxidized (*m/z* 907), mono-oxidized (*m/z* 923), di-oxidized (*m/z* 939), and tri-oxidized (*m/z* 955) triolein. These results were supported by elemental composition calculations that showed a mass accuracy of < 2 ppm for each ion.

The product-ion spectra for *m/z* 907 and *m/z* 923 are shown in Fig. 3. Many product-ions caused by CRF were observed which simplified the analysis of each structure. The A, B, J2, and G ions in the product-ion spectrum for *m/z* 923 were shifted by 16 Da when compared to the product-ion spectrum for *m/z* 907. An enlarged product-ion spectrum for *m/z* 923 is shown in Fig. 4. The correlating structures for these ions are based on the structural fragmentation assignments shown in

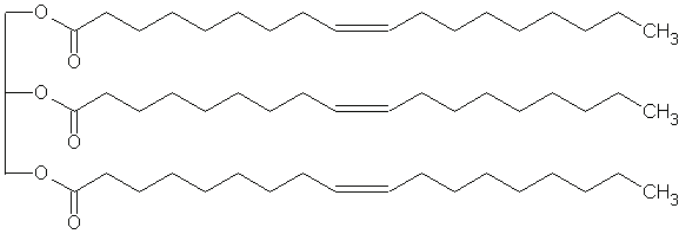

Figure 1. Structure of triolein.

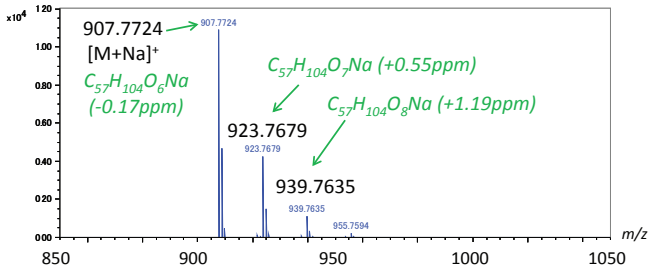

Figure 2. Mass spectrum of triolein after heating at 160°C, 60min.

Fig. 5. These results clearly show that the high-energy CID product ions collected by SpiralTOF-TOF provide a very straightforward pattern for identifying the sample structure and the position of oxidation.

Conclusion:
In this study we demonstrated the structural analysis of an oxidized triglyceride using the high-energy CID available on the MALDI-SpiralTOF-TOF. Additionally, CRF using high-energy CID is a very useful technique for assigning the position of oxidation.

Reference:
1. A.Kubo, et al., Structural analysis of complex lipids using MALDI-TOF-TOF tandem MS with high precursor-ion selectivity. 59th ASMS Conference. 2011, MP240.
2. Cheng, C., Gross, M. L.; Pittenauer, E. Complete structural elucidation of triacylgylcerols by tandem sector mass spectrometry. Anal. Chem. 1998, 70, 4417-4426.

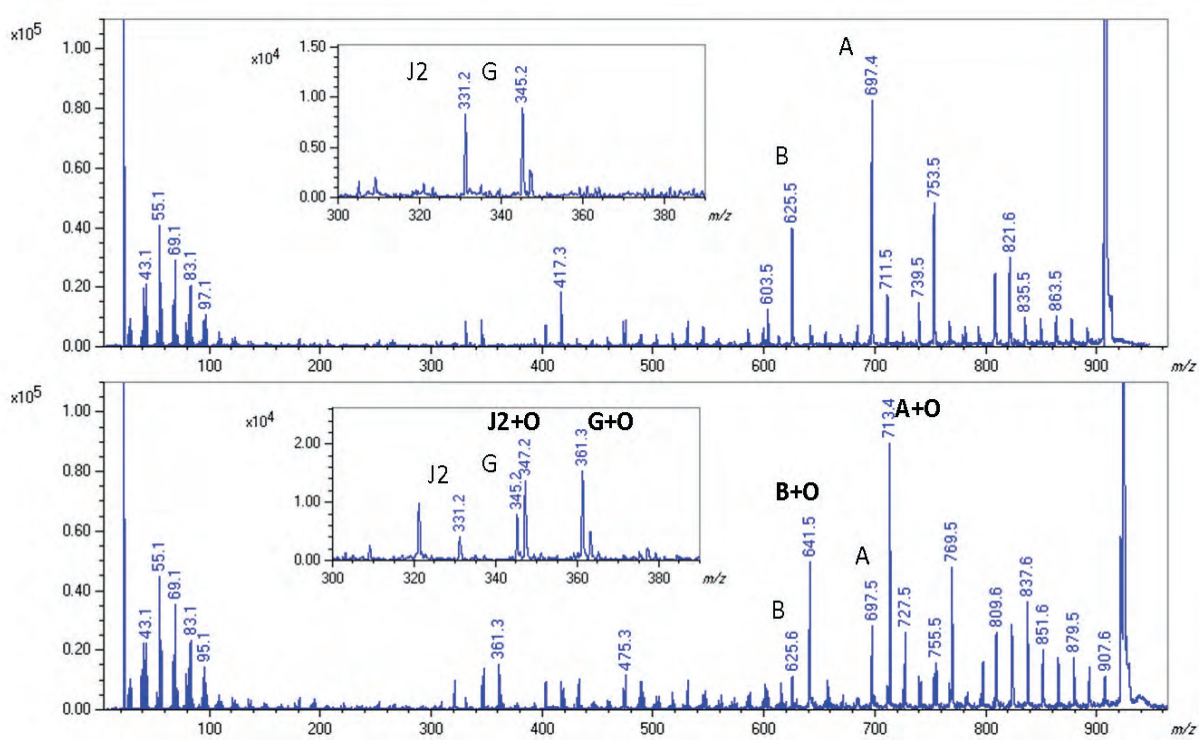

Figure 3. Product ion mass spectrum from *m/z* 907 (top) and *m/z* 923.

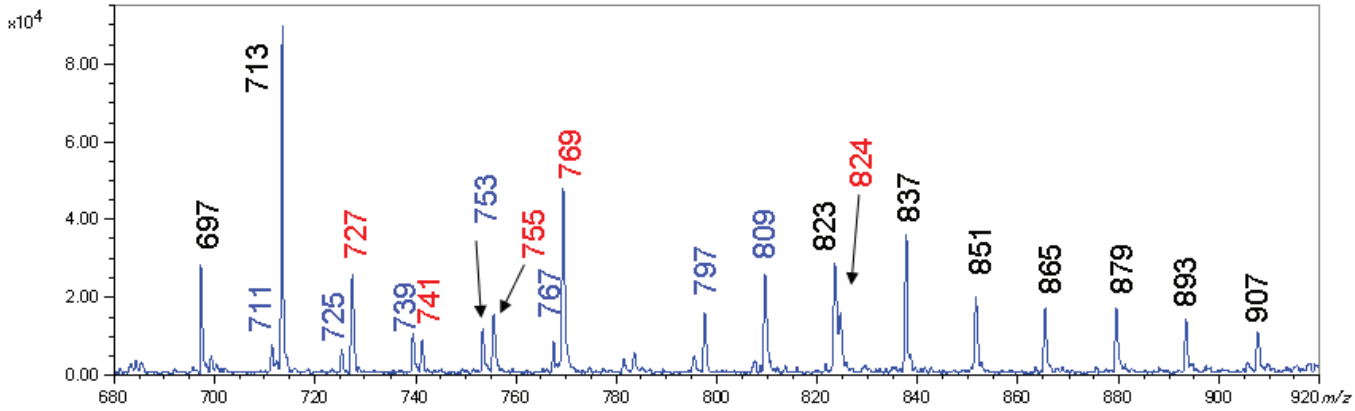

Figure 4. Product ion spectrum from *m/z* 923 (enlarged between *m/z* 680 and *m/z* 920).

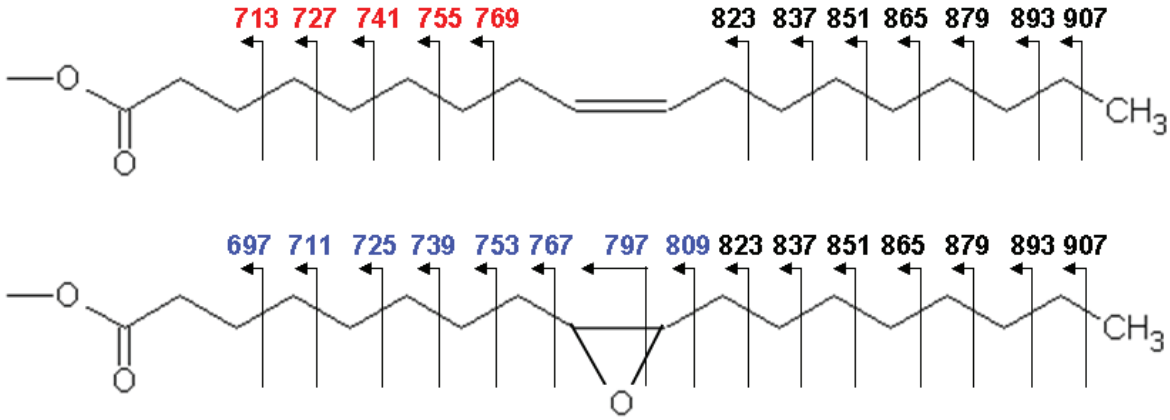

Figure.5. Assignment of product ions from *m/z* 923.

SpiralTOF™

Introduction of the JMS-S3000 SpiralTOF™

Analysis of Bovine Serum Albumin

Introduction:

The JMS-S3000 "SpiralTOF™" is a MALDI-TOF MS incorporating an innovative SpiralTOF™ ion optics system (Fig. 1). JEOL's patented technology[1] achieves a spiral ion trajectory of 17m within a compact 1m space. The ions are sent through four sets of layered toroidal electric fields, which are implemented by four pairs of cylindrical electrodes and nine Matsuda plates that are incorporated within every pair of cylindrical electrodes. Ions are accelerated to 20 kV in the ion source and fly sequentially through the layered toriodal electric fields to reach the detector (Fig. 2). With the extended flight distance, the JMS-S3000 SpiralTOF™ achieves high mass resolving power and high mass accuracy over a wide mass range.

However, ions with a very short lifetime or that undergo spontaneous dissociation during their flight (e.g., protonated molecules of high-mass proteins, multiply-phosphorylated peptides, etc.) cannot be detected by either the SpiralTOF™ or a conventional reflectron TOF. Considering the wide application of the MALDI technique, a mass analyzer that can detect such short-lived ions is necessary in addition to the SpiralTOF™. A Linear TOF option is available for the JMS-S3000 in order to satisfy this requirement (Fig. 2). In this application note, the analysis of the tryptic digest of bovine serum albumin (BSA) is shown as a Spiral mode example while the analysis of intact BSA is shown as a Linear mode example.

Figure 1. JMS-S3000 SpiralTOF™.

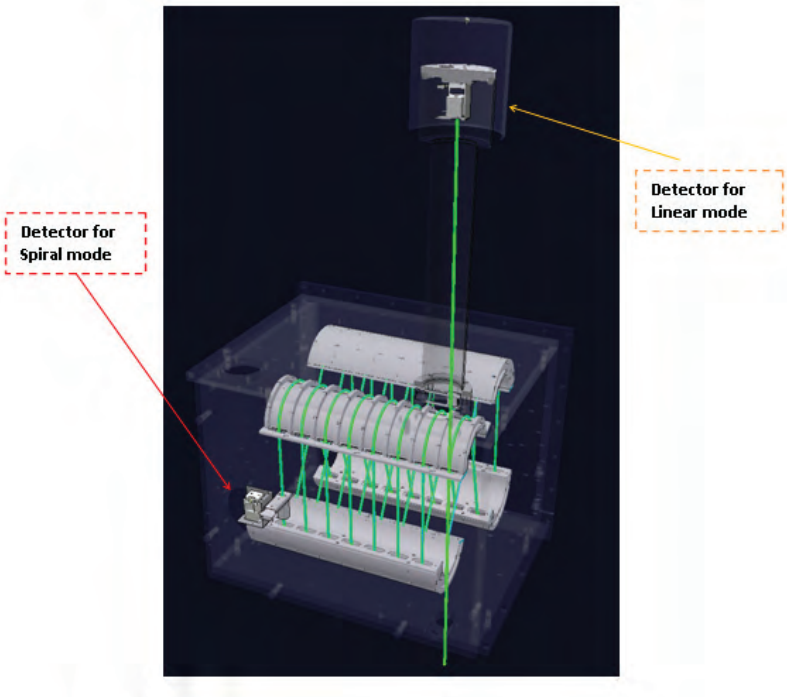

Figure 2. Ion trajectories of the JMS-S3000 SpiralTOF™.

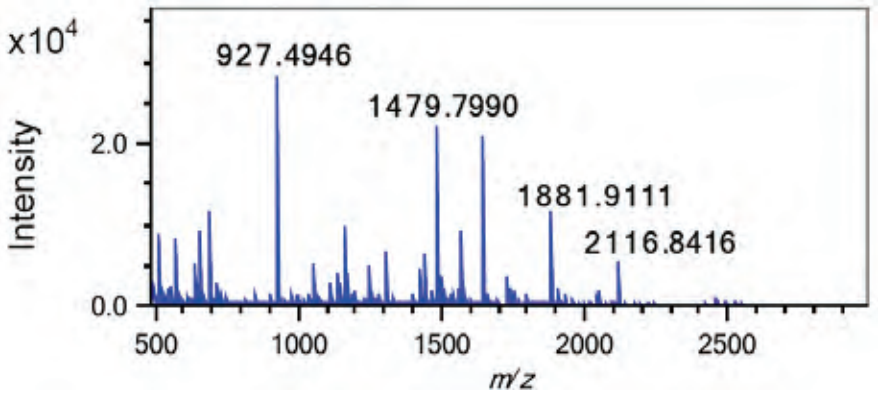

Figure 3. Mass spectrum for the tryptic digest of BSA (equivalent to 25 fmol of the protein).

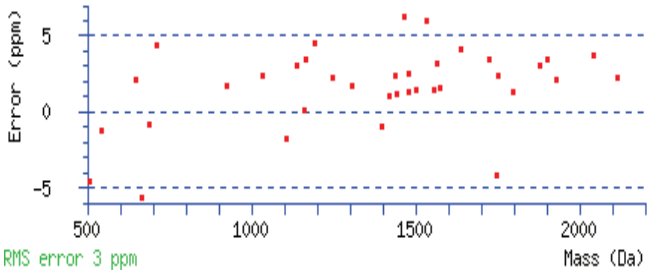

Figure 4. Mass error plot from the MASCOT PMF search result.

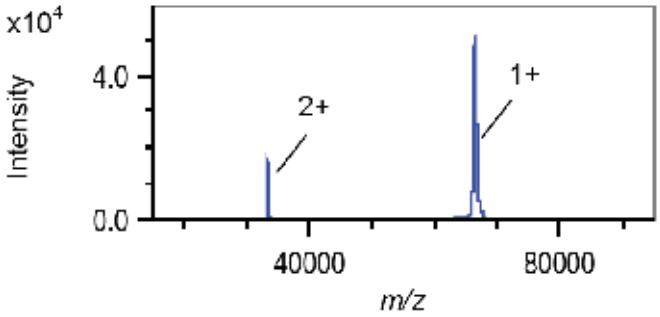

Figure 5. Mass spectrum of the intact BSA protein (2.5 pmol).

Methods:

The tryptic digest of BSA was analyzed in SpiralTOF mode. An external mass calibration was used for this data. The intact BSA was analyzed using the Linear TOF mode. The data was acquired automatically by using the msTornado™ Control, which is the instrument control and data acquisition software for the JMS-S3000.

Results and discussion:

The mass spectrum of the tryptic digest equivalent to 25 fmol of BSA is shown in Fig. 3. The peak list from this mass spectrum was submitted to the MASCOT peptide mass fingerprint (PMF) search, and the protein was identified as BSA. The mass error plot of all matched peptides is shown in Fig. 4. The RMS error was 3 ppm. The mass spectrum of the intact BSA acquired in Linear mode is shown in Fig. 5. Single- and double-charge protonated molecular ion peaks were observed at the *m/z* values expected for the primary structure of this protein.

Conclusions:

A mass spectrum of the tryptic digest of BSA with very high mass accuracy was obtained using Spiral mode. Using the MASCOT PMF search method, a peptide mass tolerance set as narrow as 10 ppm can lead to highly reliable protein identification with very few false positives. Additionally, the molecular weight of an intact protein was readily obtained by using the JMS-S3000 Linear mode.

References:

[1] US patent US7504620, Japanese patent application JP2006-12782

SpiralTOF-TOF

High-Energy CID Analysis of Bovine Serum Albumin

Introduction

The JMS-S3000 "SpiralTOF™" is a MALDI-TOFMS that uses an innovative SpiralTOF ion optics system to achieve the highest resolution currently available for a MALDI instrument (Fig. 1 and 2). Additionally, this system can be equipped with a TOF-TOF option that can acquire high-energy collision-induced dissociation (CID) product ion spectra for monoisotopically selected precursor ions. The distance to the ion gate is 15 m, more than one order of magnitude longer than that of conventional MALDI TOF-TOF instruments, thus allowing the monoisotopic selection of the precursor ion. The second TOFMS incorporates a re-acceleration mechanism and an offset parabolic reflectron, another innovative ion optical system developed by JEOL. This unique design enables the seamless observation of product ions ranging from very low *m/z* up to that of the precursor ion.

In a previous application note[1], we reported the analysis of bovine serum albumin (BSA) by Spiral and Linear modes. In this work, we show the analytical result for BSA by using the JMS-S3000 "SpiralTOF™" with the TOF-TOF option.

Results and Discussion

As a starting point, the tryptic digest of BSA (tBSA) was analyzed using just the Spiral mode. For the calibration step, a peptide mixture was used as an external mass calibrant, which resulted in an RMS error of 4 ppm. Subsequently, the mass spectrum peak list for this sample was submitted to the MASCOT (Marix Science, Ltd.)

Figure 1. JMS-S3000 SpiralTOF with TOF-TOF attachment.

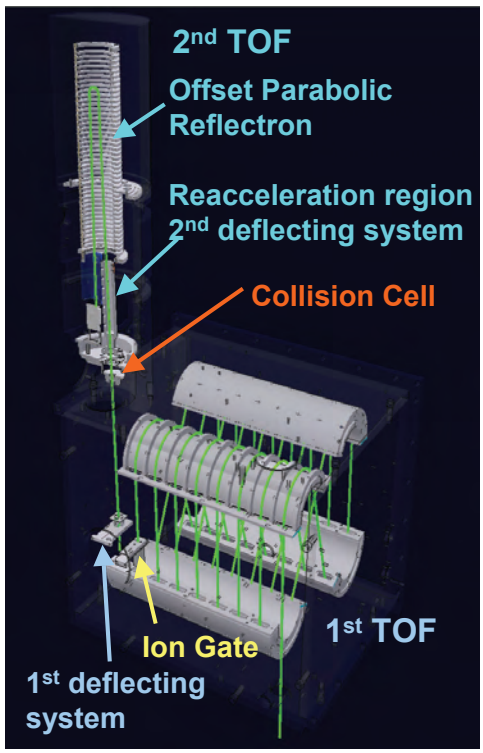

Figure 2. Ion trajectory of Spiral-TOF and TOF-TOF attachment.

peptide mass fingerprint search, and the protein was identified as BSA. These results are in very good agreement with the results ob- tained previously for Spiral mode.[1]

Next, the 10 highest intensity ions in the tBSA mass spectrum were selected as the precursor ions for auto- matic measurement using the TOF-TOF option. The product ion spectra for *m/z* 927.5, 1439.8, and 1567.7 shown in Fig.3 had an immonium ion along with the a-ion, d-ion, and w-ion series. These spectra along with the other 7 product ion spectra were then submitted to the MASCOT MS/MS Ion Search, and the protein was identified as BSA (see Fig.4).

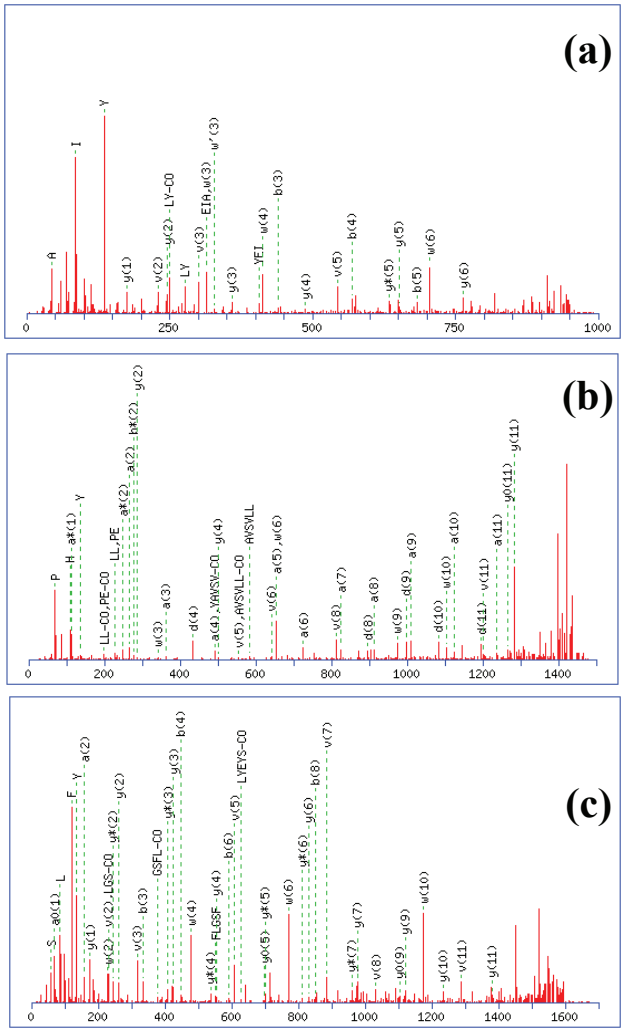

Figure 3. Product ion spectra for *m/z* (a) 927.5, (b) 1439.8, and (c) 1567.7.

Conclusions

The high resolution tBSA mass spectrum measured using Spiral mode was easily identified using the MASCOT peptide mass fingerprint method, even with a peptide mass tolerance set as narrow as 10 ppm (not shown in this note). Additionally, the high energy CID of the 10 highest intensity monoisotopically selected peaks mea- sured using the SpiralTOF-TOF mode produced product ion spectra that readily identified BSA as the protein through the MASCOT MS/MS Ion Search.

Reference

1) www.jeolusa.com/DesktopModules/Bring2mind/DMX/Download.aspx?EntryId=833&PortalId=2&DownloadMethod=attachment

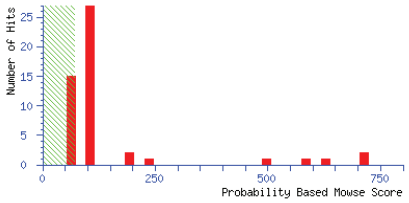

Protein Summary Report

Format As: Protein Summary (deprecated) — Help
Significance threshold p< 0.05 — Max. number of hits AUTO
Standard scoring / MudPIT scoring — Ions score or expect cut-off 0 — Show su
Show pop-ups / Suppress pop-ups — Sort unassigned Decreasing Score — Require
Re-Search All — Search Unmatched

Index

	Accession	Mass	Score	Description
1.	gi|30794280	71309	714	albumin [Bos taurus]
2.	gi|1351907	71279	696	Serum albumin precursor (Allergen Bos d 6) (BSA)
3.	gi|74267962	71221	614	ALB protein [Bos taurus]
4.	gi|229552	68118	576	albumin
5.	gi|76445989	55514	510	serum albumin [Bos indicus]

Figure 4. MASCOT MS/MS Ion search result of tBSA by TOF-TOF mode.

SpiralTOF-TOF

Structural Analysis of a High Molecular Weight Peptide

Introduction:

The JMS-S3000 SpiralTOF™ is a MALDI-TOF MS that uses an innovative spiral ion optics system to achieve the highest resolution currently available for a MALDI instrument. Additionally, the JMS-S3000 is available with a TOF-TOF option that acquires high-energy collision-induced dissociation (CID) product-ion spectra for monoisotopically selected precursor ions. In this work, we analyzed a high molecular weight peptide by using the JMS-S3000 SpiralTOF with the TOF-TOF option.

Experimental:

Sample: ACTH18-39 (Arg-Pro-Val-Lys-Val-Tyr-Pro-Asn-Gly-Ala-Glu-Asp-Glu-Ser-Ala-Glu-Ala-Phe-Pro-Leu-Glu-Phe)

Matrix: α-Cyano-4-hydroxycinnamic acid (CHCA)

Results and Discussion:

The high-energy CID product-ion spectrum for protonated ACTH18-39 $[M+H]^+$ (*m/z* 2456.2) is shown in Fig.1. Each product ion was labeled using the Biemann convention (Fig.2) in which the a-, b-, and d-ion series are fragments generated from the N terminus of the ACTH18-39 molecule. The SpiralTOF MS/MS data in Fig. 1 show that the sequence information is clearly represented by the a-ion series from a2 to a21. The immonium ions (Fig.3) and the d-ion series (produced by fragmentation of the a-ion series) were also observed in the mass spectrum.

Conclusions:

The JMS-S3000 SpiralTOF with the TOF-TOF mode produced high energy CID product ion spectra that clearly identified the sequence for the high molecular weight peptide ACTH18-39.

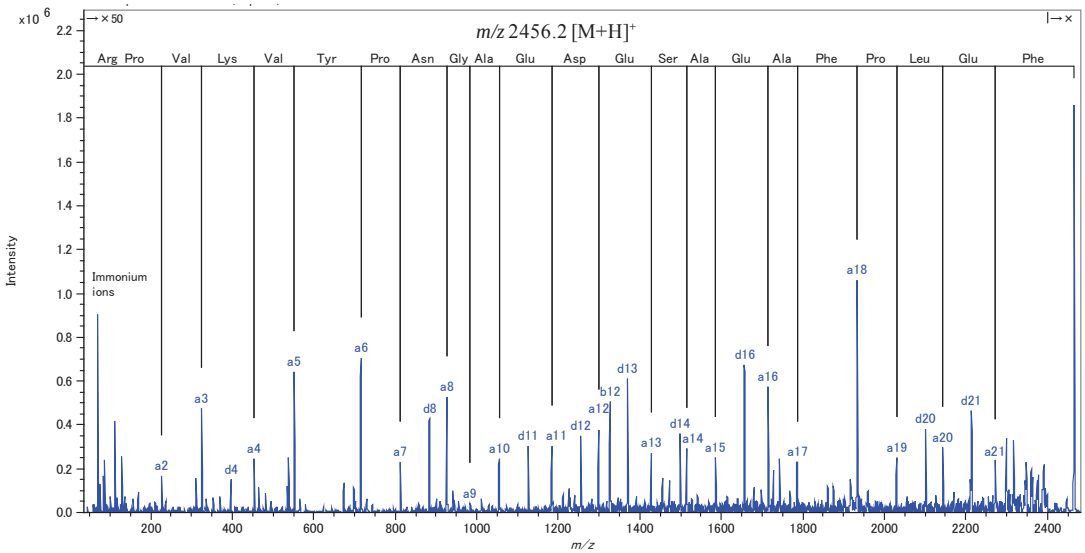

ACTH18-39 Arg-Pro-Val-Lys-Val-Tyr-Pro-Asn-Gly-Ala-Glu-Asp-Glu-Ser-Ala-Glu-Ala-Phe-Pro-Leu-Glu-Phe

Figure 1. Product ion spectrum of ACTH18-39 (*m/z* 2456.2, $[M+H]^+$).

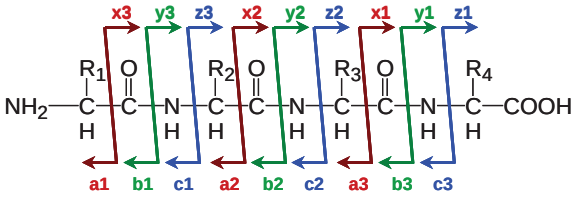

Figure 2. Fragment ion series.

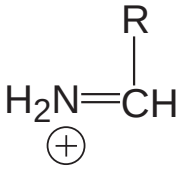

Figure 3. Immonium ion.

This page intentionally left blank for layout purpose.

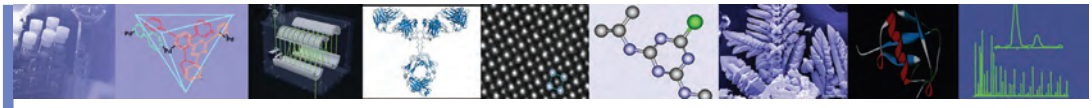

Applications Note

SpiralTOF-TOF

Analysis of Phosphopeptide Using TOF-TOF

Introduction:
Phosphorylation is a type of post-translational modification of proteins that is used for the intracellular signal transduction in a wide range of living species. For this reason, it is very important to determine where the protein (amino acid) is phosphorylated. In this work, we measure a monophosphopeptide (FQ pS EEQQQTEDELQDK) that was obtained from the tryptic digestion of β-casein (Bovine) using the TOF-TOF option that is available for the JEOL SpiralTOF™ system.

Experimental:
The monophosphopeptide sample was dissolved in water containing 0.1% trifluoroacetic acid at a concentration of 10 pmol/µL. The matrix for this analysis was made by mixing 150 µL of CHCA (Methanol) at a concentration 30 mg/mL with 35 mg of 3-Aminoquinoline. Next, the monophosphopeptide sample solution and matrix solution were mixed together 1:1 by volume. Afterwards, 0.5 µL of this mixture was placed on the MALDI target plate (2.5 pmol/spot). Finally, the sample spot was measured using the TOF-TOF option available on the JMS-S3000 SpiralTOF MS system.

Results & discussion:
The MALDI-TOF mass spectrum of the monophosphopeptide is shown in Figure 1. The peak corresponding to the protonated molecule for this compound was observed at *m/z* 2061.8. The monoisotopic peak was then selected for high-energy CID TOF-TOF analysis. The resulting product-ion mass spectrum for this protonated molecule is shown in Figure 2. Because Lysine is present at the C-terminal for basic amino acids, we were able to observe the y-ion series generated by cleavage of the main-chain peptide bonds. Additionally, the w-ion series generated by elimination of the side-chains from the corresponding y-ions were observed.

Generally, the identification of the phosphorylation position using low-energy CID is considered very difficult because the phosphate group is lost before the cleavage of the main-chain peptide bond [1]. In contrast, high-energy CID does provide information about the location of phosphorylated amino acids because the y- and w- ion series were observed without the loss of the phosphate group (Figure 2) [2]. In Figure 2, the mass difference of the y13-ion and the y14-ion is 167u, which shows the position of the phosphorylated serine.

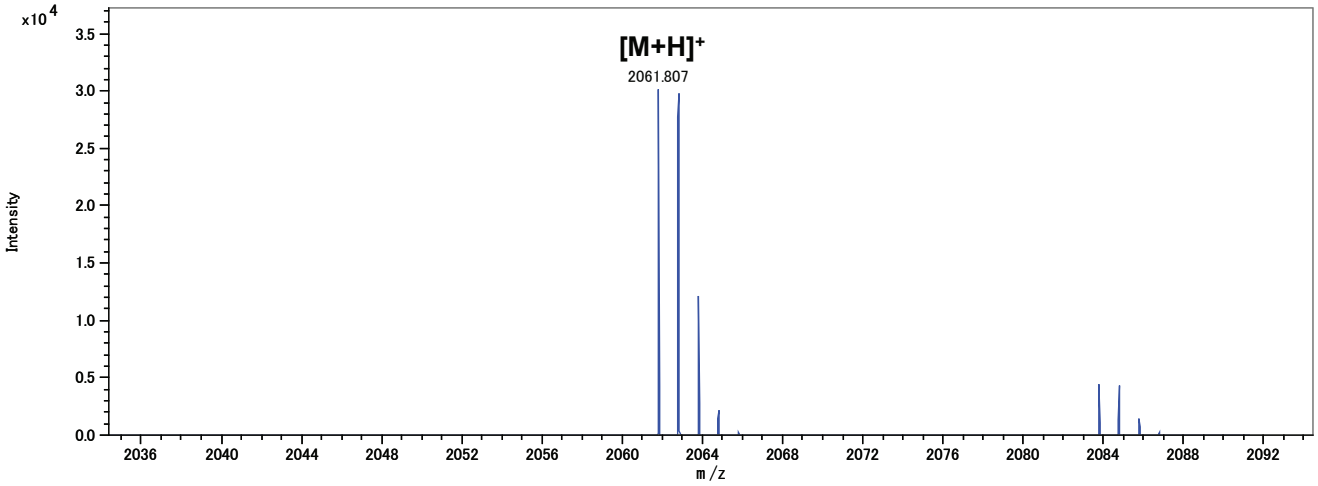

Figure 1. Mass spectrum of the monophosphopeptide.

MS-120308A

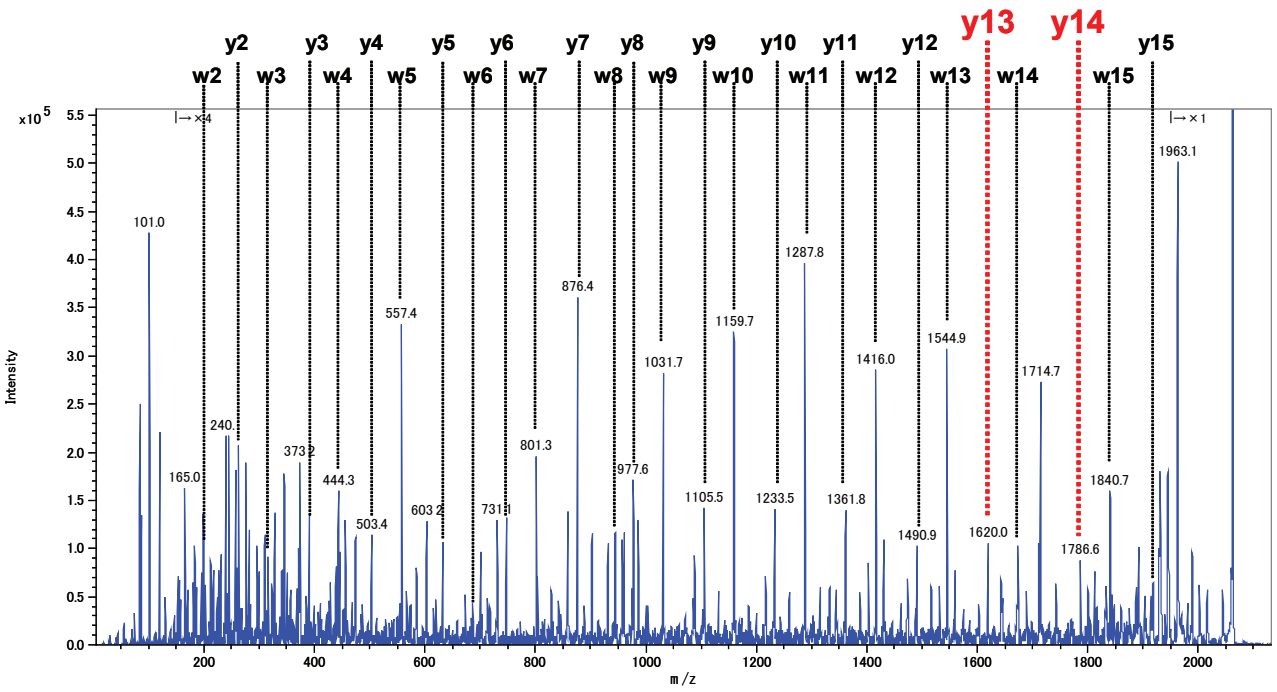

Figure 2. High-energy CID product ion spectrum of the monophosphopeptide.

Conclusions:

As this work shows, we can identify the location of phosphorylated amino acids in a peptide by using the high-energy CID TOF-TOF option available for the JMS-S3000 SpiralTOF system. Furthermore, this data shows the possibility of using this instrument for the primary structural analysis of peptides, particularly for de novo sequencing.

References:

[1] A. Stensballe, O.N. Jensen, J.V. Olsen, K.F. Haselmann, R.A. Zubarev, Rapid Communications in Mass Spectrometry 14 (2000) 1793.

[2] S. Shimma, H. Nagao, A.E. Giannakopulos, S. Hayakawa, K. Awazu, M. Toyoda, Journal of Mass Spectrometry 43 (2008) 535.

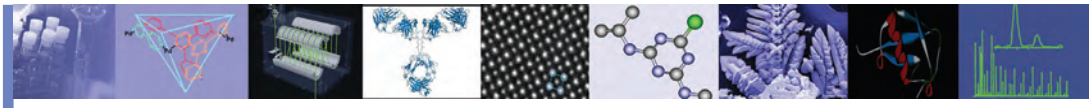

Applications Note

SpiralTOF-TOF

Distinguishing Lysine and Glutamine in a Peptide

Introduction:

Lysine and glutamine are not easily distinguished by the most common approaches to peptide sequencing which involve mass spectrometers with low to moderate resolving power and low-energy collision-induced dissociation (CID). Lysine ($C_6H_{14}N_2O_2$ with a mass of 146.1055 u) and glutamine ($C_5H_{10}N_2O_3$ with a mass of 146.0691) differ by only 0.036 u. In this study, we demonstrate the measurement of a mixture of Substance P and a synthesized peptide (3-Gln) with glutamine substituted for lysine in the Susbstance P sequence. Because the mass difference between Substance P and 3-Gln is 0.036 u, a resolving power of greater than 37,000 is required to separate each peptide. Additionally, we show that the TOF-TOF mode can be used to distinguish lysine and glutamine in these peptides by comparing the peak area ratio between a ions and d ions in the high-energy CID mass spectra.

Experimental:

Substance P standard was obtained from Sigma-Aldrich. The 3-Gln sample was synthesized and then provided by Hayashi Kasei.

1. Substance P, Arg-Pro-Lys-Pro-Gln-Gln-Phe-Phe-Leu-Met (Sigma-Aldrich)
2. 3-Gln, Arg-Pro-Gln-Pro-Gln-Gln-Phe-Phe-Leu-Met (Hayashi Kasei)

The peptide standard samples were dissolved in water containing 0.1% trifluoroacetic acid (TFA) at a concentration of 10 pmol/µL. α-Cyano-4-hydroxycinnamic acid (CHCA) was used as the matrix and was dissolved in 1:1 water/acetonitrile containing 0.1% TFA. Next, the peptide standard solution and CHCA solution were mixed together 1:1 by volume. Afterwards, 0.5 µL of this mixture was placed on the MALDI target plate (2.5 pmol/spot). Finally, the dried sample was measured using the SpiralTOF and TOF-TOF option available on the JMS-S3000 SpiralTOF MS system.

Results:

(1) SpiralTOF measurement

The MALDI mass spectra are shown in Figure 1, and expanded mass spectra are shown in Figure 2 for the monoisotopic ion of the protonated molecules $[M + H]^+$. The mass resolving power was approximately 60,000 for each of the $[M + H]^+$ peaks in both substance P and 3-Gln mass spectra. Excellent mass accuracy (less than 10 ppm) was obtained with external calibration in all mass spectra. Additionally, we demonstrated that the high resolving power of the SpiralTOF could separate both components in the mixture.

(2) TOF-TOF measurement

The product-ion mass spectra are shown in Figure 3. In both product-ion spectra, the characteristic a ions and d ions were observed in the high-energy CID. We cannot distinguish lysine and glutamine by mass accuracy and mass resolution in the product-ion mass spectra measured in TOF-TOF mode. However, we can identify lysine and glutamine by examining the a3/d3 ion intensities ratio [1]. The d3 ion intensity is higher than a3 ion for glutamine due to the stable ejected radical ($\bullet CH_2–CO–NH_2$). Conversely, the d3 ion intensity is lower than a3 ion for lysine due to the unstable ejected radical ($\bullet CH_2–CH_2–CH_2–NH_2$) [2]. This information clearly identifies the presence of lysine in Substance P and glutamine in 3-Gln, respectively, as the third amino acid in each peptide sequence.

MS-MS-0329A

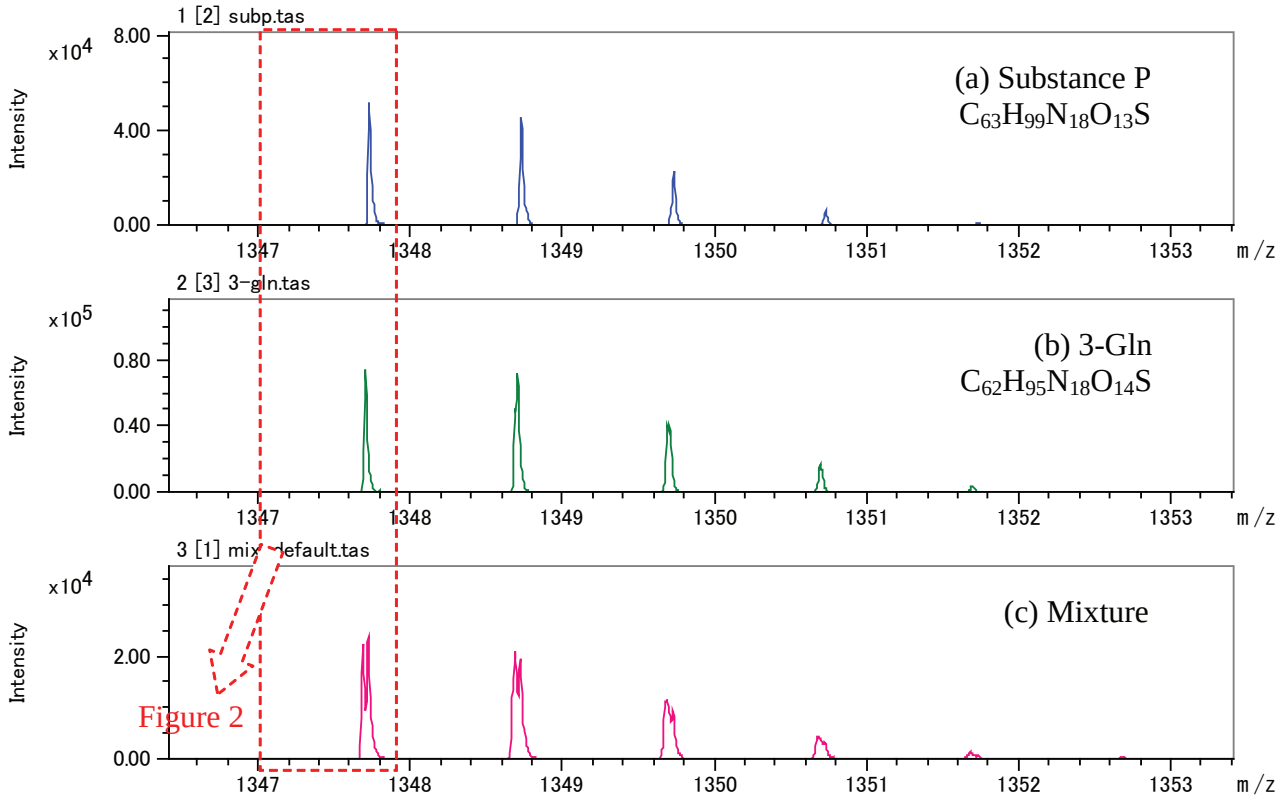

Figure 1. MALDI mass spectra of peptides: (a) Substance P, (b) 3-Gln, (c) Mixture

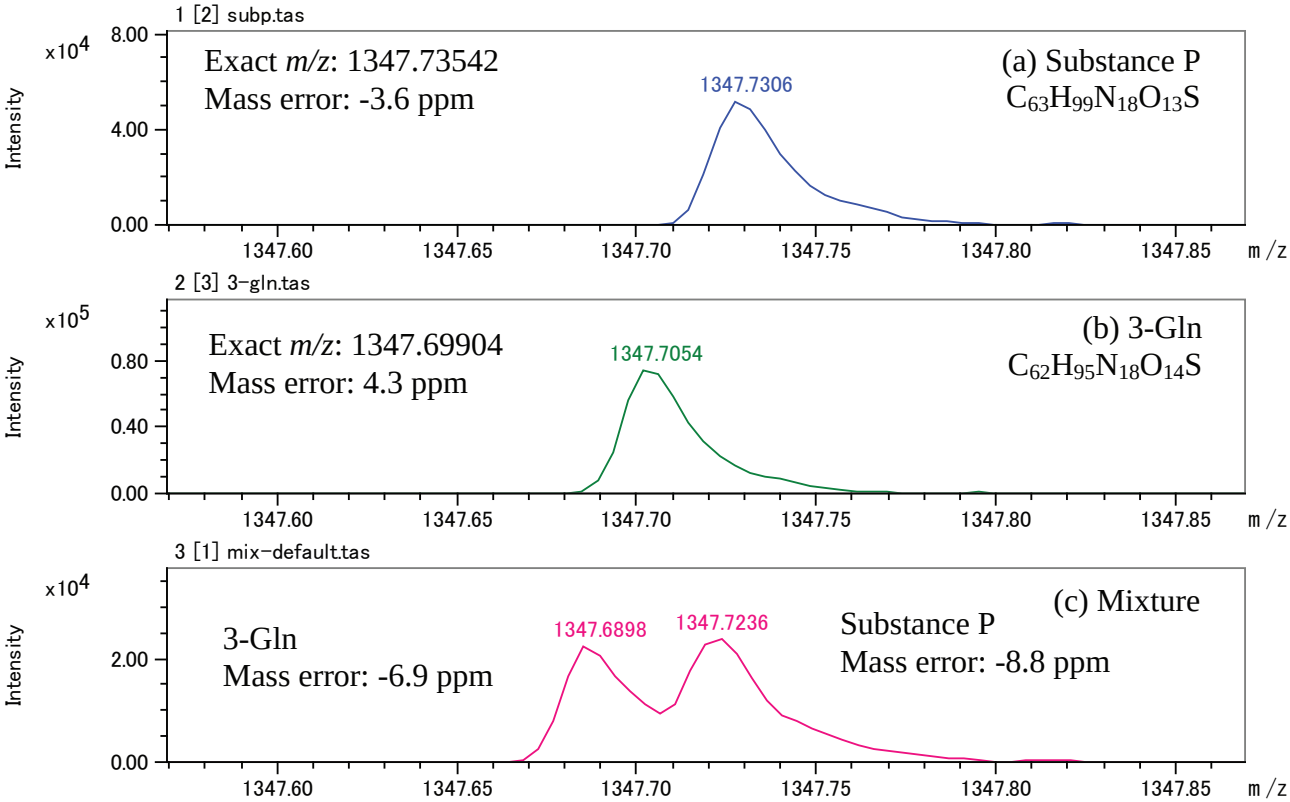

Figure 2. Expanded MALDI mass spectra showing the [M + H]+ monoisotopic ions for (a) Substance P, (b) 3-Gln, and the (c) mixture

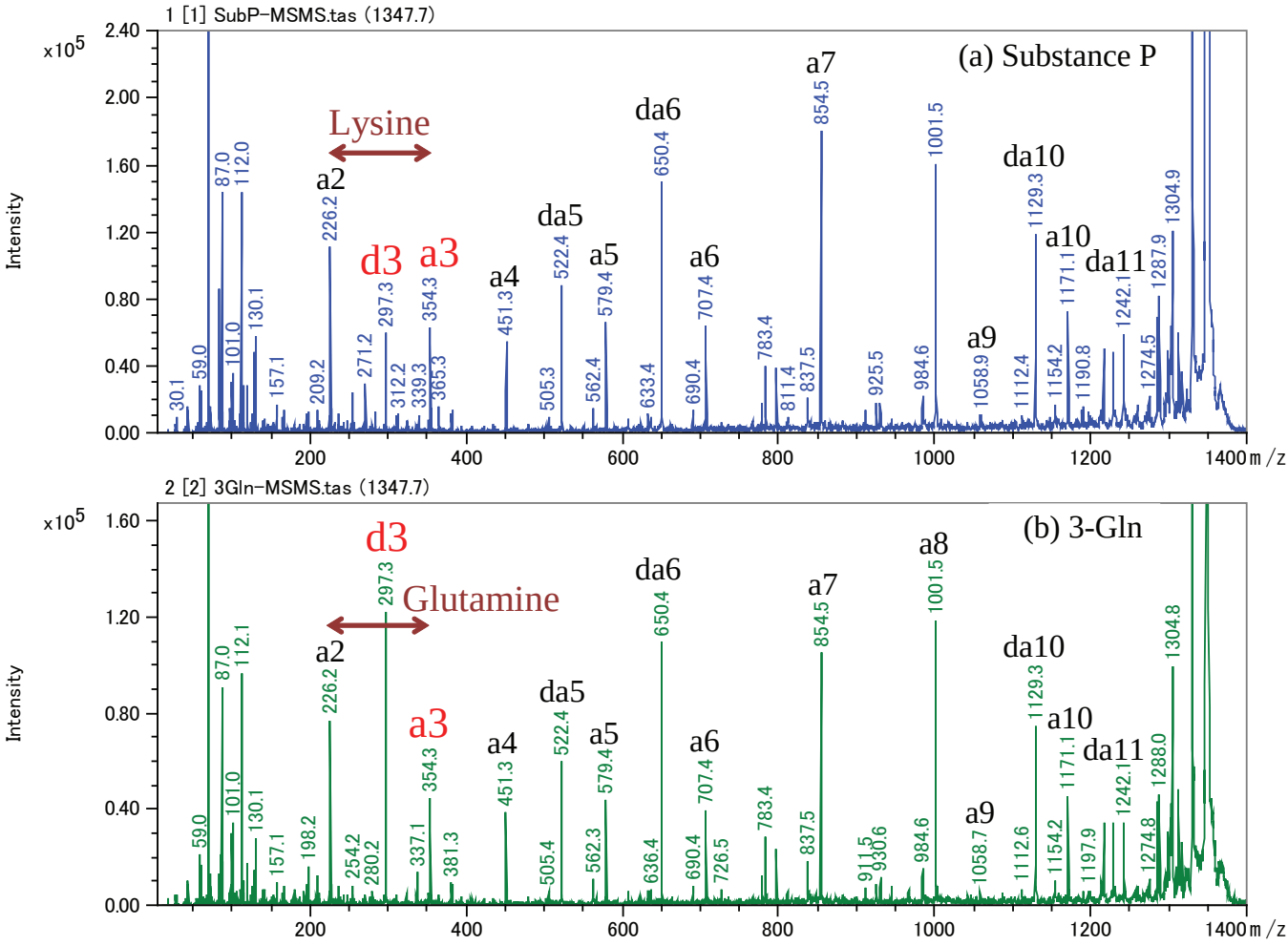

Figure 3. TOF-TOF product ion spectra for (a) Substance P and (b) 3-Gln

Conclusion:

In this study we demonstrated that the JEOL SpiralTOF MALDI mass spectrometer can distinguish lysine and glutamine in a peptide.

SpiralTOF mode provides

- Ultra high resolving power sufficient to separate isobaric ions (0.036 u in this study)
- Excellent mass accuracy with external calibration (less than 10 ppm)

TOF-TOF mode provides

- High-energy (20 kV) CID
- Lysine and glutamine can be distinguished by examining the a3/d3 peak area ratio differences

Acknowledgement:

These data were obtained through collaborative research between Mass Spectrometry Group, Department of Physics, Graduate School of Science, Osaka University and JEOL Ltd.

Reference:

[1] R.S. Johnson, S.A. Martin, K. Biemann, *International Journal of Mass Spectrometry and Ion Processes* 86 (1988) 137.

[2] M. Toyoda, A. E. Giannakopulos, A. W. Colburn, O. J. Derrick, *Review of Scientific Instuments* , 78 (2007) 074101.

This page intentionally left blank for layout purpose.

SpiralTOF-TOF

Comparison of the JMS-S3000 SpiralTOF-TOF and a 4-Sector Tandem Double-Focusing Mass Spectrometer

Introduction

The JMS-3000 SpiralTOF™ has an optional TOF-TOF mode that features monoisotopic precursor ion selectivity, elimination of post source decay (PSD) ions, and high energy collision induced dissociation (CID). The JMS-700T MStation four-sector tandem double focusing mass spectrometer, although featuring a different analyzer and ionization techniques, has similar capabilities that have been previously used for a wide variety of applications including the structural analysis of complex biological molecules.

In this work, we compare the SpiralTOF-TOF with the MStation four sector tandem double focusing mass spectrometer using the same sample for MS/MS analysis.

Experimental

The sample analyzed by both systems was renin substrate tetradecapeptide (porcine), a peptide having an amino-acid sequence of DRVYIHPFHLLVYS. Table 1 shows the measurement conditions and sample sizes used for both systems.

	JMS-S3000	JMS-700T
Ionization method	MALDI	FAB (Xe 6 kV)
Sample quantity	2.5 pmol	1 nmol
Precusor ion	mono isotopic	mono isotopic
Target gas	He	Ar
Matrix	CHCA	Glycerin, NBA
Collision energy	20000 eV	5000 eV

Table 1. Experimental conditions and specifications.

Results and Discussion

The SpiralTOF ion optics with the TOF-TOF option are shown in Fig. 1a. This design allows for the acquisition of high-energy CID product ion spectra for monoisotopically selected precursor ions. This precursor selection is made possible by the fact that the distance to the ion gate is 15 m. Additionally, the second TOF incorporates a re-acceleration mechanism into an offset parabolic reflectron (OPR) which enables the seamless observation of product ions ranging from very low *m/z* up to that of the precursor ion.

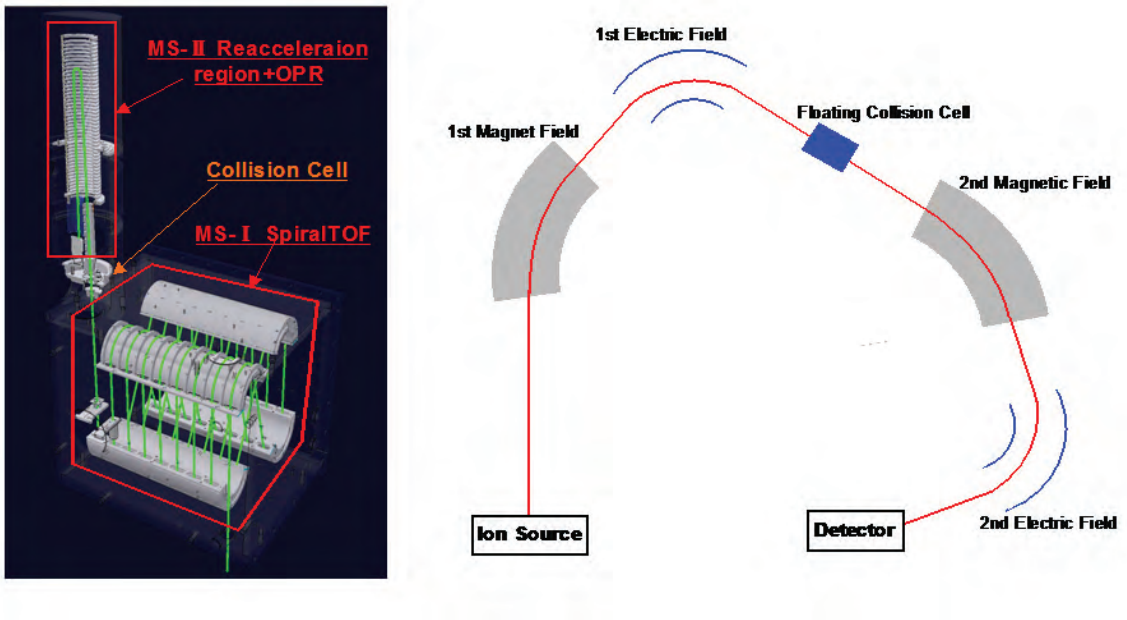

Figure 1. Ion trajectory - Left: JMS-S3000 SpiralTOF , Right: JMS-700T tandem MStation.

The MStation tandem has the ion trajectory shown in Fig. 1b, which also allows the selection of ions that have a specific *m/z* but in this case using the first magnetic and electric fields as the MS1 analyzer. The selected ions then pass into the collision chamber which is floated at a given voltage level to reduce their overall speed before colliding with the collision gas. Subsequently, the resulting product ions are re-accelerated to give them sufficient kinetic energy to be analyzed efficiently by the second magnetic and electric fields.

For comparison, the renin substrate tetradecapeptide (porcine) was analyzed using both systems. Fig. 2 shows the product ion spectra acquired for each system using the $[M+H]^+$ (*m/z* 1758.93) as the precursor ion. Because of the difference between the FAB (Fast Atom Bombardment) and MALDI (Matrix Assisted Laser Desorption/Ionization) ionization techniques, the SpiralTOF-TOF acquired the product ion spectrum using 1/100 less volume than was used to get a comparable spectrum for the MStation. The resulting spectra show the immonium ions and the same pattern of a- and d- series ions which are the characteristic product ions produced by high energy CID. For the product ion spectrum acquired with the MStation in Fig. 2, the floating voltage was set to a slightly high level of 5000 V in order to observe low mass ions efficiently. However, this actually reduced the resolution and transmission rate of the high mass ions. In contrast, the SpiralTOF was able to analyze the full mass range efficiently, as a result of the second accelerator and the OPR not requiring the process of voltage selection for the target mass range.

Conclusions

These results clearly demonstrate that the SpiralTOF-TOF produced the same structural information as a traditional four sector tandem double focusing mass spectrometer. Additionally, the SpiralTOF-TOF required a smaller sample volume and a simpler analysis procedure to produce comparable product ion spectra.

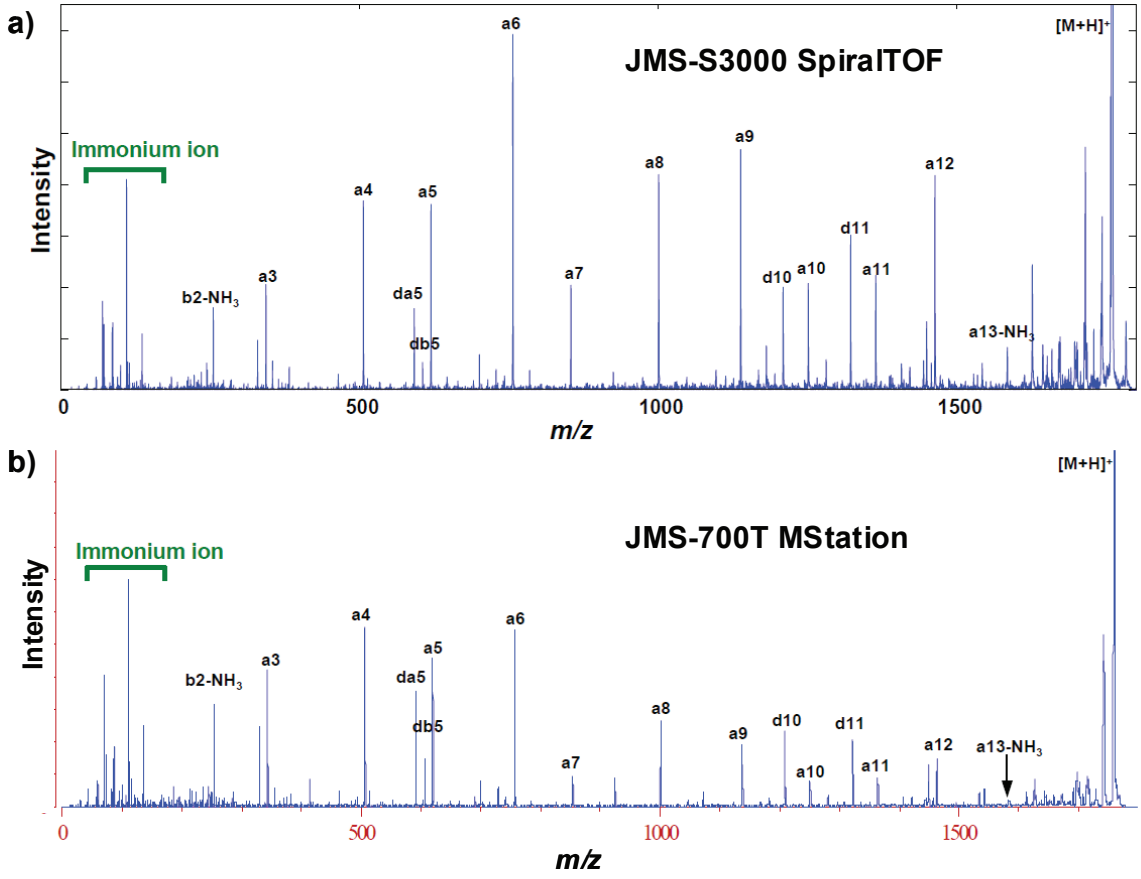

Figure 2. Product ion spectra of Renin-substrate tetradecapeptide by a) JMS-S3000 SpiralTOF-TOF and b) JMS-700T tandem MStation.

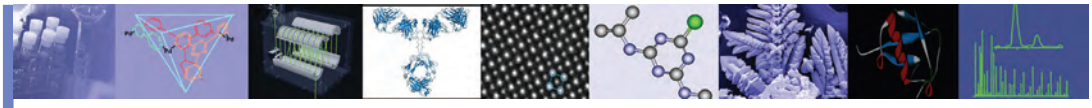

Applications Note

SpiralTOF™

High Sensitivity Peptide Measurement with the New Matrix α-Cyano-4-Chlorocinnamic Acid

Introduction:

Matrix assisted laser desorption ionization (MALDI) is a powerful and useful ionization technique that is commonly used for the analysis of biomolecules such as peptides and proteins. Typically, α-Cyano-4-hydroxycinnamic acid (CHCA) is the matrix used for MALDI peptide measurement. Recently, a new matrix "α-Cyano-4-chlorocinnamic acid (CClCA)" was investigated for peptide analysis [1]. In this study, we demonstrate the measurement of a BSA digest to evaluate the improvement in peptide sensitivity with CClCA in comparison with CHCA by using the JMS-S3000 SpiralTOF MS system.

Experimental:

Sample information and preparation conditions are shown in Table 1. The BSA digest was obtained from Michrom. The CHCA matrix and peptide standard were obtained from Sigma-Aldrich, and CClCA matrix was obtained from Cayman.

The BSA digest standard samples were dissolved in water containing 0.1% trifluoroacetic acid (TFA). CHCA was dissolved in 1:1 water/acetonitrile (ACN) containing 0.1% TFA. And CClCA was dissolved in 1:4 water/ACN containing 0.1% TFA. Next, the BSA digest standard solution and matrix solution were mixed together 1:1 by volume. Afterwards, 0.5 µL of this mixture was placed on the MALDI target plate. Finally, the dried sample was measured using the JMS-S3000 SpiralTOF MS system.

Results:

(1) Mass resolving power and mass accuracy

The comparison of mass resolving power and isotopic pattern for three of the peptide standards (Bradykinin1-7, Angiotensin II and ACTH18-39) with CHCA and CClCA are shown in Figure 1. The data for each matrix showed similar isotopic patterns and high mass-resolving power. The mass resolving power was approximately 23,000 at *m/z* 757.4 for Bradykinin1-7, over 30,000 at *m/z* 1046.5 for Angiotensin II and 73,000 at *m/z* 2466.2 for ACTH18-39. A residual plot for the calibration curves are shown in Figure 2. We used six peptides (Bradykinin1-7, Angiotensin II, Angiotensin I, P14R, ACTH1-17 and ACTH18-39) for the calibration. The Root Mean Squares (RMS) mass error of the actual measured *m/z* value against the calibration curve was just less than 0.4 ppm with both matrices. We achieved high mass resolving power and good mass calibration using the new matrix CClCA with SpiralTOF.

(2) BSA digest measurements

Next, we examined peptide sensitivity using the tryptic digest of BSA with both matrices. MALDI mass spectra of BSA digests with CClCA are shown in Figure 3. And MALDI mass spectra of BSA digests with CHCA are shown in Figure 4. There were a number of peptide peaks observed in the CClCA 250 amol/spot that had better signal-to-noise ratio than the peptide peaks observed in the CHCA 250 amol/spot (Figure 5). Additionally, the peptide mass fingerprint analysis using the peak list from CClCA 250 amol/spot mass spectrum resulted in a higher score and better coverage for the MASCOT (Matrix Science, Ltd.) search results (Figure 6). The protein was identified as BSA for this sample.

Peptide	Conc.	Solvent
BSA digest	100 fmol/µL	0.1% TFA
	10 fmol/µL	0.1% TFA
	1 fmol/µL	0.1% TFA
Matrix		
CHCA	10 mg/mL	ACN/0.1% TFA = 1/1 (v/v)
CCICA	10 mg/mL	ACN/0.1% TFA = 4/1 (v/v)
Sample		
BSA digest/Matrix = 1/1 (v/v)		
0.5 µL of this sample solution mixture was placed on the MALDI target plate		

Table 1. Sample information and preparation conditions.

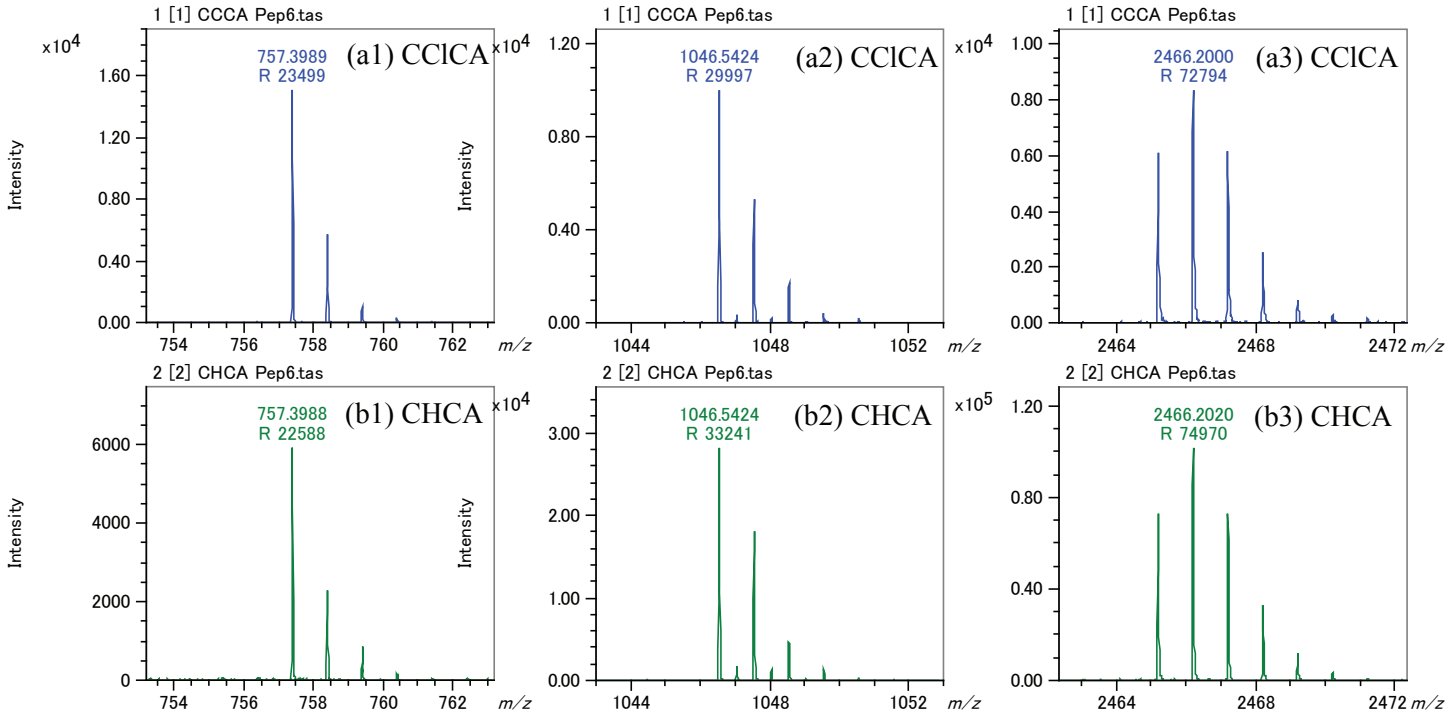

Figure 1. The comparison of mass resolving power and isotopic pattern:
(a1) Bradykinin1-7 with CClCA, (a2) Angiotensin II with CClCA and (a3) ACTH18-39 with CClCA,
(b1) Bradykinin1-7 with CHCA, (b2) Angiotensin II with CHCA and (b3) ACTH18-39 with CHCA.

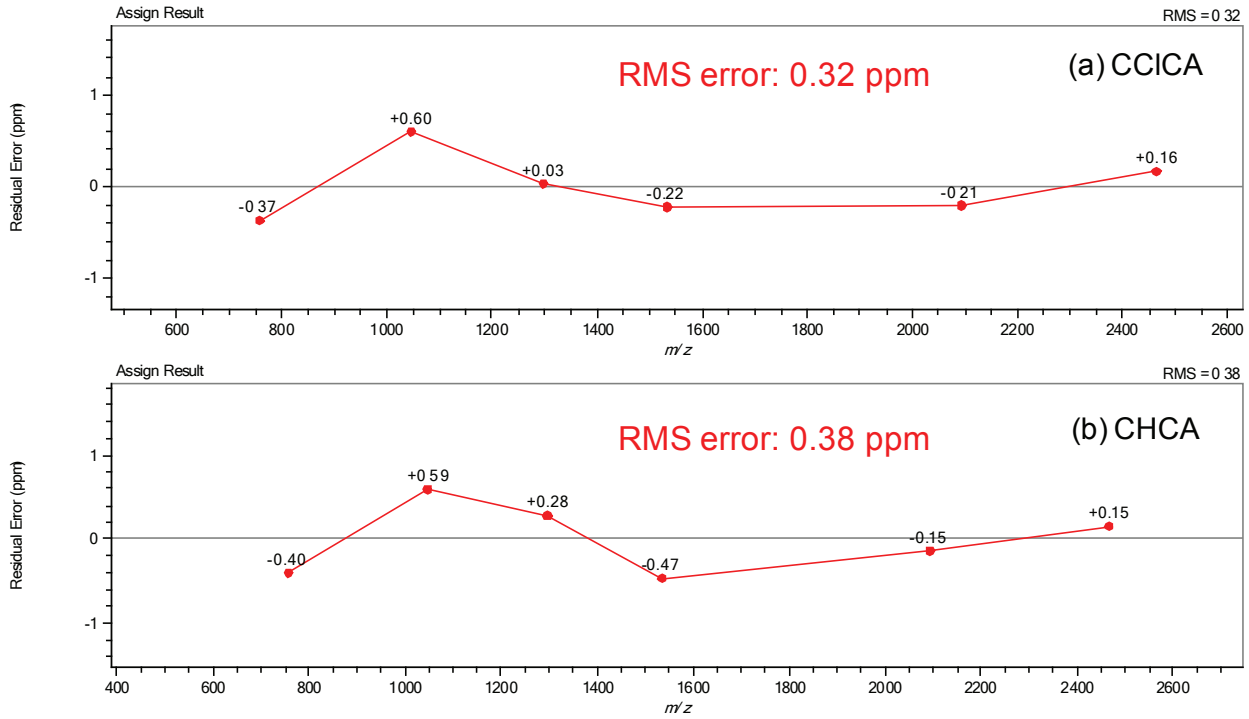

Figure 2. The residual plot for the calibration curves obtained by using six-peptide mixture:
(a) CClCA and (b) CHCA.

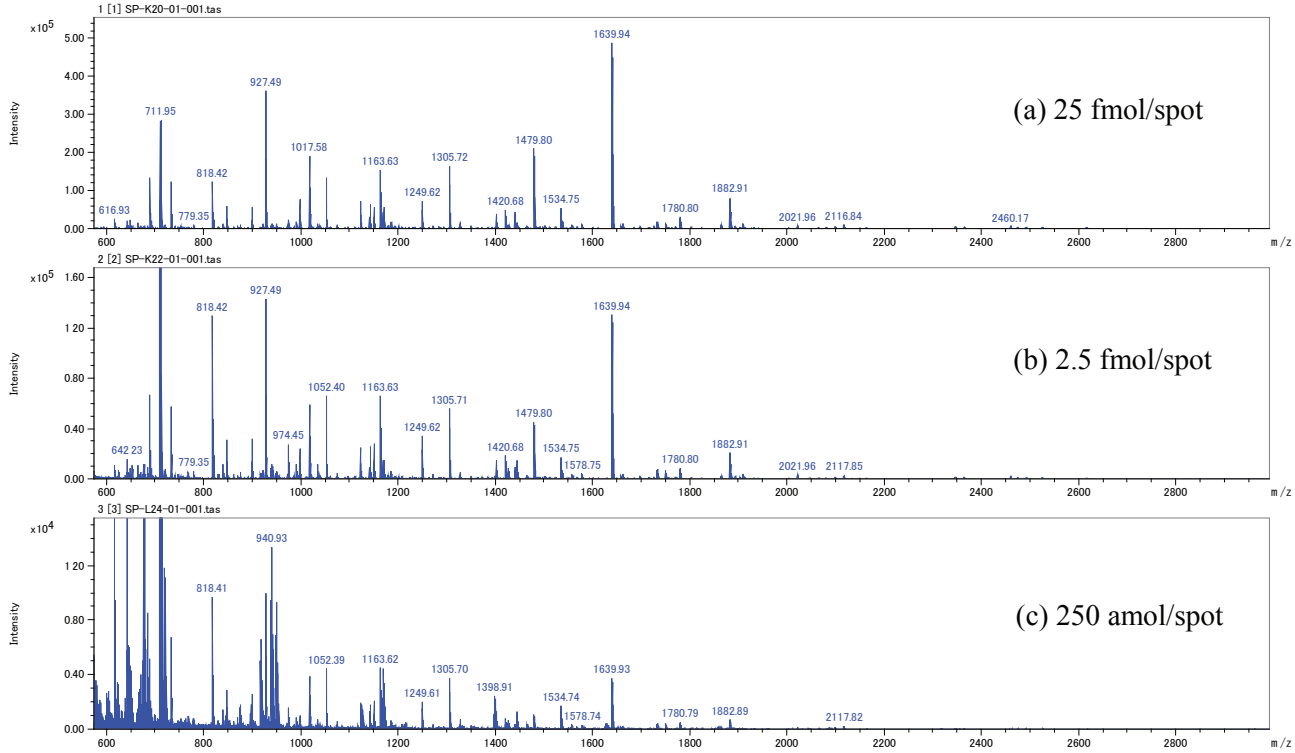

Figure 3. MALDI mass spectra of BSA digests with CClCA: (a) 25 fmol/spot, (b) 2.5 fmol/spot, (c) 250 amol/spot.

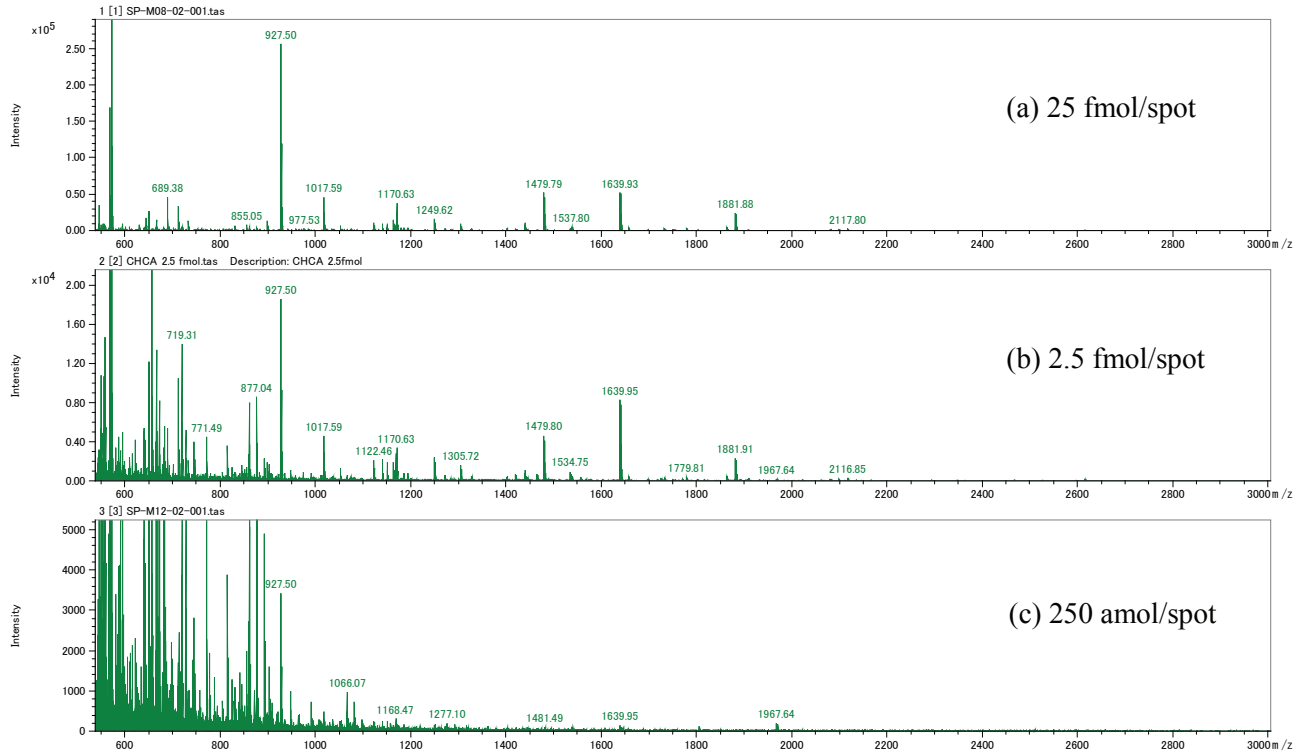

Figure 4. MALDI mass spectra of BSA digests with CHCA: (a) 25 fmol/spot, (b) 2.5 fmol/spot, (c) 250 amol/spot.

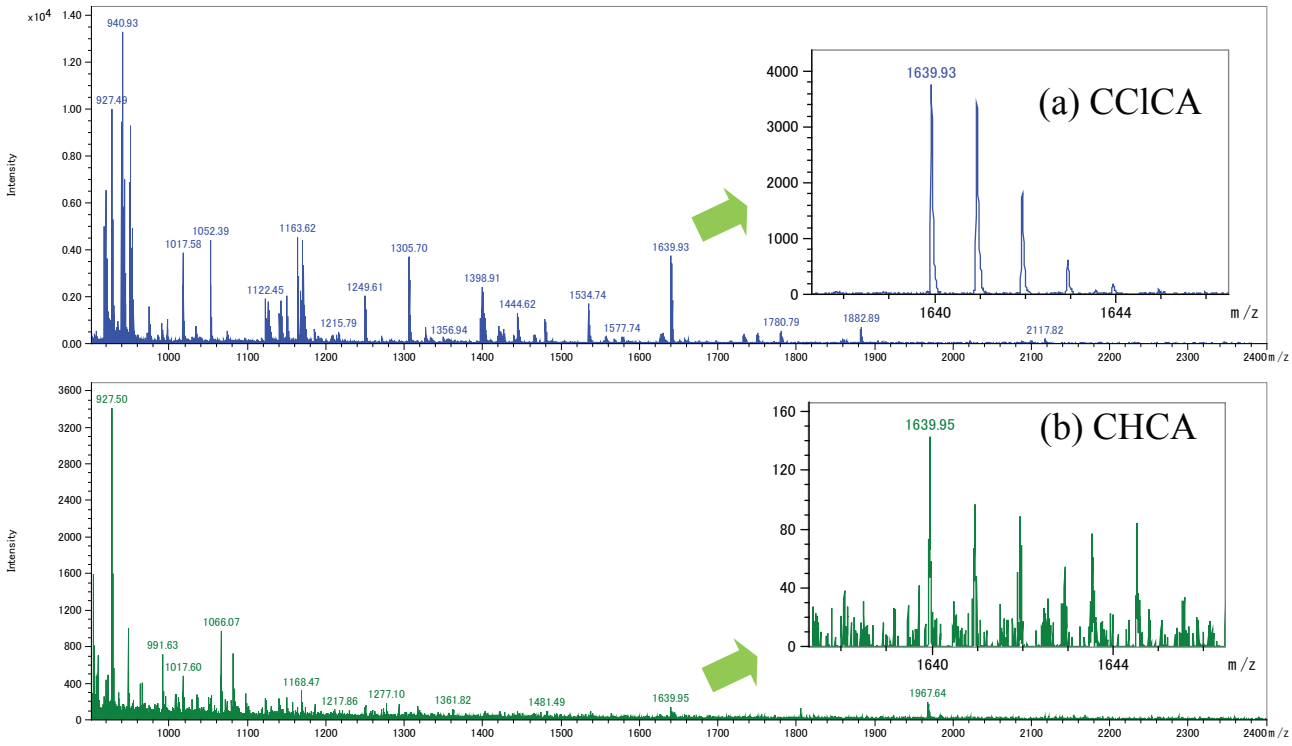

Figure 5. Comparison of BSA digests mass spectra each 250 amol/spot: (a) CClCA, (b) CHCA.

Mascot Score Histogram

Protein score is -10*Log(P), where P is the probability that the observed match is a random event.
Protein scores greater than 61 are significant (p<0.05).

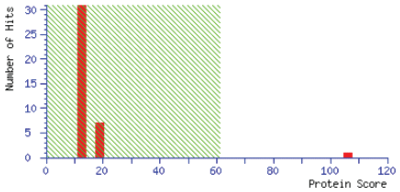

Concise Protein Summary Report

Format As | Concise Protein Summary | Help

Significance threshold p< 0.05 | Max. number of hits AUTO

Re-Search All | Search Unmatched

1. ALBU_BOVIN Mass: 71279 Score: 106 Expect: 1.7e-06 Matches: 28
Serum albumin OS=Bos taurus GN=ALB PE=1 SV=4
RL27A_PIG Mass: 6179 Score: 13 Expect: 3.4e+03 Matches: 2
60S ribosomal protein L27a (Fragment) OS=Sus scrofa GN=RPL27A PE=3 SV=3

2. APOE_ZALCA Mass: 37980 Score: 19 Expect: 8.1e+02 Matches: 11
Apolipoprotein E OS=Zalophus californianus GN=APOE PE=2 SV=1

Figure 6. MASCOT search result using 250 amol/spot of CClCA.

Conclusion:

We have done an initial study in which the new matrix "α-cyano-4-chlorocinnamic acid (CClCA)" was coupled with the SpiralTOF. The CClCA matrix provides high mass resolving power and excellent mass calibration curves that are comparable to the CHCA matrix. Additionally, the CClCA matrix improves the sensitivity of peptides. This new matrix will be a powerful and useful tool for the analysis of peptides and proteins.

Reference:

[1] John D. Leszyk, Evaluation of the New MALDI Matrix 4-Chloro-α-Cyanocinnamic Acid, J. Biomol Tech. 2010 July; 21(2): 81–91.

MS-0402A

SpiralTOF™

High Sensitivity Analysis of Intact Proteins Using Linear TOF

Introduction:
The JMS-S3000 SpiralTOF has a unique 17m flight path that offers the highest resolution MALDI-TOF MS system currently available. However, ions with a very short lifetime or that undergo spontaneous dissociation during their flight cannot be detected by the SpiralTOF (or a conventional reflectron TOF). To address this situation, the SpiralTOF with Linear TOF option can be used for the high sensitivity analysis of intact proteins.

In this work, we demonstrate the measurement of intact proteins by using the Linear TOF option for the JEOL SpiralTOF system.

Experimental:
Protein standards were obtained from Sigma-Aldrich.
a. Pepsin (porcine gastric mucosa), P-6887
b. Albumin (bovine serum), A8471
c. Conalbumin (chicken egg white), C0755
d. IgG (bovine serum), I5506
The protein standard samples were dissolved in water at a concentration of 1 pmol/µL. Sinapinic acid (SA) was used as the matrix and was dissolved in 1:1 water/acetonitrile containing 0.1% trifluoroacetic acid. Next, the protein standard solution and SA solution were mixed together 1:1 by volume. Afterwards, 0.5µL of this mixture was placed on the MALDI target plate (250 fmol/spot). Finally, the dried sample was measured using the Linear TOF option available on the JMS-S3000 SpiralTOF MS system.

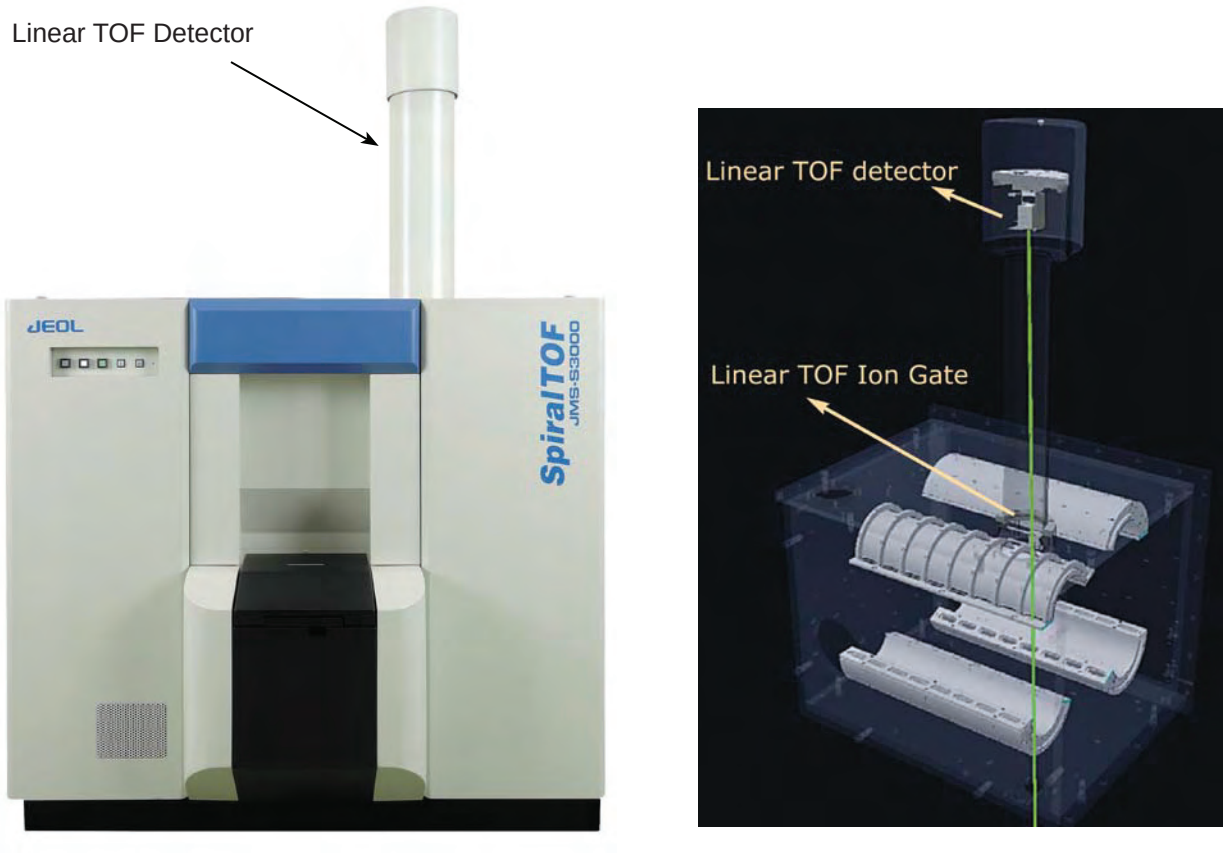

Figure 1. SpiralTOF with Linear TOF option.

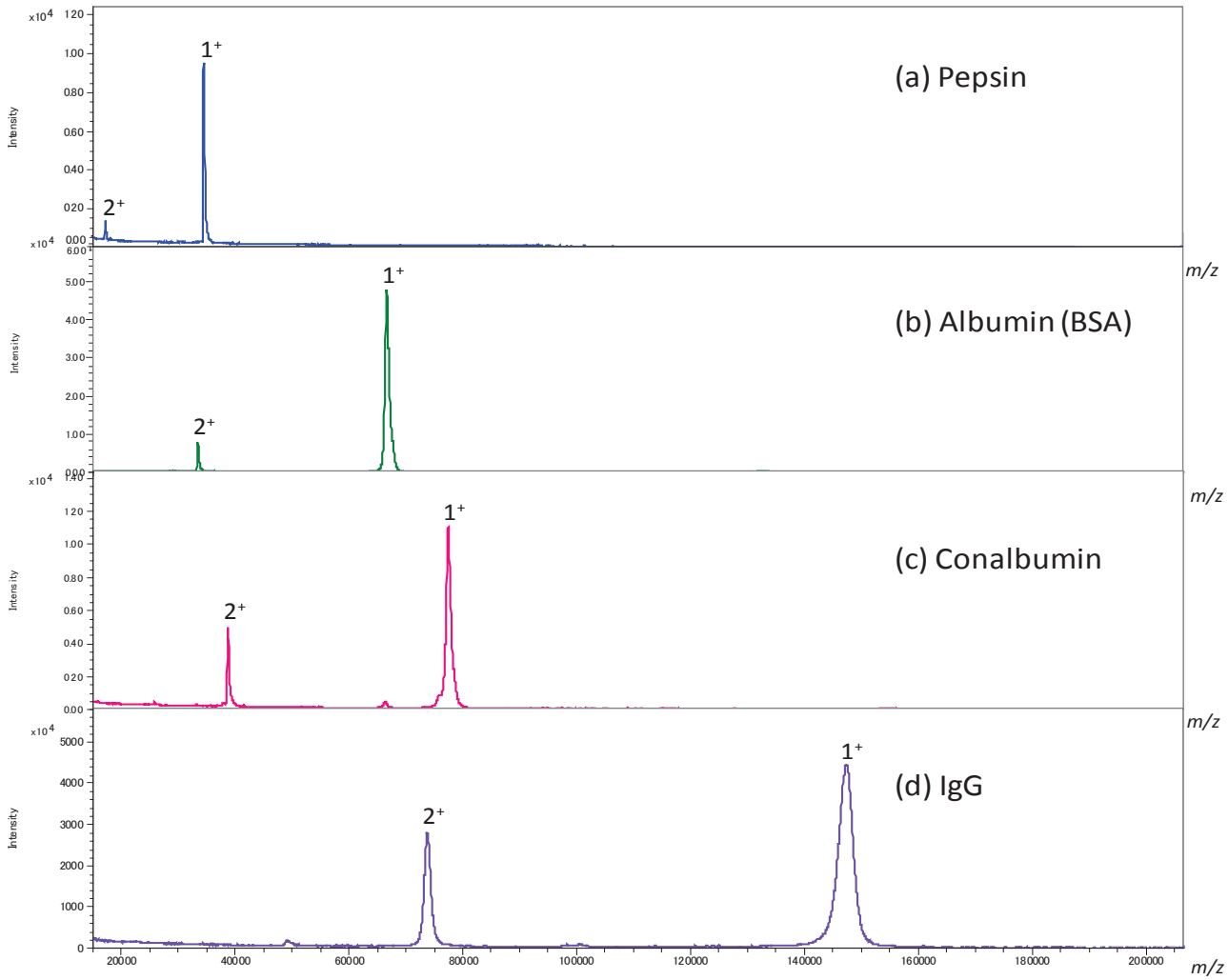

Figure 2. MALDI mass spectrum of protein standard, (a) Pepsin (250 fmol/spot), (b) Albumin (250 fmol/spot) (c) Conalbumin (250 fmol/spot), (d) IgG (250 fmol/spot).

Results & discussion:
The MALDI mass spectra are shown in Figure 2 for each protein sample. Peaks corresponding to single- and double-charge protonated molecules were observed at the expected m/z values for the primary structure of these proteins.

The SpiralTOF with Linear TOF option provided:
- Good peak shape in the high m/z region
- Excellent signal-to-noise ratio for these samples at this concentration (250 fmol)

High-quality mass spectra were achieved for intact proteins by using the JEOL JMS-S3000 system. Also worth noting, the Linear TOF can measure intact molecules up to m/z 500,000 (data not shown in these examples).

SpiralTOF™

MALDI-ISD Measurements Using Both the SpiralTOF Mode and the LinearTOF Mode

Introduction

Matrix assisted laser desorption/ionization (MALDI) combined with in-source decay (ISD) is a useful tool for doing top-down sequencing of intact proteins. In this work, we measured and compared the ISD fragment ions generated for several proteins by using both the high resolution MALDI-Spiral mode and the high sensitivity MALDI-Linear mode available on the JEOL SpiralTOF MALDI-MS system.

Experimental

Myoglobin and Bovine serum albumin (BSA) protein samples were separately dissolved into 0.1% trifluoroacetic acid aqueous with the concentration fixed at 10 pmol/µL. 1,5-diaminonaphthalene (DAN), which can provide good S/N for ISD fragment ions [1], was used as the MALDI matrix. The DAN matrix was dissolved to 0.1% trifluoroacetic acid aqueous/ 50% acetonitrile with the matrix concentration fixed at 10 mg/mL. Subsequently, the matrix and the sample solutions were mixed 1/1 (v/v), and then 1 µL of each solution was deposited and dried on the MALDI target plate. Afterwards, each sample was analyzed in triplicate on the JEOL JMS-3000 SpiralTOF by using both the SpiralTOF mode and the LinearTOF mode.

Results

The Myoglobin and BSA ISD mass spectra for both the LinearTOF and SpiralTOF measurements are shown in Figures 1 and 2, respectively. Both sets of ISD spectra were dominated by the c-ion series. The Linear mode mass spectra showed higher sensitivity overall, especially for ions over *m/z* 5,000 (shown in the *m/z* 4000-7000 zoomed regions). However, as expected, the Linear TOF did not provide full isotopic separation of these c-ions (see insets for the myoglobin c35 and BSA c33 ions). Conversely, the Spiral mode measurements fully resolved these ions and their associated isotopes, as shown in the Figures 1b and 2b insets, respectively, but had less sensitivity at higher *m/z* values.

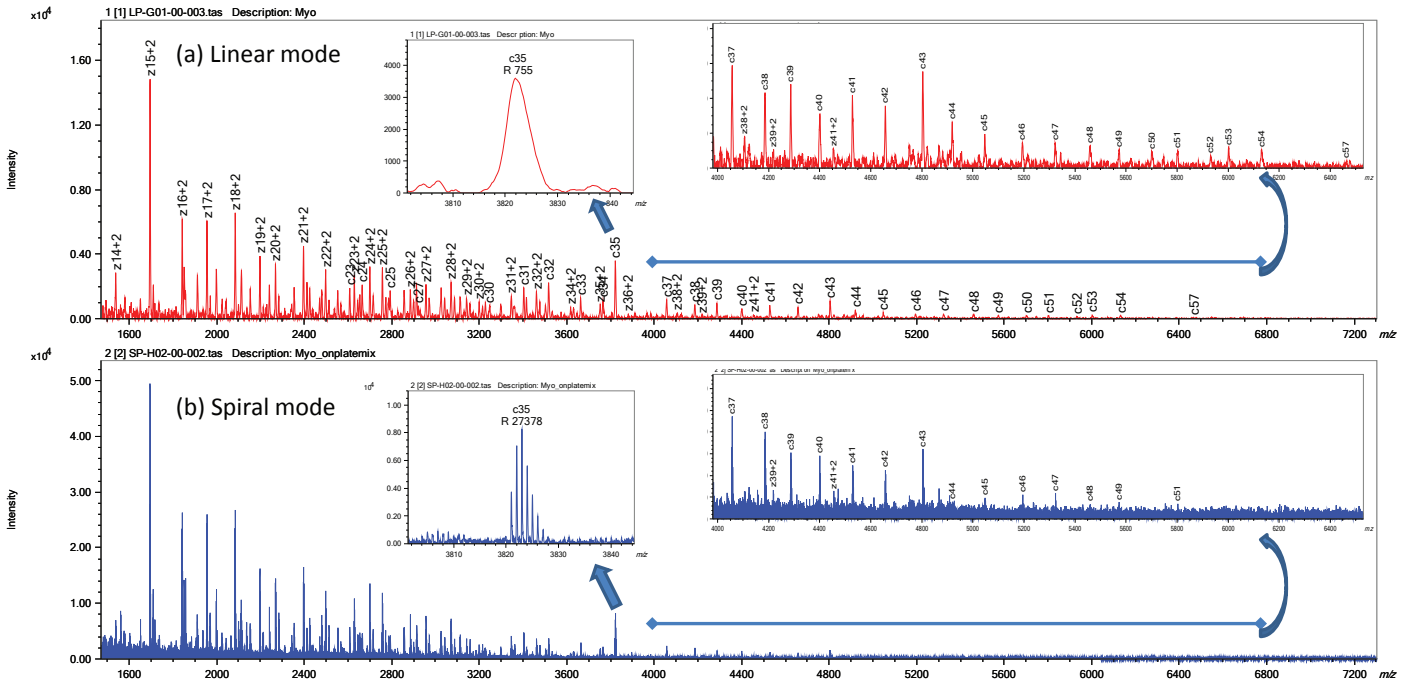

Figure 1. ISD Spectra of myoglobin (MW: 16,952Da) using (a) LinearTOF mode, (b) SpiralTOF mode.

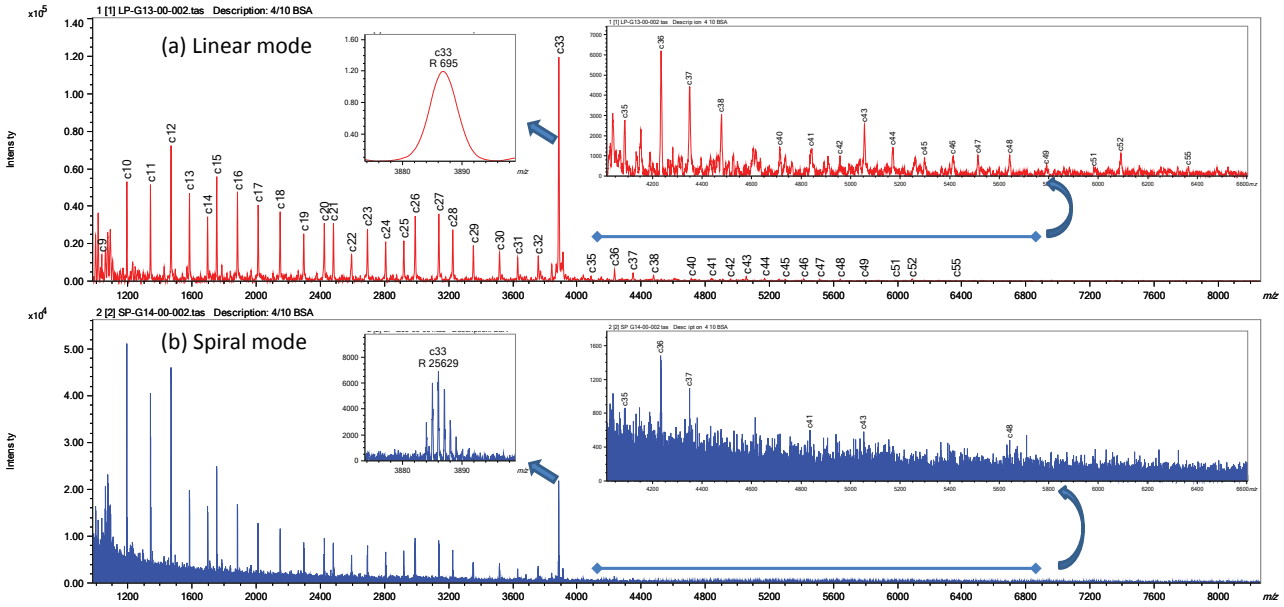

Figure 2. ISD spectra of BSA (MW: 66,430Da) using (a) LinearTOF mode, (b) SpiralTOF mode.

Figure 3. MASCOT search result for the myoglobin sample.

A MASCOT (Matrix Science, Ltd.) MS/MS Database Search using the LinearTOF data identified each sample as myoglobin and BSA, respec- tively. As an example, Figure 3 shows the Mascot database search result for the myoglobin sample. These results showed that, despite the fact that the ISD Linear data does not contain exact masses and does not provide isotopic separation of the ions, the data can still be used with a database search function like MASCOT to identify proteins.

Conclusion

In this work, we showed a brief study in which the ISD measurements for standard proteins were measured by using the SpiralTOF mode and the LinearTOF mode. The SpiralTOF mode provides high mass accuracy and fully separated isotopic ions while the LinearTOF mode provides higher sensitivity, particularly for ions in the higher *m/z* region. Additionally, the LinearTOF data can be used in conjunction with a database search analysis to identify proteins.

Reference

[1] Issey Osaka, Mami Sakai, Mitsuo Takayama, 5-Amino-1-naphthol, a novel 1,5-naphthalene derivative matrix suitable for matrix-assisted laser desorption/ionization in-source decay of phosphorylated peptides, Rapid Communications in Mass Spectrometry, Volume 27, Issue 1, pages 103–108, 15 January 2013.

SpiralTOF™

High Resolution and High Mass Accuracy MALDI-ISD Measurements

Introduction

Matrix assisted laser desorption/ionization (MALDI) combined with in-source decay (ISD) is a useful tool for doing top-down sequencing of intact proteins. This technique can provide enough information to determine both N- and C-terminal sequences. In this work, we measured the ISD fragment ions generated for several peptides using the JEOL SpiralTOF MALDI-MS system.

Experimental

ACTH18-39 and oxidized Insulin B chain peptide samples were separately dissolved in 0.1% trifluoroacetic acid aqueous with the concentration fixed at 10 pmol/µL. 1,5-diaminonaphtalene (DAN), which can provide good S/N for ISD fragment ions [1], was used as the MALDI matrix. The DAN matrix was dissolved to 0.1% trifluoroacetic acid aqueous/50% acetonitrile with the matrix concentration fixed at 10 mg/mL. Subsequently, the matrix and sample solutions were mixed 1/1 (v/v), and then 1 µL of each solution was deposited and dried on the MALDI target plate. Afterwards, each sample was analyzed in triplicate on the JEOL JMS-3000 SpiralTOF MALDI-MS system.

Results

As a starting point, MALDI imaging was used to visualize the location of the sample ion distributions within the DAN crystal matrix. A comparison between an optical microscope image and the MALDI image for the oxidized Insulin B chain y10 fragment ion (*m/z* 1215.6) are shown in Figure 1. These results clearly showed that the ISD fragment ions were concentrated along the edges of the DAN matrix crystals. As a result, the MALDI laser irradiation for each sample spot was focused on the crystal edges in order to obtain sufficient sensitivity for the ISD measurements.

Afterwards, the ISD mass spectra were measured for each peptide, and the results are shown in Figure 2. The ACTH18-39 peptide produced ISD spectra that mostly consisted of the c-ion series. However, for the oxidized Insulin B chain, y-ion series dominated the ISD spectra. It should be noted here that when the basic amino acids are located on the N-terminal side, c-ion series are the dominant ions generated during ISD. However, when the basic amino acids are located on the C-terminal side, the y-ion series are the dominant ions generated during ISD [2]. These results highlight the difference in location for the basic amino acids for each of the peptide chains tested.

Next, each ISD fragment ion series was evaluated for mass accuracy using an external calibration. These analyses showed an average RMS of 4.0 ppm for the ACTH18-39 c ion series and an average RMS of 4.7 ppm for the y-ion series produced from the oxidized Insulin B chain, as shown in Tables 1 and 2, respectively.

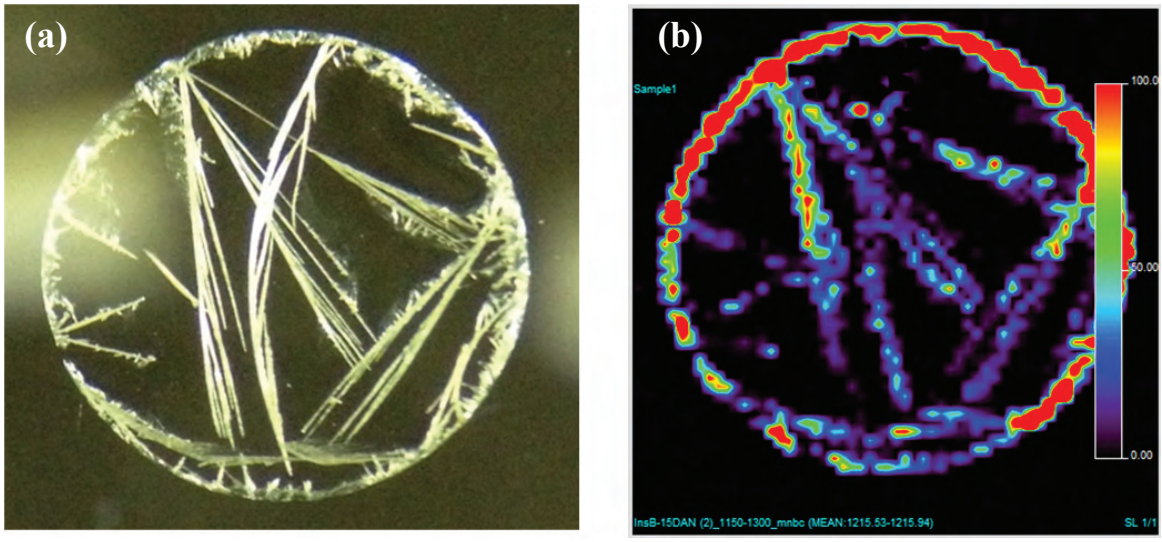

Figure 1. (a) Optical microscope image of DAN crystal, (b) MALDI imaging of *m/z* 1215.6 (y10 ISD fragment ion of oxidized Insulin B chain (width 3.0mm x height 3.0mm, interval 0.05mm).

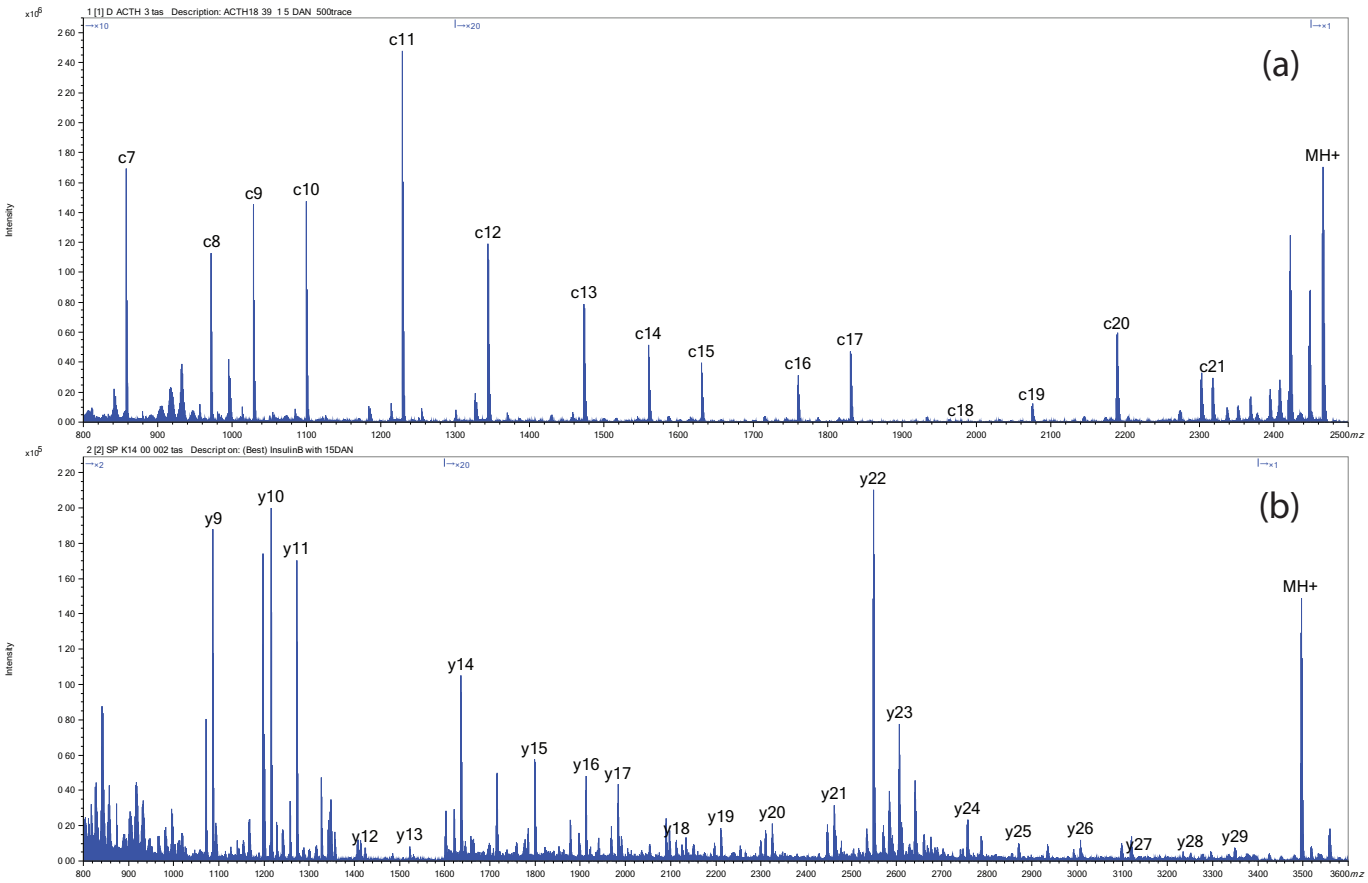

Figure 2. ISD mass spectra for (a) ACTH18-39, (b) oxidized Insulin B chain.

Ion species	Calc. m/z	Mass error (ppm)		
		Data 1	Data 2	Data 3
c7	857.5356	3.73	13.18	2.92
c8	971.5785	1.96	12.87	3.50
c9	1028.6000	0.49	11.76	3.01
c10	1099.6371	0.36	11.55	2.46
c11	1228.6797	1.06	10.09	2.28
c12	1343.7066	0.52	7.59	0.52
c13	1472.7492	0.95	6.52	0.88
c14	1559.7812	0.26	4.62	1.15
c15	1630.8184	0.06	3.07	1.59
c16	1759.8610	1.88	1.99	2.84
c17	1830.8981	0.66	0.44	4.64
c18	1977.9665	6.77	3.08	6.32
c19	2075.0192	1.11	0.82	5.73
c20	2188.1033	5.12	4.30	8.91
c21	2317.1459	4.19	3.88	8.03
Abs. Average		1.94	6.38	3.65

Table 1. Accurate mass measurement results for c-ion series of ACTH18-39.

Ion species	Calc. m/z	Mass error (ppm)		
		Data 1	Data 2	Data 3
y9	1086.5731	1.76	0.10	0.08
y10	1215.6157	0.76	0.48	1.22
y11	1272.6372	0.98	0.04	1.06
y12	1423.6311	11.51	11.51	9.12
y13	1522.6995	9.25	4.98	7.81
y14	1635.7836	4.19	5.41	3.82
y15	1798.8469	4.55	6.27	7.49
y16	1911.9310	8.29	4.89	9.81
y17	1982.9681	3.56	6.33	5.33
y18	2112.0107	2.30	6.37	3.29
y19	2211.0791	4.42	8.94	5.69
y20	2324.1631	3.97	5.31	8.92
y21	2461.2220	1.15	1.15	0.96
y22	2548.2541	2.77	4.42	3.44
y23	2605.2755	3.82	4.81	2.28
y24	2756.2695	5.68	5.43	2.96
y25	2869.3535	4.47	8.76	2.87
y26	3006.4124	5.47	0.55	4.40
y27	3134.4710	6.13	13.47	16.65
y28	3248.5139	1.40	16.76	13.22
y29	3347.5824	3.33	6.83	4.04
Abs. Average		4.37	5.10	4.55

Table 2. Accurate mass measurement results for y-ion series of oxidized Insulin B chain.

Conclusion

In this work, we showed a brief study in which the ISD measurements for standard peptides were measured by using the SpiralTOF. It should be noted that ISD measurements generally require a relatively high laser power to generate ISD fragment ions which in turn detrimentally impacts the mass resolving power of the instrument. As a result, it is generally very difficult to achieve high mass resolving power using a high laser power. However, the Spiral trajectory ion optics provides a 17m flight path that overcame this problem to produce resolving powers of 20,000-35,000 for each of the measured ions. Furthermore, as shown with these peptide sequences, the system provided excellent mass accuracy even when an external calibration was used for the data.

Reference

[1] Issey Osaka, Mami Sakai, Mitsuo Takayama, 5-Amino-1-naphthol, a novel 1,5-naphthalene derivative matrix suitable for matrix-assisted laser desorption/ionization in-source decay of phosphorylated peptides, Rapid Communications in Mass Spectrometry, Volume 27, Issue 1, pages 103–108, 15 January 2013.

[2] Mitsuo Takayama, The Characteristics of In-source Decay in Mass Spectrometric Degradation Methods _Hydrogen-Attachment Dissociation (HAD)_, J. Mass Spectrom. Soc. Jpn., Vol. 50, No. 6, 2002.

This page intentionally left blank for layout purpose.

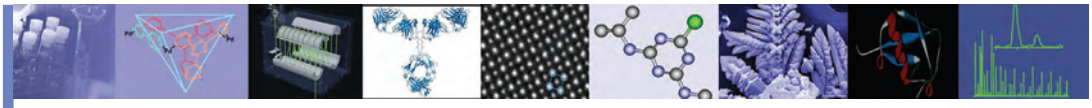

SpiralTOF-TOF

Analysis of the Natural Organic Compound SAAF by Using the TOF-TOF Option

Introduction

Sperm activating and attracting factor (SAAF) is a naturally occurring substance produced by ascidians (sea squirts) to promote the fertilization process. Previously, the structure of this compound was characterized by high-energy collision induced dissociation (CID) using a traditional four sector tandem double focusing mass spectrometer.[1]

In this work, we analyzed the SAAF from a ciona intestinalis by using a JMS-S3000 SpiralTOF™ equipped with the optional TOF-TOF analyzer to generate a high energy CID product ion spectrum for this compound.

Results and Discussion

Fig. 1 shows the SAAF mass spectrum acquired using PEG sulfate 600 as an external calibrant. The spectrum shows a peak at *m/z* 515.301, which is suspected to be the monoisotopic ion $[M\text{-}2Na\text{-}SO_3+H]^-$ (calculated value 515.305). In addition, peaks from SAAF are observed at two other masses: $[M\text{-}2Na+H]^-$ at *m/z* 595.255 (calculated value 595.261) and $[M\text{-}Na]^-$ at *m/z* 617.237 (calculated value 617.242). Among these peaks, the product ion spectrum was acquired for the $[M\text{-}2Na\text{-}SO_3+H]^-$ ion, which had been previously analyzed using a traditional four sector tandem double focusing mass spectrometer.[1] Fig. 2 shows the high energy CID results generated by the SpiralTOF-TOF. The negative charge was fixed to the sulfate ester end of the molecule, causing charge remote fragmentation (CRF) to occur. As a result, the spectrum showed peaks that systematically reflected the structure of SAAF, as

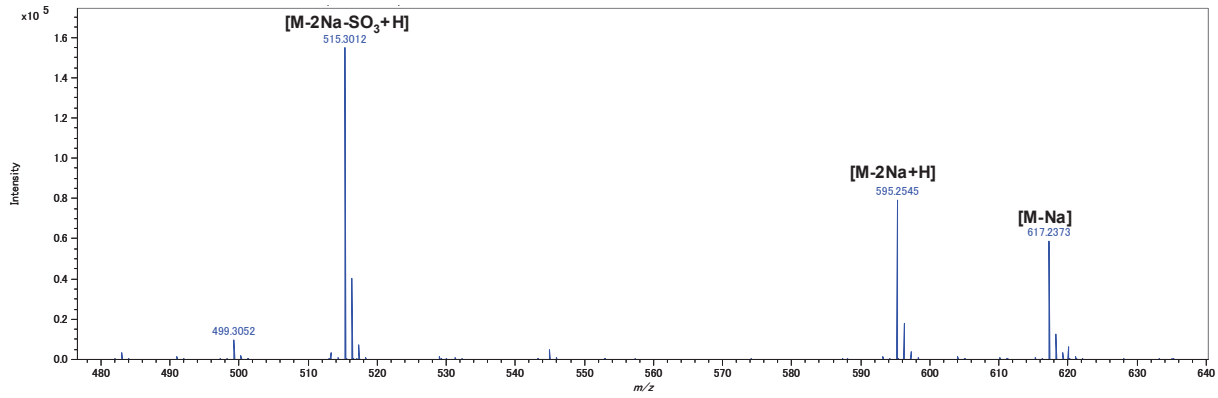

Figure 1. Mass spectrum of SAAF.

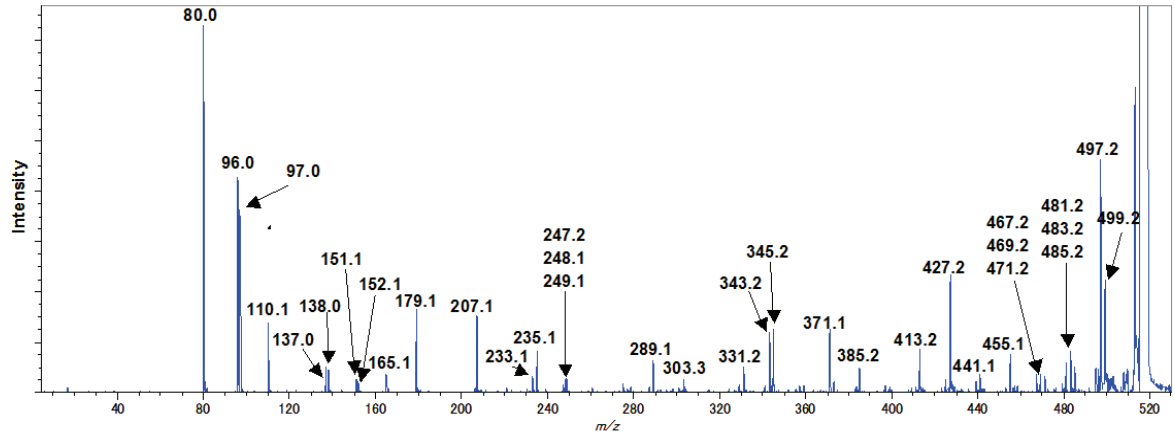

Figure 2. Product ion spectrum of $[M\text{-}2Na\text{-}SO_3+H]^-$.

shown in Fig. 3. This data closely resembles the results obtained using a traditional four sector MS/MS system.[1]

Conclusions

As this data demonstrates, high energy CID analysis by using SpiralTOF-TOF clearly detected the peaks resulting from CRF, which enabled the analysis of samples that are complex in structure, such as natural organic compounds like SAAF.

Acknowledgment

The analysis above was conducted in collaboration with the Mass Analysis Group, Department of Physics, Graduate School of Science, Osaka University.
We wish to express our thanks to Prof. Michio Murata of the Department of Biomolecular Sciences, Department of Physics, Graduate School of Science, Osaka University, for providing the SAAF samples.

Reference

[1] M. Yoshida, M. Murata, K. Inaba, and M. Morisawa, Proceeding of the National Academy of Sciences of the United States of America 99 (2002) 14831-14836.

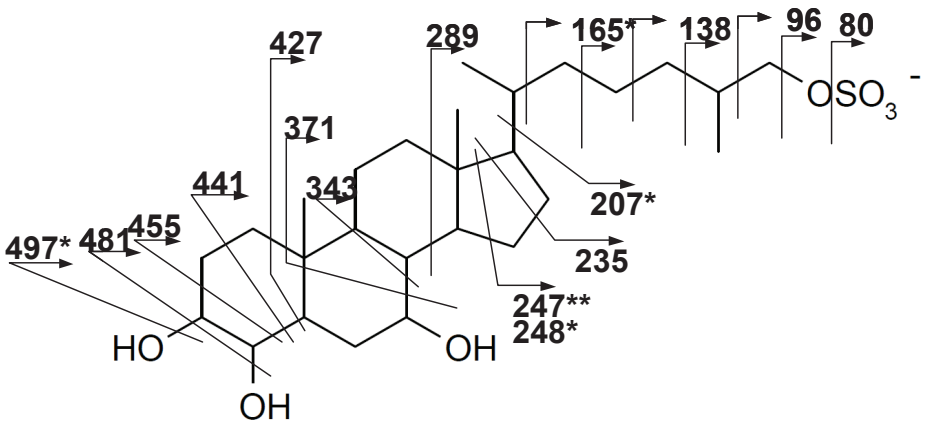

Figure 3. Structure of of SAAF and fragmentation pattern. (Asterisks show dehydrated ions.)

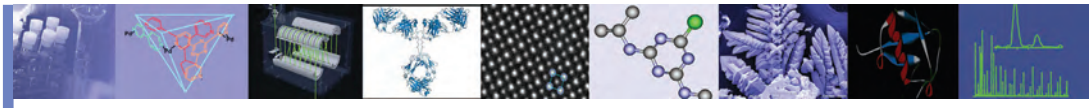

SpiralTOF-TOF

Analysis of the Natural Organic Compound YTX by Using TOF-TOF Option

Introduction

Yessotoxin (YTX) is one of the substances that cause food poisoning when humans consume toxic shellfish. The structure of this compound has been previously analyzed by high-energy collision induced dissociation (CID) using a traditional four sector tandem double focusing mass spectrometer.[1]

In this work, we analyzed YTX by using a JMS-S3000 SpiralTOF™ equipped with the optional TOF-TOF analyzer to generate a high energy CID product ion spectrum.

Results and Discussion

Fig. 1 shows the YTX mass spectrum acquired using polyalanine as an external calibrant. The spectrum shows a peak at *m/z* 1061.513, which is suspected to be the monoisotopic ion $[M-2Na-SO3+H]^-$ (calculated value 1061.609). There was also a $[M-Na]^-$ peak observed for YTX at *m/z* 1164.450 (calculated value 1163.548). Among these peaks, the product ion spectrum was acquired from $[M-2Na-SO_3+H]^-$, which had been previously analyzed using a traditional four sector tandem double focusing mass spectrometer.1 Fig. 2 shows the high-energy CID results generated by the SpiralTOF-TOF. The negative charge was fixed to the sulfate ester end of the molecule, causing charge remote fragmentation (CRF) to occur. As a result, the spectrum showed peaks that systematically reflected the structure of YTX, as shown in Fig. 3. This data closely resembles the results obtained using a traditional four sector MS/MS system.[1]

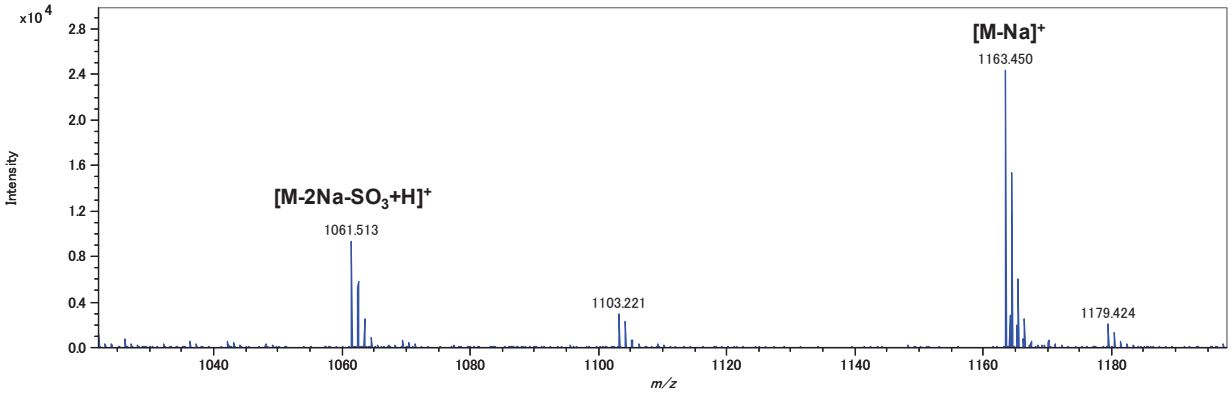

Figure 1. Mass spectrum of YTX.

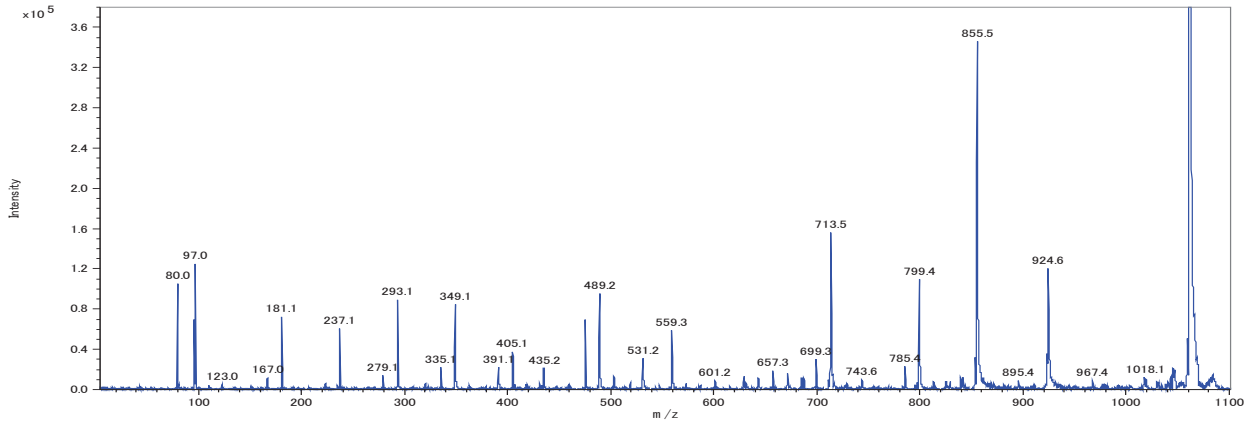

Figure 2. Product ion spectrum of $[M-2Na-SO_3+H]^-$

Conclusions

As this data demonstrates, high energy CID analysis using SpiralTOF-TOF clearly detected the peaks resulting from CRF, Which enabled analysis of samples that are complex in structure such, as natural organic compounds.

Acknowledgement

We wish to express our thanks to Prof. Michio Murata of the Department of Biomolecular Sciences, Department of Physics, Graduate School of Science, Osaka University, for providing the YTX samples.

Reference

[1] H. Naoki, M. Murata, T. Yasumoto, Rapid Communication of Mass Spectrometry 7 (1993) 179

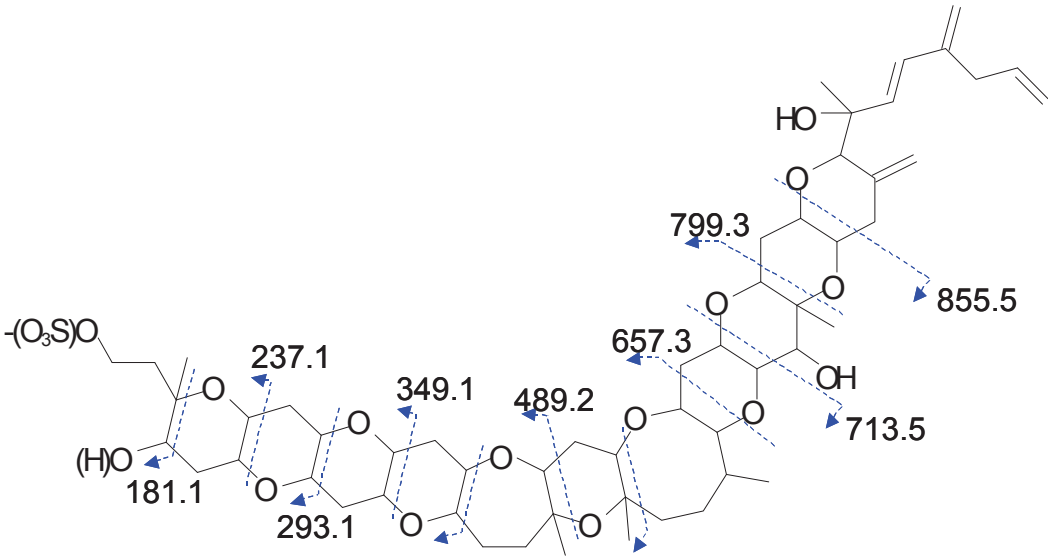

Figure 3. Structure of YTX and fragmentation pattern.

SpiralTOF-TOF

High-energy CID Mass Spectrometry of Oligosaccharides

Introduction:

Matrix assisted laser desorption ionization (MALDI) is a powerful and useful ionization technique that is commonly used for the analysis of biomolecules such as oligosaccharides. There are many applications of oligosaccharides in which various ionization techniques and mass spectrometers were used for their analysis [1]. In particular, tandem mass spectrometry techniques are often used to sequence these molecules.

Recently, JEOL developed a new tandem TOF-TOF instrument coupled with MALDI that is called the SpiralTOF. The 1st TOF consists of 4 toroidal electric sectors that fold a 17 meter flight path into a one meter box. This design provides several unique advantages for TOF-TOF analysis. The 2nd TOF has (a) 20 kV high-energy CID, (b) monoisotopic precursor ion selection, and (c) no PSD ions in the product ion mass spectrum.

In this study, we analyzed several oligosaccharides by using the JMS-S3000 SpiralTOF-TOF tandem mass spectrometer system.

Experimental:

All oligosaccharides (Laminaritetraose, Stachyose, α-Cyclodextrin, β-Cyclodextrin, γ-Cyclodextrin) were commercially available items that were used without further purification. Each oligosaccharide standard solution was dissolved in water. 2,5-Dihydroxybeozoic acid (DHB) was dissolved in 40% ethanol at a concentration of 10 mg/mL. Next, the oligosaccharides standard solution and matrix solution were mixed together 1:1 by volume. Afterwards, 0.5 µL of this mixture was placed on the MALDI target plate. Finally, the dried sample was measured using the JMS-S3000 SpiralTOF-TOF.

Results:

The A, B and C fragment ions for oligosaccharides are labeled as the non-reducing terminal ends while the X, Y and Z fragment ions are labeled as the reducing terminal ends. The nomenclature fragmentation pathway of oligosaccharides by tandem MS is shown in Figure 1[modified from Reference 2].

In this study, we did not do further purification for all oligosaccharide standards, matrix and solvents. As a result, the sodiated molecules were the most intense peak in each positive-ion MALDI mass spectrum (see Figure 2). Therefore, these sodiated molecules were selected as the precursor ions for the SpiralTOF-TOF analysis. MALDI TOF-TOF spectra of Laminaritetraose and Stachyose are shown in Figure 3. Laminaritetraose is a tetrasaccharide that consists of four β-D-glucose units that are linked as Glc(β1→3)Glc(β1→3)Glc(β1→3)Glc. Stachyose is also a tetrasccharide that consists of two α-D-galactose units, one α-D-glucose unit, and one β-D-fructose unit that are linked as Gal(α1→6)Gal(α1→6)Glc(α1→2β)Fru. These isomers showed significantly different mass spectral patterns. B and Y fragment ions were generated from the glycosidic bond cleavage were observed as the dominant components in each MALDI TOF-TOF spectrum. The fragmentation scheme for Laminaritetraose is shown in Figure 4. High-energy CID fragmentation occurs within a shorter time-scale than low-energy CID, which means that it provides a cross-ring cleavage that gives useful structural information about the oligosaccharides and their glycoconjugates. This cross-ring cleavage was also observed for both oligosaccharides, as indicated by the presence of the fragment ions m/z 599, 569, 555, etc. (see Figure 3). All of this information is essential for determining the structure of each oligosaccharide and differentiating structural isomers from each other.

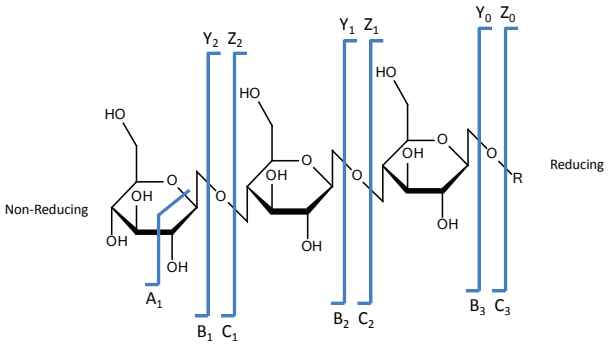

Figure 1. Fragmentation pathways.

Cyclodextrins are cyclic oligosaccharides consisting of five or more α-D-glucose units that are linked as Glc(α1→4)Glc. The MALDI TOF-TOF spectrum for each Cyclodextrin is shown in Figure 5. In each case, the B ion series from glycosidic bond cleavage were the dominant ions observed in the TOF-TOF spectra. Additionally, a number of fragment ions were observed that were the result of cross-ring cleavage.

MS-MS-012313

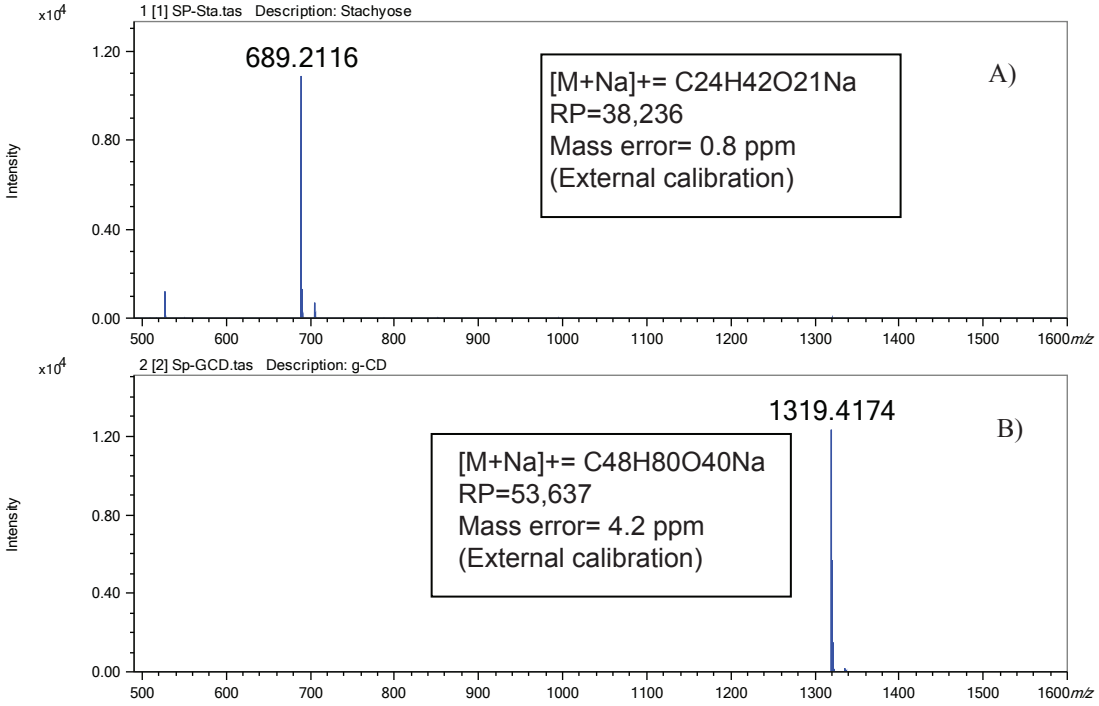

Figure 2. MALDI TOF spectra. A) Stachyose, B) γ-Cyclodextrin

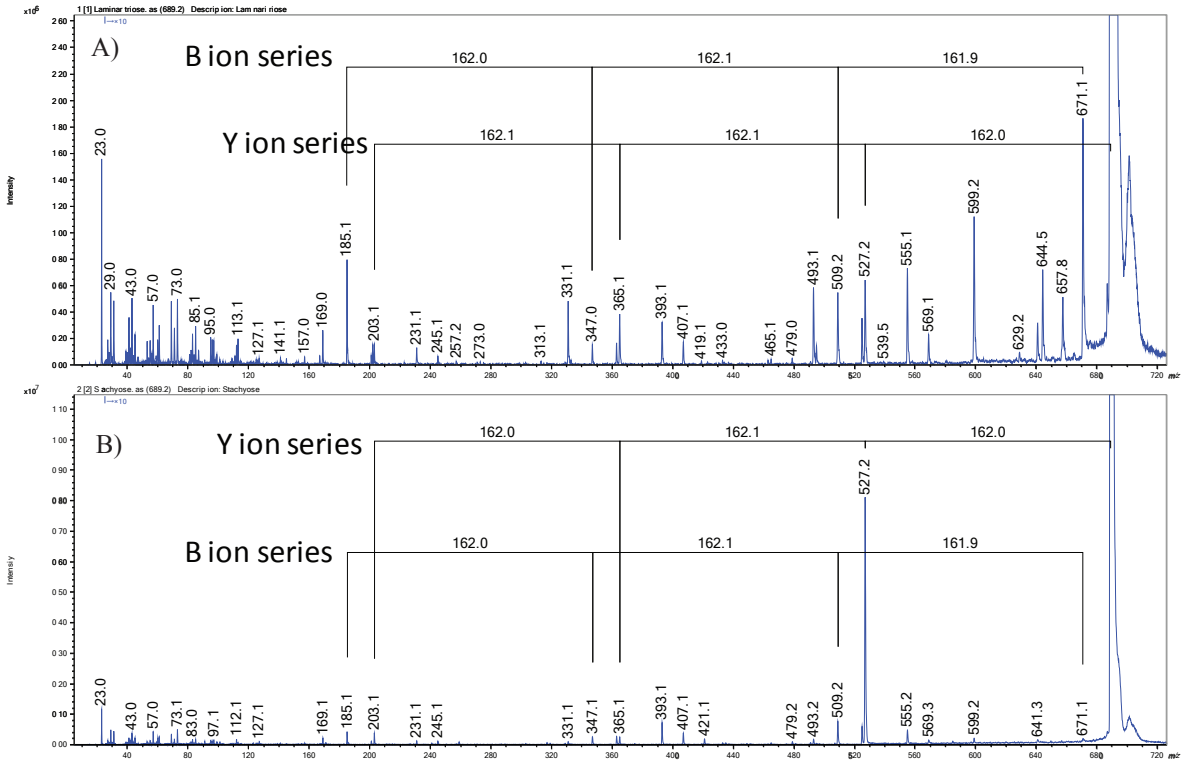

Figure 3. MALDI TOF-TOF spectra. A) Laminaritetraose, B) Stachyose

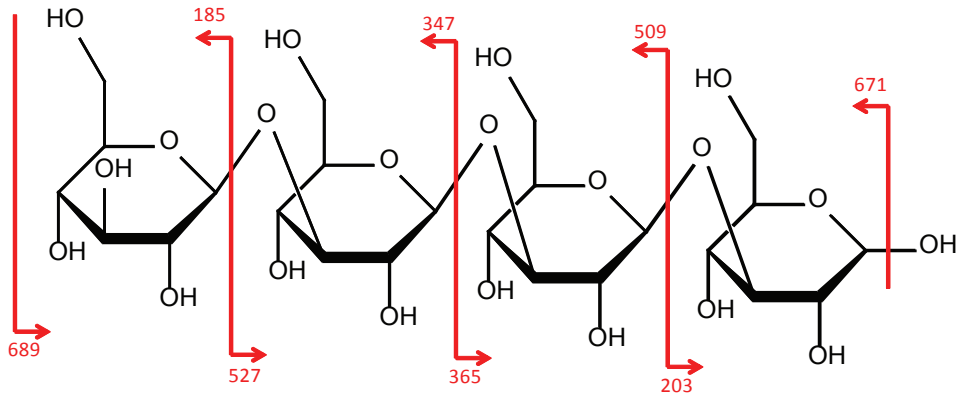

Figure 4. The glycosidic bond cleavage to generate B and Y ion series for Laminaritetraose

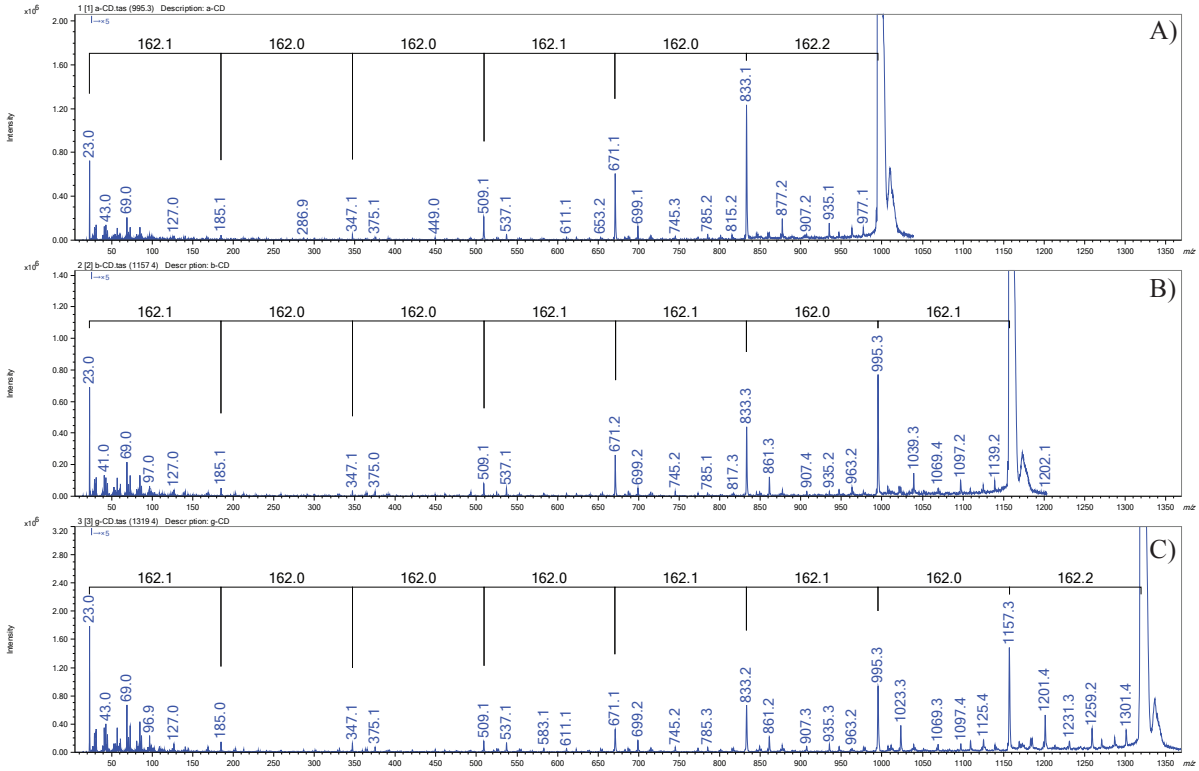

Figure 5. MALDI TOF-TOF spectra. A) α-Cyclodextrin, B) β-Cyclodextrin, C) γ-Cyclodextrin

Conclusion:

In this work, we showed a brief study in which the high-energy CID measurements for several oligosaccharides were measured by using the SpiralTOF-TOF. The B and Y ion series were observed as the main components in each TOF-TOF spectrum. Furthermore, we could also see a number of fragment ions that were generated from cross-ring cleavage, which was helpful in differentiating structural isomers. These results show that high-energy CID coupled with MALDI provides a good platform for determining oligosaccharide structural information that will not generally be available when analyzing these compounds by other mass spectrometry techniques.

Reference:

[1] Joseph Zaia, Mass Spectrometry of Oligosaccharides, ***Mass Spectrometry Reviews***, Volume 23, Issue 3, pages 161–227, May/June 2004

[2] Domon B, Costello CE. 1988b. A systematic nomenclature for carbohydrate fragmentations in FAB-MS/MS spectra ofglycoconjugates. ***Glycoconjugate J*** 5:397–409.

This page intentionally left blank for layout purpose.

JMS-S3000 *SpiralTOF* bibliography

6 May 2016

1 Satoh, T., Sato, T. & Tamura, J. Development of a high-performance MALDI-TOF mass spectrometer utilizing a spiral ion trajectory. *J Am Soc Mass Spectrom* **18**, 1318-1323, doi:10.1016/j.jasms.2007.04.010 (2007).

2 Satoh, T. Analytical Capability of a High Performance Matrix-Assisted Laser Desorption/Ionization Time-of-Flight Mass Spectrometer for Peptide Mass Fingerprinting 高性能マトリックス支援レーザー脱離イオン化飛行時間質量分析計を利用したペプチドマスフィンガープリント法によるタンパク質解析能力の検討. *Journal of the Mass Spectrometry Society of Japan* **55**, 173-181, doi:10.5702/massspec.55.173 (2007).

3 Satoh, T. Development of a Time-of-Flight Mass Spectrometer Utilizing a Spiral Ion Trajectory らせん状のイオン軌道を利用した飛行時間質量分析計の開発. *Journal of the Mass Spectrometry Society of Japan* **57**, 363-369, doi:10.5702/massspec.57.363 (2009).

4 佐藤貴弥. らせん状のイオン軌道を利用した飛行時間質量分析計の開発. *ぶんせき*, 688-691 (2009).

5 Hitora, Y., Takada, K., Okada, S. & Matsunaga, S. Miyakosynes A–F, cytotoxic methyl branched acetylenes from a marine sponge Petrosia sp. *Tetrahedron* **67**, 4530-4534, doi:10.1016/j.tet.2011.04.085 (2011).

6 Ishii, Y., Sakashita, T., Kawasaki, S., Kato, H. & Takatori, M. Fusing Treatment of Pentacenes: Toward Giant Graphene-Like Molecule. *Materials Express* **1**, 36-42, doi:10.1166/mex.2011.1005 (2011).

7 Naka, T. *et al.* Lipid phenotype of two distinct subpopulations of Mycobacterium bovis Bacillus Calmette-Guerin Tokyo 172 substrain. *J Biol Chem* **286**, 44153-44161, doi:10.1074/jbc.M111.310037 (2011).

8 Satoh, T., Sato, T., Kubo, A. & Tamura, J. Tandem time-of-flight mass spectrometer with high precursor ion selectivity employing spiral ion trajectory and improved offset parabolic reflectron. *J Am Soc Mass Spectrom* **22**, 797-803, doi:10.1007/s13361-011-0090-3 (2011).

9 Tsujita, T. *et al.* Purification and characterization of polyphenols from chestnut astringent skin. *Journal of agricultural and food chemistry* **59**, 8646-8654, doi:10.1021/jf201679q (2011).

10 佐藤貴弥. らせん状のイオン軌道をもつタンデム飛行時間質量分析装置の開発と応用例. *ぶんせき*, 532-536 (2011).

11 Degawa, T., Shimma, S. & Toyoda, M. Rapid sequencing of a peptide containing a single disulfide bond using high-energy collision-induced dissociation. *European Journal of Mass Spectrometry* **18**, 345, doi:10.1255/ejms.1188 (2012).

12 Hamamoto, Y. *et al.* Brevisulcenal-F: A polycyclic ether toxin associated with massive fish-kills in New Zealand. *Journal of the American Chemical Society* **134**, 4963-4968, doi:10.1021/ja212116q (2012).

13 Holland, P. T. *et al.* Novel toxins produced by the dinoflagellate Karenia brevisulcata. *Harmful Algae* **13**, 47-57, doi:10.1016/j.hal.2011.10.002 (2012).

14 Li, K. *et al.* A rheological and chemical investigation of canadian heavy oils from the McMurray Formation. *Energy & Fuels* **26**, 4445-4453, doi:10.1021/ef300608w (2012).

15 Moyori, T., Tang, T. & Takasu, A. Dehydration Polycondensation of Dicarboxylic Acids and Diols Using Sublimating Strong Brønsted Acids. *Biomacromolecules* **13**, 1240-1243, doi:10.1021/bm300231d (2012).

16 Mukosaka, S., Teramoto, K. & Koike, H. in *Biological Data Visualization (BioVis), 2012 IEEE Symposium on.* 63-68 (IEEE).

17 Mukosaka, S., Teramoto, K. & Koike, H. Visual Analytics of Repeating Structures Using Mass Spectrometry. *Journal of the Mass Spectrometry Society of Japan* **60**, 27-32, doi:10.5702/massspec.11-34 (2012).

18 Oda, M. *et al.* Stathmin is involved in the cooperative effect of Zoledronic acid and gefitinib on bone homing breast cancer cells in vitro. *J Bone Oncol* **1**, 40-46, doi:10.1016/j.jbo.2012.06.001 (2012).

19 Satoh, T., Kubo, A., Shimma, S. & Toyoda, M. Mass spectrometry imaging and structural analysis of lipids directly on tissue specimens by using a spiral orbit type tandem time-of-flight mass spectrometer, SpiralTOF-TOF. *Mass Spectrometry* **1**, A0013-A0013, doi:10.5702/massspectrometry.A0013 (2012).

20 Shimma, S., Kubo, A., Satoh, T. & Toyoda, M. Detailed structural analysis of lipids directly on tissue specimens using a MALDI-SpiralTOF-Reflectron TOF mass spectrometer. *PLoS One* **7**, e37107, doi:10.1371/journal.pone.0037107 (2012).

21 Voorhees, K. J., McAlpin, C. R. & Cox, C. R. Lipid profiling using catalytic pyrolysis/metal oxide laser ionization-mass spectrometry. *Journal of Analytical and Applied Pyrolysis* **98**, 201-206, doi:10.1016/j.jaap.2012.07.004 (2012).

22 Wang, X., Nagata, K. & Higuchi, M. Formation and electrochemical investigation of ordered cobalt coordinated peptide monolayers on gold substrates. *Thin Solid Films* **520**, 2884-2891, doi:10.1016/j.tsf.2011.12.009 (2012).

23 Yamazaki, M. *et al.* Origins of oxygen atoms in a marine ladder-frame polyether: evidence of monooxygenation by 18O-labeling and using tandem mass spectrometry. *The Journal of organic chemistry* **77**, 4902-4906, doi:10.1021/jo300531t (2012).

24 佐藤崇文, 寺本華奈江, 佐藤貴弥 & 上田祥久. MALDI Spiral-TOF/TOF によるエチレンオキサイド–プロピレンオキサイドブロック共重合体の分析. *高分子論文集 KOBUNSHI RONBUNSHU* **69**, 502-502, doi:10.1295/koron.69.502 (2012).

25 Hari, Y. *et al.* Base-pair recognition ability of hydroxyphenyl nucleobases in parallel triplex DNA. *Tetrahedron* **69**, 6381-6391, doi:10.1016/j.tet.2013.05.107 (2013).

26 Hari, Y., Nakahara, M. & Obika, S. Triplex-forming ability of oligonucleotides containing 1-aryl-1, 2, 3-triazole nucleobases linked via a two atom-length spacer. *Bioorganic & medicinal chemistry* **21**, 5583-5588, doi:10.1016/j.bmc.2013.05.034 (2013).

27 Kubo, A. *et al.* Structural analysis of triacylglycerols by using a MALDI-TOF/TOF system with monoisotopic precursor selection. *J Am Soc Mass Spectrom* **24**, 684-689, doi:10.1007/s13361-012-0513-9 (2013).

28 Matsumori, N. *et al.* A novel sperm-activating and attracting factor from the ascidian Ascidia sydneiensis. *Organic letters* **15**, 294-297, doi:10.1021/ol303172n (2013).

29 Mizuta, Y., Takasu, A. & Higuchi, M. Synthesis of Cell - Penetrating S - Galactosyl–Oligoarginine Peptides as Inducers of Recombinant Protein Expression under the Control of lac Operator/Repressor Systems. *ChemPlusChem* **78**, 677-683, doi:10.1002/cplu.201300130 (2013).

30 Moyori, T., Hayashi, T. & Takasu, A. Aldol - type group - transfer polymerization of silyl vinyl ethers using silyl perfluoroalkaneimides as nonmetal catalysts. *Journal of Polymer Science Part A: Polymer Chemistry* **51**, 3516-3522, doi:10.1002/pola.26753 (2013).

31 Nomura, N., Shinoda, K., Takasu, A., Nagata, K. & Inomata, K. Emulsion polymerization of vinyl acetate using iodine - transfer and RAFT radical polymerizations. *Journal of Polymer Science Part A: Polymer Chemistry* **51**, 534-545, doi:10.1002/pola.26424 (2013).

32 Sato, H., Ishii, Y., Momose, H., Sato, T. & Teramoto, K. Application of High-Resolution MALDI-TOFMS with a Spiral Ion Trajectory for the Structural Characterization of Free Radical Polymerized Methacrylate Ester Copolymers. *Mass Spectrom (Tokyo)* **2**, A0014, doi:10.5702/massspectrometry.A0014 (2013).

33 Teramoto, K. *et al.* Simple and rapid characterization of mycolic acids from Dietzia strains by using MALDI spiral-TOFMS with ultra high mass-resolving power. *The Journal of antibiotics* **66**, 713-717, doi:10.1038/ja.2013.79 (2013).

34 Tsujita, T., Shintani, T. & Sato, H. α-Amylase inhibitory activity from nut seed skin polyphenols. 1. Purification and characterization of almond seed skin polyphenols. *Journal of agricultural and food chemistry* **61**, 4570-4576, doi:10.1021/jf400691q (2013).

35 Voorhees, K. J. *et al.* Modified MALDI MS fatty acid profiling for bacterial identification. *Journal of Mass Spectrometry* **48**, 850-855, doi:10.1002/jms.3215 (2013).

36 Wang, X., Fukuoka, S., Tsukigawara, R., Nagata, K. & Higuchi, M. Electric-field-enhanced oriented cobalt coordinated peptide monolayer and its electrochemical properties. *Journal of colloid and interface science* **390**, 54-61, doi:10.1016/j.jcis.2012.08.079 (2013).

37 Yamada, S., Takasu, A. & Kawamura, K. The effect of microwave irradiation on the kinetics and activation thermodynamics of ring - opening polymerization of ε - caprolactone. *Journal of Polymer Science Part A: Polymer Chemistry* **51**, 3732-3739, doi:10.1002/pola.26776 (2013).

38 Akabane-Nakata, M., Obika, S. & Hari, Y. Synthesis of oligonucleotides containing N, N-disubstituted 3-deazacytosine nucleobases by post-elongation modification and their triplex-forming ability with double-stranded DNA. *Organic & biomolecular chemistry* **12**, 9011-9015, doi:10.1039/C4OB01760A (2014).

39 Chen, Y.-T., Hong, P.-F., Wen, L. & Lin, C.-T. Molecular cloning and characterization of a thioredoxin from Taiwanofungus camphorata. *Botanical Studies* **55**, 1-8, doi:10.1186/s40529-014-0077-z (2014).

40 Ito, M., Shimasaki, T., Teramoto, N. & Shibata, M. Photo-cured organic–inorganic hybrid composites of methacrylate-terminated 4-arm star-shaped ε-caprolactone oligomer and methacrylate-or thiol-substituted polysilsesquioxane. *Journal of Polymer Research* **21**, 1-10, doi:10.1007/s10965-014-0507-3 (2014).

41 Kawasaki, T., Imai, T. & Tsukiyama, K. Use of a Mid-Infrared Free-Electron Laser (MIR-FEL) for Dissociation of the Amyloid Fibril Aggregates of a Peptide. *Journal of Analytical Sciences, Methods and Instrumentation* **04**, 9-18, doi:10.4236/jasmi.2014.41002 (2014).

42 Ken, C.-F., Chang, C.-C., Wen, L., Huang, J.-K. & Lin, C.-T. Biochemical characterization of a functional recombinant aryl-alcohol dehydrogenase from Taiwanofungus camphorata. *Botanical Studies* **55**, 14, doi:10.1186/1999-3110-55-14 (2014).

43 Kim, B.-J. *et al.* Preparation of carbon fibers with excellent mechanical properties from isotropic pitches. *Carbon* **77**, 747-755, doi:10.1016/j.carbon.2014.05.079 (2014).

44 Kurashige, W. *et al.* Au25 Clusters Containing Unoxidized Tellurolates in the Ligand Shell. *The journal of physical chemistry letters* **5**, 2072-2076, doi:10.1021/jz500901f (2014).

45 Niihori, Y., Matsuzaki, M., Uchida, C. & Negishi, Y. Advanced use of high-performance liquid chromatography for synthesis of controlled metal clusters. *Nanoscale* **6**, 7889-7896, doi:10.1039/C4NR01144A (2014).

46 Nishikawa, K. *et al.* Detection of changes in the structure and distribution map of triacylglycerol in fatty liver model by MALDI - SpiralTOF. *FEBS open bio* **4**, 179-184, doi:10.1016/j.fob.2014.02.005 (2014).

47 Ohtani, H. & Iura, T. Complementary Characterization of End Groups in Radically Polymerized Poly(methyl methacrylate) by Matrix-Assisted Laser Desorption/Ionization Mass Spectrometry and Pyrolysis-Gas Chromatography-Mass Spectrometry. *Mass Spectrom (Tokyo)*

3, S0041, doi:10.5702/massspectrometry.S0041 (2014).

48 Okabe, T., Kuzuhara, D., Aratani, N. & Yamada, H. Synthesis and electronic properties of acetylene-and butadiyne-linked 3, 3′-porphycene dimers. *Journal of Porphyrins and Phthalocyanines* **18**, 849-855, doi:10.1142/S1088424614500631 (2014).

49 Sanai, Y., Morita, Y., Asano, Y., Ishizaki, K. & Kubota, K. Chain - end lactonization of polyacrylates prepared by photopolymerization. *Journal of Polymer Science Part A: Polymer Chemistry* **52**, 1161-1171, doi:10.1002/pola.27100 (2014).

50 Sato, H., Nakamura, S., Teramoto, K. & Sato, T. Structural characterization of polymers by MALDI spiral-TOF mass spectrometry combined with Kendrick mass defect analysis. *J Am Soc Mass Spectrom* **25**, 1346-1355, doi:10.1007/s13361-014-0915-y (2014).

51 Satoh, T., Kubo, A., Hazama, H., Awazu, K. & Toyoda, M. Separation of Isobaric Compounds Using a Spiral Orbit Type Time-of-Flight Mass Spectrometer, MALDI-SpiralTOF. *Mass Spectrom (Tokyo)* **3**, S0027, doi:10.5702/massspectrometry.S0027 (2014).

52 Shibata, T., Fujimoto, M. & Otani, T. Synthesis of macrocyclic heteroarylenes by consecutive inter-and intramolecular cycloadditions of thiophenylene-tethered triynes. *Tetrahedron* **70**, 8453-8461, doi:10.1016/j.tet.2014.09.077 (2014).

53 Shigeri, Y. *et al.* Hydrazide and hydrazine reagents as reactive matrices for MALDI - MS to detect gaseous aldehydes. *Journal of Mass Spectrometry* **49**, 742-749, doi:10.1002/jms.3408 (2014).

54 Suzuki, R. *et al.* Brevisulcatic acids, marine ladder-frame polyethers from the red tide dinoflagellate Karenia brevisulcata in New Zealand. *Org Lett* **16**, 5850-5853, doi:10.1021/ol502700h (2014).

55 Takagi, K., Kawagita, E. & Kouchi, R. Synthesis and characterization of polythiophene derivatives with nitrogen heterocycles on the side chain. *Journal of Polymer Science Part A: Polymer Chemistry* **52**, 2166-2174, doi:10.1002/pola.27228 (2014).

56 Tsujita, T., Shintani, T. & Sato, H. Preparation and characterisation of peanut seed skin polyphenols. *Food chemistry* **151**, 15-20, doi:10.1016/j.foodchem.2013.11.072 (2014).

57 Wambua, D. M., Ubukata, M., Dane, J., Cody, R. B. & Chiu, N. H. Bottom-up mass spectrometric sequencing of microRNA. *Analytical Methods* **6**, 8829-8839, doi:10.1039/C4AY01519C (2014).

58 Yamaguchi, I. & Nagano, T. Synthesis, chemical, and thermoelectric properties of n - type π - conjugated polymer composed of 1, 2, 4 - triazole and pyridine rings and its metal complexes. *Journal of Applied Polymer Science* **131**, doi:10.1002/app.39928 (2014).

59 Yamakado, R. *et al.* Synthesis, reaction, and optical properties of cyclic oligomers bearing 9, 10-diphenylanthracene based on an aromatic tertiary amide unit. *RSC Advances* **4**, 6752-6760, doi:10.1039/C3RA46652C (2014).

60 Yamazoe, S., Kurashige, W., Nobusada, K., Negishi, Y. & Tsukuda, T. Preferential Location of Coinage Metal Dopants (M= Ag or Cu) in [Au25–x M x (SC2H4Ph) 18]−(x~ 1) As Determined by Extended X-ray Absorption Fine Structure and Density Functional Theory Calculations. *The Journal of Physical Chemistry C* **118**, 25284-25290, doi:10.1021/jp5085372 (2014).

61 Yan, Y., Ubukata, M., Cody, R. B., Holy, T. E. & Gross, M. L. High-energy collision-induced dissociation by MALDI TOF/TOF causes charge-remote fragmentation of steroid sulfates. *J Am Soc Mass Spectrom* **25**, 1404-1411, doi:10.1007/s13361-014-0901-4 (2014).

62 Yu, M., Tang, T., Takasu, A. & Higuchi, M. pH-and thermo-induced morphological changes of an amphiphilic peptide-grafted copolymer in solution. *Polymer journal* **46**, 52-58, doi:10.1038/pj.2013.61 (2014).

63 Abe, T., Matsuzaka, M., Isoda, K. & Tadokoro, M. Liquid-Crystalline and Electronic Properties

of Racemic-Alkoxy Chains-Substituted Tetraazanaphthacene. *Molecular Crystals and Liquid Crystals* **615**, 70-77, doi:10.1080/15421406.2015.1066963 (2015).

64 Asamizu, S., Ozaki, T., Teramoto, K., Satoh, K. & Onaka, H. Killing of Mycolic Acid-Containing Bacteria Aborted Induction of Antibiotic Production by Streptomyces in Combined-Culture. *PLoS One* **10**, e0142372, doi:10.1371/journal.pone.0142372 (2015).

65 Hayakawa, T., Song, H., Ishii, Y. & Kawasaki, S. Facile Synthesis of Coronene Dimers Having Unique Optical Properties. *J. Chem* **9**, 442-447, doi:10.17265/1934-7375/2015.07.002 (2015).

66 Hayakawa, Y. *et al.* Complementary DNA display selection of high - affinity peptides binding the vacuolating toxin (VacA) of Helicobacter pylori. *Journal of Peptide Science* **21**, 710-716, doi:10.1002/psc.2795 (2015).

67 Hubin, E. A. *et al.* Structural, functional, and genetic analyses of the actinobacterial transcription factor RbpA. *Proc Natl Acad Sci U S A* **112**, 7171-7176, doi:10.1073/pnas.1504942112 (2015).

68 Ikawa, T. *et al.* 2 - [(Neopentyl glycolato) boryl] phenyl Triflates and Halides for Fluoride Ion - Mediated Generation of Functionalized Benzynes. *Advanced Synthesis & Catalysis* **357**, 2287-2300, doi:10.1002/adsc.201500315 (2015).

69 Itoh, Y. *et al.* Identification of SNAIL1 Peptide-Based Irreversible Lysine Specific Demethylase 1-Selective Inactivators. *Journal of medicinal chemistry*, doi:10.1021/acs.jmedchem.5b01323 (2015).

70 Iura, T. & Ohtani, H. Fragmentation behavior of poly(methyl methacrylate) during matrix-assisted laser desorption/ionization. *Rapid Commun Mass Spectrom* **29**, 155-162, doi:10.1002/rcm.7087 (2015).

71 Kano, H. *et al.* A novel analytical pyrolysis device applicable for measurements of less volatile pyrolyzates. *Journal of Analytical and Applied Pyrolysis* **113**, 165-173, doi:10.1016/j.jaap.2014.12.008 (2015).

72 Kurimoto, K., Yamamura, H. & Miyagawa, A. Chemical approach for the syntheses of GM4 isomers with sialic acid to non-natural linkage positions on galactose. *Carbohydrate research* **401**, 39-50, doi:10.1016/j.carres.2014.10.018 (2015).

73 Miyagawa, A., Matsuda, T. & Yamamura, H. Synthesis of Branched Tetrasaccharide Derivatives of Schizophyllan-like ß-Glucan. *Journal of Carbohydrate Chemistry* **34**, 215-246, doi:10.1080/07328303.2015.1044754 (2015).

74 Mizukado, J. *et al.* High - resolution MALDI - TOF MS study on analysis of low - molecular - weight products from photo - oxidation of poly (3 - hexylthiophene). *Journal of Mass Spectrometry* **50**, 1006-1012, doi:10.1002/jms.3614 (2015).

75 Mori, S., Morihiro, K., Kasahara, Y., Tsunoda, S.-i. & Obika, S. Synthesis and Properties of 2'-Deoxyuridine Analogues Bearing Various Azobenzene Derivatives at the C5 Position. *Chemosensors* **3**, 36-54, doi:10.3390/chemosensors3020036 (2015).

76 Negishi, Y. *et al.* A critical size for emergence of nonbulk electronic and geometric structures in dodecanethiolate-protected Au clusters. *Journal of the American Chemical Society* **137**, 1206-1212, doi:10.1021/ja5109968 (2015).

77 Niihori, Y., Kikuchi, Y., Kato, A., Matsuzaki, M. & Negishi, Y. Understanding Ligand-Exchange Reactions on Thiolate-Protected Gold Clusters by Probing Isomer Distributions Using Reversed-Phase High-Performance Liquid Chromatography. *ACS nano* **9**, 9347-9356, doi:10.1021/acsnano.5b03435 (2015).

78 Nishikawa, K. *et al.* Resveratrol increases CD68+ Kupffer cells colocalized with adipose differentiation - related protein and ameliorates high - fat - diet - induced fatty liver in mice. *Molecular nutrition & food research* **59**, 1155-1170, doi:10.1002/mnfr.201400564 (2015).

79 Ono, K. *et al.* Self-Assembly of Nanometer-Sized Boroxine Cages from Diboronic Acids. *Journal of the American Chemical Society* **137**, 7015-7018, doi:10.1021/jacs.5b02716 (2015).

80 Sakano, T., Ohashi, T., Yamanaka, M. & Kobayashi, K. Photoresponsive self-assembled hexameric capsules based on calix [4] resorcinarenes bearing azobenzene dendron conjugates as side chains. *Organic & biomolecular chemistry* **13**, 8359-8364, doi:10.1039/C5OB00997A (2015).

81 Satoh, T. *et al.* Imaging Mass Spectrometry Using Ultra-high Mass Resolution Matrix-Assisted Laser Desorption/Ionization Time-of-Flight Mass Spectrometer, SpiralTOF. *Microscopy and Microanalysis* **21**, 2059-2060, doi:10.1017/S1431927615011071 (2015).

82 Segawa, Y., Kuwabara, T., Matsui, K., Kawai, S. & Itami, K. Palladium-free synthesis of [10] cycloparaphenylene. *Tetrahedron* **71**, 4500-4503, doi:10.1016/j.tet.2015.02.066 (2015).

83 Sharma, S., Kurashige, W., Nobusada, K. & Negishi, Y. Effect of trimetallization in thiolate-protected Au(24-n)Cu(n)Pd clusters. *Nanoscale* **7**, 10606-10612, doi:10.1039/c5nr01491c (2015).

84 Shigeri, Y. *et al.* Hydrazide and hydrazine reagents as reactive matrices for matrix-assisted laser desorption/ionization mass spectrometry to detect steroids with carbonyl groups. *European Journal of Mass Spectrometry* **21**, 79-90, doi:10.1255/ejms.1336 (2015).

85 Spring, A. M. *et al.* An analysis of the structural, thermal and optical characteristics as well as the electrical resistivity of tert-butyldiphenylsilyl substituted poly (norbornene-dicarboximide) s. *Polymer* **56**, 189-198, doi:10.1016/j.polymer.2014.11.043 (2015).

86 Takanashi, E. *et al.* Cytotoxic linear acetylenes from a marine sponge Pleroma sp. *Tetrahedron* **71**, 9564-9570, doi:10.1016/j.tet.2015.10.062 (2015).

87 Teramoto, K. *et al.* Characterization of Mycolic Acids in Total Fatty Acid Methyl Ester Fractions from Mycobacterium Species by High Resolution MALDI-TOFMS. *Mass Spectrom (Tokyo)* **4**, A0035, doi:10.5702/massspectrometry.A0035 (2015).

88 Wang, C. *et al.* A novel D–π–A small molecule with N-heteroacene as acceptor moiety for photovoltaic application. *Dyes and Pigments* **122**, 231-237, doi:10.1016/j.dyepig.2015.06.029 (2015).

89 Wang, C. *et al.* Synthesis, Characterization, and Memory Performance of Two Phenazine/Triphenylamine‐Based Organic Small Molecules through Donor‐Acceptor Design. *Asian Journal of Organic Chemistry* **4**, 646-651, doi:10.1002/ajoc.201500087 (2015).

90 Yamanoi, T., Oda, Y., Katsuraya, K., Inazu, T. & Hattori, K. Synthesis, structure, and evaluation of a ß-cyclodextrin-artificial carbohydrate conjugate for use as a doxorubicin-carrying molecule. *Bioorganic & medicinal chemistry*, doi:10.1016/j.bmc.2015.12.030 (2015).

91 Zheng, Q., Morimoto, M., Sato, H. & Takanohashi, T. Molecular composition of extracts obtained by hydrothermal extraction of brown coal. *Fuel* **159**, 751-758, doi:10.1016/j.fuel.2015.07.042 (2015).

92 橋詰峰雄 *et al.* 体液類似環境におけるアパタイト結合性ペプチド樹状オリゴマーによるミネラリゼーション. *高分子論文集* **73**, 55-61, doi:10.1295/koron.2015-0050 (2015).

93 小林大祐 *et al.* 超音波を用いたポリピロール微粒子合成. *化学工学論文集* **41**, 153-156, doi:10.1252/kakoronbunshu.41.153 (2015).

94 Fouquet, T., Nakamura, S. & Sato, H. MALDI SpiralTOF high-resolution mass spectrometry and Kendrick mass defect analysis applied to the characterization of poly(ethylene-co-vinyl acetate) copolymers. *Rapid Commun Mass Spectrom* **30**, 973-981, doi:10.1002/rcm.7525 (2016).

95 Hayakawa, T., Ishii, Y. & Kawasaki, S. Sodium ion battery anode properties of designed graphene-layers synthesized from polycyclic aromatic hydrocarbons. *RSC Advances* **6**,

22069-22073, doi:10.1039/C6RA00955G (2016).

96 Kakizawa, T. *et al.* Evaluation of phenylcyclopropylamine compounds by enzymatic assay of lysine-specific demethylase 2 in the presence of NPAC peptide. *Bioorganic & Medicinal Chemistry Letters*, doi:10.1016/j.bmcl.2016.01.036 (2016).

97 Katagiri, K., Takasu, A. & Higuchi, M. Synthesis of Glycopolymer Containing Cell-Penetrating Peptide as Inducers of Recombinant Protein Expression under the Control of Lac Operator/Repressor Systems. *Biomacromolecules*, doi:10.1021/acs.biomac.6b00368 (2016).

98 Kim, B.-J. *et al.* Enhancing the tensile strength of isotropic pitch-based carbon fibers by improving the stabilization and carbonization properties of precursor pitch. *Carbon* **99**, 649-657, doi:10.1016/j.carbon.2015.12.082 (2016).

99 Peršurić, Ž., Osuga, J., Grbac, T. G., Peter - Katalinić, J. & Pavelić, S. K. MALDI - SpiralTOF technology for assessment of triacylglycerols in Croatian olive oils. *European Journal of Lipid Science and Technology*, doi:10.1002/ejlt.201500375 (2016).

100 Shigeri, Y. *et al.* 2-hydrazinoquinoline: a reactive matrix for MALDI-MS to detect gaseous carbonyl compounds. *European Journal of Mass Spectrometry* **22**, 0-0, doi:10.1255/ejms.1413 (2016).

101 Takahira, Y., Murotani, E., Fukuda, K., Vohra, V. & Murata, H. Design, synthesis, and properties of a series of charged iridium (III) complexes with a neutral bidentate ligand for deep-blue phosphorescent emitter. *Journal of Fluorine Chemistry* **181**, 56-60, doi:10.1016/j.jfluchem.2015.10.016 (2016).

102 Yang, J., Nakabayashi, K., Miyawaki, J. & Yoon, S.-H. Preparation of isotropic pitch-based carbon fiber using hyper coal through co-carbonation with ethylene bottom oil. *Journal of Industrial and Engineering Chemistry* **34**, 397-404, doi:10.1016/j.jiec.2015.11.026 (2016).

This page intentionally left blank for layout purpose.

*Specifications subject to change without prior notice.

Certain products in this brochure are controlled under the "Foreign Exchange and Foreign Trade Law" of Japan in compliance with international security export control. JEOL Ltd. must provide the Japanese Government with "End-user's Statement of Assurance" and "End-use Certificate" in order to obtain the export license needed for export from Japan. If the product to be exported is in this category, the end user will be asked to fill in these certificate forms.

JEOL Ltd.

1-2 Musashino 3-chome Akishima Tokyo 196-8558 Japan Sales Division Tel. +81-3-6262-3560 Fax. +81-3-6262-3577

www.jeol.com ISO 9001・ISO 14001 Certified

• **AUSTRALIA & NEW ZEALAND** /JEOL(AUSTRALASIA) Pty.Ltd. Suite 1, L2 18 Aquatic Drive - Frenchs Forest NSW 2086 Australia • **BELGIUM** /JEOL (EUROPE) B.V. Planet II, Gebouw B Leuvensesteenweg 542, B-1930 Zaventem Belgium • **CANADA** /JEOL CANADA, INC. 3275 1ere Rue, Local #8 St-Hubert, QC J3Y-8Y6, Canada • **CHINA** /JEOL(BEIJING) CO., LTD. Zhongkeziyuan Building South Tower 2F, Zhongguancun Nansanjie Street No. 6, Haidian District, Beijing, P.R.China • **EGYPT** /JEOL SERIVCE BUREAU 3rd Fl. Nile Center Bldg., Nawal Street, Dokki, (Cairo), Egypt • **FRANCE** /JEOL (EUROPE) SAS Espace Claude Monet, 1 Allee de Giverny 78290, Croissy-sur-Seine, France • **GERMANY** /JEOL (GERMANY) GmbH Oskar-Von-Miller-Strasse 1a, 85386 Eching, Germany • **GREAT BRITAIN & IRELAND** /JEOL (U.K.) LTD. JEOL House, Silver Court, Watchmead, Welwyn Garden City, Herts AL7 1LT, U.K. • **ITALY** /JEOL (ITALIA) S.p.A. Palazzo Pacinotti - Milano 3 City, Via Ludovico il Moro, 6/A 20080 Basiglio(MI) Italy • **KOREA** /JEOL KOREA LTD. Dongwoo Bldg. 7F, 1443, Yangjae Daero, Gangdong-Gu, Seoul, 134-814, Korea • **MALAYSIA** /JEOL(MALAYSIA) SDN.BHD. 508, Block A, Level 5, Kelana Business Center, 97, Jalan SS 7/2, Kelana Jaya, 47301 Petaling Jaya, Selangor, Malaysia • **MEXICO** /JEOL DE MEXICO S.A. DE C.V. Arkansas 11 Piso 2 Colonia Napoles Delegacion Benito Juarez, C.P. 03810 Mexico D.F., Mexico • **SCANDINAVIA** /SWEDEN JEOL (Skandinaviska)AB Hammarbacken 6A, Box 716, 191 27 Sollentuna Sweden • **SINGAPORE** /JEOL ASIA PTE.LTD. 2 Corporation Road #01-12 Corporation Place Singapore 618494 • **TAIWAN** /JIE DONG CO., LTD. 7F, 112, Chung Hsiao East Road, Section 1, Taipei, Taiwan 10023 Republic of China • **THE NETHERLANDS** /JEOL (EUROPE) B.V. Lireweg 4, NL-2153 PH Nieuw-Vennep, The Netherlands • **USA** /JEOL USA, INC. 11 Dearborn Road, Peabody, MA 01960, U.S.A.